UNIVERSITÉ DE MONTRÉAL

PERFORMANCE EVALUATION AND ANALYSIS OF MIMO SCHEMES IN LTE NETWORKS ENVIRONMENT

ALI JEMMALI
DÉPARTEMENT DE GÉNIE ÉLECTRIQUE
ÉCOLE POLYTECHNIQUE DE MONTRÉAL

THÈSE PRÉSENTÉE EN VUE DE L'OBTENTION
DU DIPLÔME DE PHILOSOPHIÆ DOCTOR
(GÉNIE ÉLECTRIQUE)
DÉCEMBRE 2013

UNIVERSITÉ DE MONTRÉAL

ÉCOLE POLYTECHNIQUE DE MONTRÉAL

Cette thèse intitulée :

PERFORMANCE EVALUATION AND ANALYSIS OF MIMO SCHEMES IN LTE NETWORKS ENVIRONMENT

présentée par : JEMMALI Ali
en vue de l'obtention du diplôme de : Philosophiæ Doctor
a été dûment acceptée par le jury d'examen constitué de :

M. CARDINAL Christian, Ph.D., président
M. CONAN Jean, Ph.D., membre et directeur de recherche
M. WU Ke, Ph.D., membre et codirecteur de recherche
M. AKYEL Cevdet, D.Sc.A, membre
M. AJIB Wessam, Ph.D., membre

To my dear mother, my dear wife and dear son,
In memory of my father...

ACKNOWLEDGEMENTS

I would like to express the deepest appreciation to my director of research, Dr Jean Conan and my co-director of research, Dr Ke Wu. My sincere gratitude goes to my director of research for his continuous support of my Ph.D study and research, for his motivation, enthusiasm and immense knowledge. His guidance helped me in all the time of research and writing of this thesis. I also wish to express my truthful recognition to Dr Ke Wu for his continuous encouragement and support. Without the support, encouragement of my supervisors, this thesis would not have been possible.

My sincere gratitude goes towards my thesis examiners :

– Prof. Cardinal Christian (Committee Chair), Dept. Electrical Engineering, École Polytechnique, Montréal,
– Prof. Ajib Wessam (External Examiner), Dept. Computer Science, UQAM, Montréal,
– Prof. Cevdet Akyel, Dept. Electrical Engineering, École Polytechnique, Montréal,

for accepting reviewing my work and for their valuable comments towards the improvement of my final thesis report, as well as putting me through a stimulating, albeit a bit stressful, defense experience.

Special thanks go also go to my student colleagues in the laboratory for the technical exchanges and fruitful discussions. I mention for memory Wael, Jihed and Tarek. My truthful recognition goes to Mohammad Torabi for his precious help and advises. Big thanks also goes to my colleagues, namely Vladan Jevromovic and Benoit Courchesne for their encouragement and for giving me one day off for more than one year to help me finalize my thesis work.

Last but not least, I would like to thank my dear wife for her patience, support and sacrifice.

RÉSUMÉ

Dans cette thèse, nous proposons d'évaluer et d'analyser les performances des configurations radio à antennes multiples à l'émission et/ou la réception (MIMO) dans l'environnement des réseaux LTE (Long Term Evolution). Plus spécifiquement, on s'intéresse à la couche physique de l'interface radio OFDM-MIMO de ces réseaux. Après une introduction rapide aux réseaux LTE et aux techniques MIMO, on présente dans une première étape, une analyse théorique du taux d'erreur binaire en fonction du rapport signal sur bruit des deux principaux codes spatio-temporels de la norme LTE, à savoir le codage SFBC 2×1 (Space Frequency Block Coding) et le codage FSTD 4×2 (Frequency Switch Transmit Diversity). On développe les équations analytiques du taux d'erreur binaire de ces codes dans un canal à évanouissement de Rayleigh sans corrélation spatiale qui sont par la suite comparées à des valeurs obtenues par simulations Monte-Carlo. Dans une deuxième étape, on considère l'évaluation de la capacité du canal résultant de l'utilisation de ces mêmes codes dans un canal à évanouissement de Rayleigh. Pour fin de comparaison, on propose par la suite d'évaluer par simulation leur débit effectif. Les résultats montrent que la capacité peut effectivement être presque atteinte en pratique. Le deuxième volet de cette thèse considère les performances des systèmes MIMO utilisant la sélection d'antennes. Nous utilisons la théorie d'ordre statistique pour développer des équations analytiques relatives au taux d'erreur binaire des systèmes avec sélection d'antennes du coté récepteur dans un canal d'évanouissement de Rayleigh sans corrélation spatiale. Afin de valider numériquement les résultats de notre analyse, un algorithme à sélection d'antenne au récepteur a été développé et utilisé en simulation. Dans un dernier temps, on évalue l'effet de la corrélation spatiale entre les antennes. L'étude est faite à partir de simulations et d'un modèle de corrélation spatiale basé sur le produit Kronecker de deux matrices de corrélation relatives respectivement à l'émission et à la réception.

ABSTRACT

This thesis considers both an analysis and a numerical evaluation of the performance of MIMO radio systems in the LTE network environment. More specifically we consider the physical layer of the OFDM-MIMO based radio interface. As a first step we present a theoretical analysis of the bit error rate of the two space-time codes adopted by the LTE norm, namely the SFBC 2×1 and FSTD 4×2 codes, as a function of the signal upon noise ratio. Analytical expressions are given for transmission over a Rayleigh channel without spatial correlation which are then compared with Monte-Carlo simulations. As a second step, we consider the capacity of the channel obtained by using these codes on a Rayleigh fading channel. Results show that simulated throughput almost reaches the capacity limit. As a different topic, this thesis considers also MIMO systems based on antenna selection. By using order statistics we develop analytical expressions for the error rate on a Rayleigh channel without antenna correlation. In order to validate our numerical results, an algorithm implementing antenna selection at the receiver has been developed and used in the simulations. As a last step the effect of antenna correlation is investigated through the use of simulations and a model of spatial antenna correlation based on the Kronecker product of two correlation matrices related to the transmitting and receiving elements of the MIMO scheme.

TABLE OF CONTENTS

LIST OF TABLES

LIST OF FIGURES

LIST OF APPENDICES

LIST OF ACRONYMS

MIMO	Multi-Input Multi-Output
SIMO	Single-Input Multi-Output
MISO	Multi-Input Single-Output
LTE	Long Term Evolution
SAE	System Architecture Evolution
OFDM	Orthogonal Frequency Division Multiplex
OFDMA	Orthogonal Frequency Division Multiplex Access
IFFT	Inverse Fast Fourier Transform
FFT	Fast Fourier Transform
BER	Bit Error Rate
SNR	Signal to Noise Ratio
MGF	Moment Generating Function
PDF	Probability Density Function
CDF	Cumulative Distribution Function
EPC	Evolved Packet Core
E-UTRAN	Evolved Universal Terrestrial Radio Access Network
DL	Uplink Channel
UL	Downlink Channel
CRC	Cyclic Redundancy Check
MAC	Medium Access Control
RLC	Radio Link Control
RRC	Radio Resource Control
CW	Code Word
RE	Resource Element
RB	Resource Block
FDD	Frequency Division Duplex
TDD	Time Division Duplex
TTI	Transmission Time Interval
CP	Cyclic Prefic
UpPTS	Uplink Pilot Time Slot
DwPTS	Downlink Pilot Time Slot
N_{DL}^{RB}	Number of RB in the Downlink Link
PSS	Primary Synchronization Signal

SSS	Secondary Synchronization Signal
PBCH	Physical Broadcast Channel
PCFICH	Physical Control Format Indicator Channel
PHICH	Physical Hybrid ARQ Indicator Channel
PDCCH	Physical Downlink Control Channel
PDSCH	Physical Downlink Shared Channel
PMCH	Physical Multicast Channel
MRC	Maximum Ratio Combining
AWGN	Additive White Gaussian Noise
STBC	Space Time Block Coding
SFBC	Space Frequency Block Coding
N_t	Number of Transmit Antennas
N_r	Number of Receive Antennas
γ	Instantaneous Signal to Noise Ratio
γ_i	Instantaneous Signal to Noise Ratio at ith Branch
γ_c	Instantaneous Combined Signal to Noise Ratio
$\overline{\gamma}$	Average Signal to Noise Ratio
N_d	Diversity Order
CSI	Channel State Information
CSIT	Channel State Information at the Transmitter
UE	User Equipment
TB	Transport Block
FSTD	Frequency Switched Transmit Diversity
CQI	Channel Quality Indicator
HARQ	Hybrid Automatic Repeat reQuest
MMSE	Minimum Mean Square Error
SIC	Successive Interference Cancelation
RI	Rank Indicator
CDD	Cyclic Delay Diversity
3GPP	3rd Generation Partnership Project
RS	Reference Signal
$\Re\{x\}$	Real Part of x
$\Im\{x\}$	Imaginary Part of x
LLS	Link Level Simulator
PMI	Precoding Matrix Indicator
QAM	Quadrature Amplitude Modulation

CHAPTER 1

INTRODUCTION

1.1 Introduction

To increase the capacity and speed of wireless communication systems, a new type of wireless data networks has recently emerged and been standardized by the 3rd Generation Partnership Project (3GPP). This new standard comes as a natural evolution to the existing second (2G) and third (3G) generation wireless networks in order to respond to the growing demand in terms of extended data rates and speed and is marketed as the 4G Long Term Evolution (LTE) network. It was first proposed by NTT DoCoMo of Japan in 2004, and studies on the new standard officially commenced in 2005. In may 2007, the LTE and the System Architecture Evolution (SAE) Trial Initiative (LSTI) was founded as a global collaboration between vendors and operators with the goal of verifying and promoting the new standard in order to ensure as quickly as possible the global introduction of the new technology. The LTE standard was finalized in December 2008, and the first publicly available LTE service was launched by TeliaSonera in Oslo and Stockholm on December 2009 as a data connection with a Universal Serial Bus (USB) modem. By the end of 2012 already 113 commercial LTE networks in 51 countries have been deployed and the Global mobile Suppliers Association (GSA) forecasts, by the end of 2013, that the number of deployed commercial LTE networks will reach 209 in 75 countries. In Canada, Rogers Wireless was the first wireless network operator to launch LTE network on July, 2011 offering the Sierra Wireless AirCard USB mobile broadband modem known as the LTE Rocket stick. Initially, CDMA operators planned to upgrade to rival standards called Ultra Mobile Broadband (UMB) and WiMAX, but finally all the major CDMA operators in the world have announced that they intended to migrate to LTE after all. The most recent evolution of LTE has been standardized in March 2011 and is known as LTE-Advanced. The LTE-Advanced services are expected to begin in 2013. Comparing with other standards, the key aim of UMTS and GPRS/EDGE was the expansion of service provision beyond voice calls towards a multi service air interface. This objective was achieved by circuit switching and packet switching. In contrast to the former technology family of standards, LTE was designed from the start with the goal of evolving the the radio access technology under the assumption that all services would be packet switched, rather than following the circuit switching model of earlier systems.

1.2 Motivation

The third generation (3G) wireless communication systems, mainly based on the WCDMA technology, have been confronted with a number of new challenges regarding to the design of the required wireless communication systems. The main challenges the 3G technology has been facing can be summarized as follows:

- The data rate of the 3G system needs to be increased by introducing new techniques such as HSPA and HSPA+. Since the 3G is based on WCDMA technology in a 5 MHz bandwidth, the data rate couldn't be improved as much as planned.

- The typical delay spread observed in wireless channel puts a strong limitation on the symbol duration period if it is transmitted serially. To struggle with the time delay spread of the wireless channel, the delay spread should be smaller than the symbol period, which is not the case for high data rate serial transmission, where, in general, the delay spread is much bigger than the transmitted symbol period. It is well known that the delay spread of the channel causes Inter Symbol Interference (ISI) which can be undone often only partially by means of complex equalization procedures. In WCDMA, since the signal is transmitted serially in time it is highly challenging to increase the data rate of the transmitted signal.

To contend with the above mentioned challenges and to achieve good system performance, the choice of an appropriate modulation and multiple access schemes applicable to mobile wireless communication systems is then critical. In this context, the parallel multi carriers schemes have shown their efficiency in many wireless applications. More specifically, the Orthogonal Frequency Division Multiplexing (OFDM) which is a special case of multi carrier transmission is a good choice. In OFDM, the frequency selective fading wide band channel is used as frequency multiplex of non frequency selective (flat fading) narrow band parallel sub channels. To avoid the need to separate the carriers by means of guard-bands and therefore make OFDM highly spectrally efficient, the sub channels in OFDM are overlapping and orthogonal. Initially, only analog design was considered, using banks of sinusoidal signal generators and demodulators to process the signal for multiple sub channels. The tremendous advancement in digital signal processing made the implementation of digitally designed OFDM possible and cost effective using the Discrete Fast Fourier Transform (DFFT). The OFDM became the modulation of choice for many applications for both wired systems (such us Asymmetric Digital Subscriber Line (ADSL)) and wireless broadcasting systems such as Digital Audio Broadcasting (DAB) and Digital Video Broadcasting (DVB) as well as Wireless

Local Area Network (WLAN). In addition to the mentioned benefits of OFDM technology, this multi carrier modulation has the ability to be adapted in a straightforward manner to operate in different channel bandwidth according to spectrum availability. All above mentioned benefits have strongly motivated the choice of OFDM in the LTE system. Beside the OFDM schemes, the use of multi antenna techniques always been known to be of value in improving the performance of general wireless communication systems including early line of sight systems. Nevertheless, most of the theoretical development in understanding their fundamental benefits has appeared only in the last 15 years, driven by advancement in signal processing and Shannon's information theory. A key innovation being accomplished with the introduction of the concept of so-called Multiple Input Multiple Output (MIMO) systems in the mid-1990s. In fact, serious attention to the utilization of multiple antenna techniques in mass market commercial wireless networks has only been granted since around 2000. The key role that MIMO technology plays in the latest wireless communication standards for personal area networks testifies to its importance. The MIMO technique was adopted for the first time in the release 7 version of HSDPA (High Speed Downlink Packet Access) and LTE is the first wireless communication system to be developed with MIMO as a key component form the start. In chapter 2, we will provide the necessary theoretical background for a good understanding of the role and advantage promised by MIMO techniques in general wireless communication.

1.3 Research Objective and Contributions

Nowadays, the performance evaluation of LTE systems is mainly obtained through rather time consuming simulators and it is extremely difficult to evaluate the influence of the different parameters. The objective of this dissertation is to derive analytical models that will partially compensate for these drawbacks. More specifically, we focus on the link level performance of the physical layer. Three main key performance indicators are considered in this study, namely the Bit Error Rate (BER), Channel Capacity as well as the data throughput, all in terms of Signal to Noise Ratio (SNR). We also consider to analyze and evaluate MIMO systems using antenna selection techniques. In a first step, we analyze the BER performance of MIMO system when antenna selection is applied at the receiver side. In a second step, we evaluate the impact of antenna correlation on the BER performance of MIMO systems using receive antenna selection. A subject rarely considered in the current literature.

1.4 Dissertation Outline

In this work we provide several analytical performance analysis of MIMO schemes defined in the 4G LTE standard as well as comparison with simulations results which we believe are significant contributions. The document pertaining to this thesis is organized as follows:

- In Chapter 2, we present a technical overview of LTE systems. More specifically, the system architecture of LTE is highlighted and explained. Since our study concentrates on the physical layer of LTE systems, we emphasize particularly the OFDMA and MIMO schemes used by the LTE systems. The overall frame structure of the LTE signal is also considered with some depth.
- The main performance analysis of different MIMO scheme scenarios in LTE are given in Chapter 3. At first, we describe the system model used for the analysis. Then, the detailed Bit Error Rate analysis with mathematical derivation for different modulation order and different MIMO arrangements are developed. The approach used for this analysis is based on the Probability Density Function (PDF) of the instantaneous Signal to Noise Ratio (SNR) and the Moment Generating Function (MGF) approach. The channel capacity as well as data throughput are also derived in this chapter. To validate the accuracy of our analysis, simulation results of the analysed schemes are shown and compared to the analytical results.
- In Chapter 4, the principles and performance analysis of the Antenna selection algorithm of MIMO Systems are presented. After a brief introduction, the system model used for our analysis is given. A subsection dedicated to the BER performance analysis for receive antenna selection follows the introduction. The theory of order statistics used for this analysis is also introduced in this section. To validate the analytical results, the simulations results of antenna selection algorithm are shown and compared to the numerical results. In the second part of this chapter, the impact of antenna correlation on the performance of MIMO systems using antenna selection is evaluated. The system model used for this evaluation is also shown in this section.
- The summary and conclusion of this dissertation are made in Chapter 5, where we outline the basic contributions of the overall work and present an outline of possible future extensions.

CHAPTER 2

TECHNICAL OVERVIEW OF LTE SYSTEMS

In this chapter, a brief technical overview of the LTE systems is provided. We start by a brief description of the high level overall LTE system architecture, which consists of two parts; namely the *radio* and *core network parts* as shown in Figure 2.1. Since our main work in this thesis is related to the performance of the LTE physical layer, we will detail, more specifically, the physical layer of the radio part of LTE system. Due to its significant importance and relevance in our analysis and evaluation, one section is dedicated to the frame structure of the physical layer in which we explain how the data is organized in the time and frequency domains as well as how the data is transmitted over the air. Finally, we conclude the chapter by presenting the MIMO-OFDM schemes as defined in LTE which are relevant to our study.

2.1 LTE System Architecture

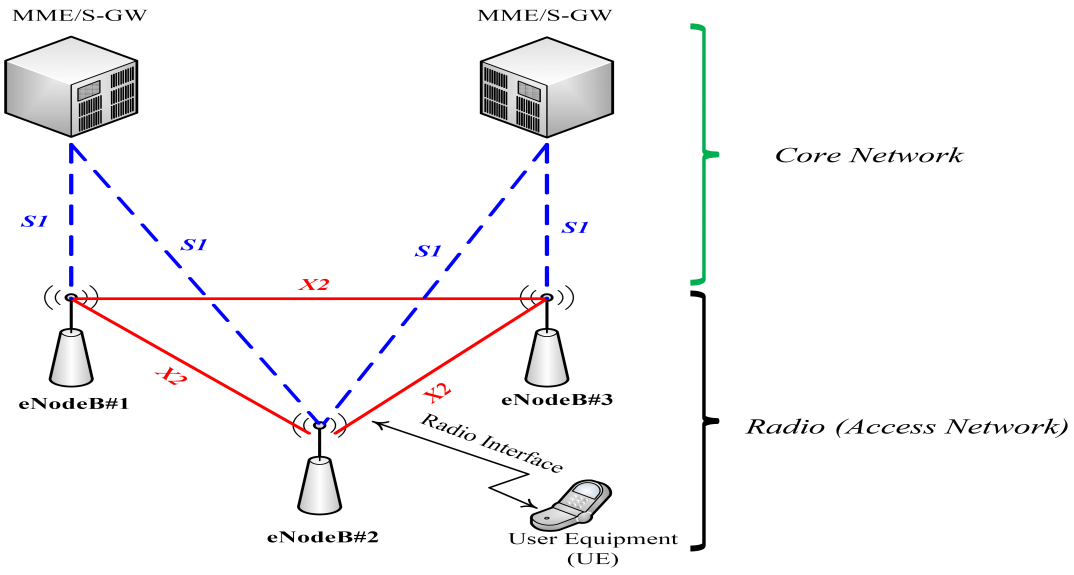

Figure 2.1 LTE System Architecture.

To understand the general structure of 4G (also called Evolved 3G) wireless communications systems, it is primordial to know its overall network architecture as well as the

functionalities of each element. As any other wireless communications network, the 4G system consists of two main parts, namely the *core network part* and the *radio part*. The core side of the network is called System Architecture Evolution (SAE) and the radio part is known as Long Term Evolution (LTE). The term LTE encompasses the Evolved Universal Terrestrial Radio Access Network (E-UTRAN) and represents the radio access network. The description of each part will be presented separately in the following subsections.

2.1.1 Core Network

At the beginning of the standardization process, the core network of the Evolved 3G network was designated by SAE but nowadays the core network is also called Evolved Packet Core (EPC) and the term SAE is used in parallel with EPC. The main functionality of the EPC is to provide access to external packet networks based on Internet Protocol (IP) and performs a number of functions for idle and active terminals. The whole functionalities of the core network (EPC) are performed using the following main logical nodes:

- Packet Data Network (PDN) Gateway (P-GW)
- Serving Gateway (S-GW)
- Mobility Management Entity (MME)

The main functionality of P-GW is to allocate IP addresses for the user equipment (UE). It is responsible for the filtering of downlink user's IP packets into the different radio services. Serving Gateway acts as the local mobility anchor for the data transmission when user equipment moves between eNodeBs. A mobile anchor means that the data for a specific user equipment pass through the S-GW regardless of the serving eNodeB to which the mobile is connected. The main functionality of the Mobility Management Entity is to process the signaling between the user equipment and the core network.

2.1.2 The Access Network

The access network of LTE, i.e., E-UTRAN, consists of a network of base stations called eNodeBs, as illustrated in Figure 2.1 above. In this Figure, a user equipment (UE) is connected to eNodeB#2 using the radio interface. The elements of the core network; namely the MME and S-GW as described in the previous section are also shown in this Figure. The eNodeBs are connected to the core network (EPC) via S1 interfaces. Two types of S1 interfaces are standardized in LTE. The S1-U, referred to as S1 User plan interface and S1-C, referred to as S1 Control plan interface. The communications between eNodeBs is also possible in LTE and it is assured by the so called X2 interfaces which enable a meshed radio access

network (RAN) architecture. The E-UTRAN is responsible of all functions related to the radio interface and its main function can be summarized briefly as follows:

- *Connectivity to the EPC*: This function handles the radio communications between the mobile user and the EPC network.
- *Radio Resource Management (RRM)*- This covers all functions related to the radio bearers such as radio bearer control, radio admission control, radio mobility control, scheduling and dynamic allocation of resources to UE in both uplink and downlink. Radio bearer can be defined as a pipeline connecting two or more points in the communication system in which data traffic follow through.
- *Header compression*: This function helps to provide efficient use of the radio interface by compressing the IP packet headers that could otherwise cause a significant overhead, especially for small packets such as voice over IP.
- *Security*: All data sent over the radio interface is encrypted.

In LTE, the radio interface, also called Uu interface, protocols that run between eNodeBs and an UE are divided into two plans, namely the *user plan* and the *control plan*. The control plan protocols are responsible for managing the control signaling whereas the user plan is responsible for transporting user traffic data. In Figure 2.2, the protocol stacks of the user plan are shown, where PDCP (Packet Data Convergence Protocol), RLC (Radio Link Control), MAC (Medium Access Control) and PHY (Physical) sublayers perform functions, such as header compression, retransmissions during handover, segmentation and reassembly of upper layers packets, scheduling and multiplexing data from different control channels. To be complete, the protocol stacks of the interface between the eNodeB and the serving GW, called S1-U interface, is also shown in Figure 2.2.

The protocols stacks of the control plan appear in Figure 2.3. It can be seen from the figure that the control plan protocols differ only by the so-called Radio Resource Control (RRC) sublayer with respect to the user plan protocols. In fact, all other sublayers perform the same functions as in the user plan. For the control plan, the eNodeB interfaces with the MME entity and the interface between them are designated by S1-MME as shown in Figure 2.3.

The above is just an outline of the actual architecture of the LTE concept. Since our main work in this thesis is related to the LTE physical layer aspects, more details about the LTE physical layer will be presented in the forthcoming sections.

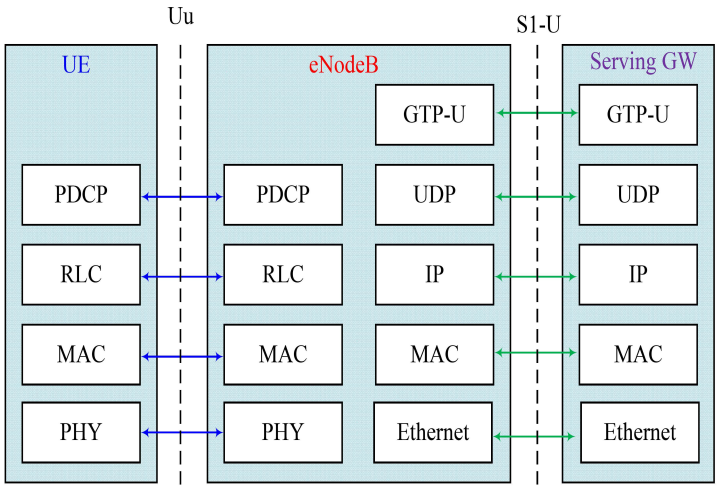

Figure 2.2 User Plan Protocols.

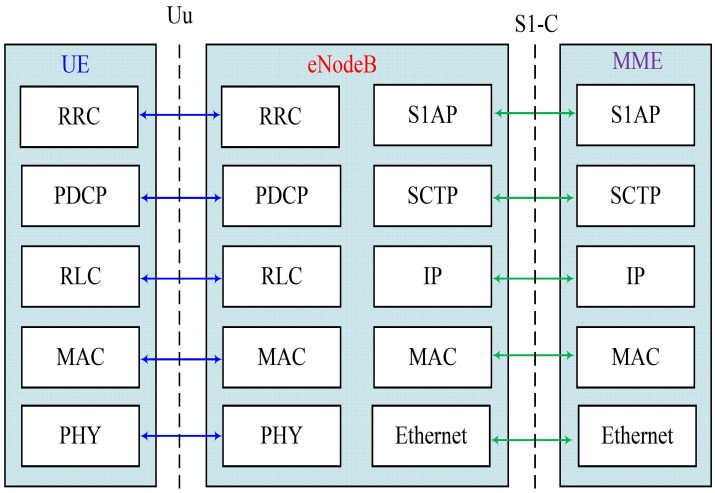

Figure 2.3 Control Plan Protocols.

2.2 LTE Physical Layer

The role of the physical layer in LTE is mainly to transform the base-band data into a reliable signal for transmissions across the radio interface between the eNodeB and the User Equipment (UE) in both directions, i.e., from eNodeB to UE, (Downlink Channel (DL)), and from UE to eNodeB, (Uplink Channel (UL)). The simplified block diagram of the LTE downlink physical layer is shown in Figure 2.4.

Each block of data, received from the upper layer (MAC layer) (See Figures 2.2 and 2.3) is first protected against transmission errors, usually first with Cyclic Redundancy Check (CRC). Then using Turbo codes, the block of data is coded to form a *codeword* (CW). After

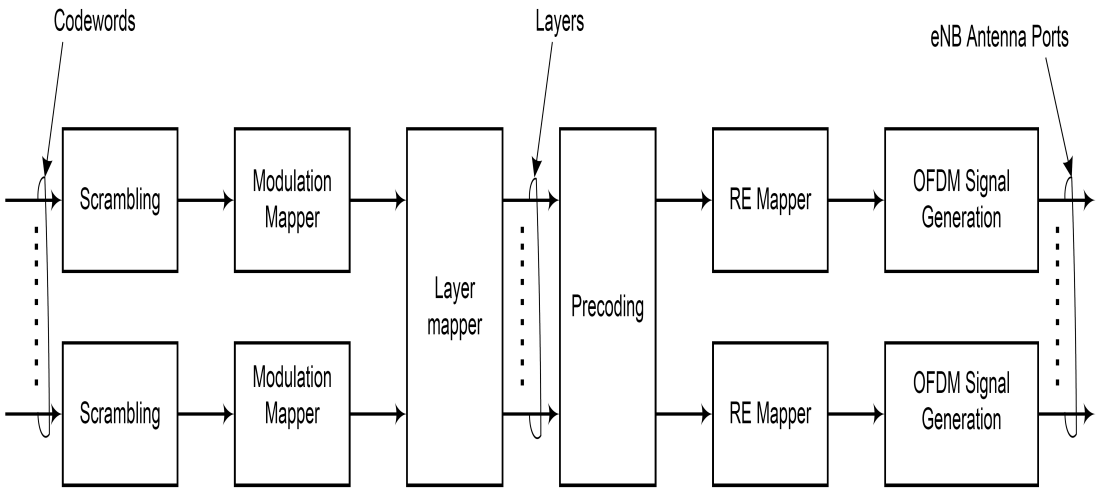

Figure 2.4 LTE downlink Physical Layer Block Diagram.

channel coding, an initial step of scrambling is applied to the physical channel, and serves the purpose of interference rejection. The scrambling task is performed using an order 31 Gold code, that can provide 2^{31} sequences with no cyclic shifts. The attractive feature of Gold codes is that they can be generated with very low implementation complexity, as they can be derived from the modulo-2 addition of two maximum length sequences, which can be generated by a simple shift register. Following the scrambling operation, the transmitted data bits are mapped into modulated complex value symbols depending on the modulation scheme which is used. After modulation task, a layer mapping is applied to the modulated codewords (CW). In LTE, a layer mapper maps the modulated symbols belonging to either 1 or 2 codewords into a number of layers less or equal to the number of *antennas ports*. In LTE, *antenna port* is a new term used to differentiate with the *physical antenna*. Usually, antenna ports map into physical antenna elements. A more formal definition of antenna port will be given later in this chapter. An operation of precoding follows the layer mapping, which consists of applying coding to the layers of modulated symbols prior to mapping onto Resource Element (RE). The concept of Resource Element will be explained later in section 2.3. The final stage of the LTE block diagram is the transformation of the complex modulated symbols at the output of RE mapper into a complex valued OFDM signal by means of an Inverse Fast Fourier Transform (IFFT).

As indicated in Figure 2.4, the LTE downlink transmission is based on Orthogonal Frequency Division Multiplexing Access (OFDMA). OFDMA is known as a technique of encoding digital data on multiple carrier frequencies. The principle of OFDMA is to convert a wide band frequency-selective channel into a set of many flat-fading subchannels using optimum receivers that can be implemented with a reasonable system complexity, in contrast

to WCDMA systems. Another important advantage of OFDMA is the easy frequency domain scheduling, typically by assigning only good channels (i.e., channels with high SNRs) to the users. It is well known that OFDMA is an efficient technique to improve the spectral efficiency of wireless systems [38]. By converting the wide-band frequency-selective channel into a set of several flat fading sub-channels, OFDM becomes more resistant to frequency selective fading than single carrier systems. Since OFDM signals are in time and frequency domains, in addition to the use of time domain scheduling, a frequency domain scheduling can also be used. The role of the user scheduler at the transmitter side is to assign the data rate for each user according to the channel conditions from the serving cell, the interference level from other cells, and the noise level at the receiver side. It has been proven [43] that in LTE, for a given transmission power, the system data throughput and the coverage area can be optimized by employing Adaptive Modulation and Coding (AMC) techniques.

2.3 LTE Frame Structure

Two types of LTE frame structures are defined depending on the duplexing mode of the transmission. Two duplexing methods are defined in LTE, namely Time Division Duplex (TDD) and Frequency Division Duplex (FDD). In the FDD mode, the downlink path (DL), from the eNodeB to UE, and the uplink path (UL), from the UE to eNodeB, operate on different carrier frequencies. In the TDD mode, the downlink and the uplink paths operate on the same carrier frequency but in different time slots. In other word, in FDD, the downlink and uplink transmissions are separated in the frequency domain, whereas in TDD the downlink and uplink transmissions are separated in the time domain. The Type 1 frame structure of LTE is associated with the FDD duplexing mode whereas the Type 2 frame structure of LTE is associated with the TDD duplexing mode. For both types of LTE frame structure, the DL and UL transmissions in LTE systems are arranged into radio frames. The duration of a radio frame is fixed at 10 ms. The radio frame is comprised of ten 1ms subframes, which represent the shortest Transmission Time Interval (TTI). Each subframe consists of two slots of duration 0.5 ms. The Type 1 LTE FDD frame structure is shown in Figure 2.5. In case of Type 2 TDD frame structure, as shown in Figure 2.6, each radio frame consists of 2 half frames of 5 subframes each. Subframes can be either uplink subframes, downlink subframes or special subframes. Special subframes include the following fields: Downlink Pilot Time Slot (DwPTS) and Uplink Pilot Time Slot (UpPTS).

Depending on the length of the Cyclic Prefix (CP) and the subcarriers spacing, each time slot consists of 6 or 7 OFDM symbols. In fact, the cyclic prefix represents a guard period at the beginning of each OFDM symbol which provides protection against multi-path delay

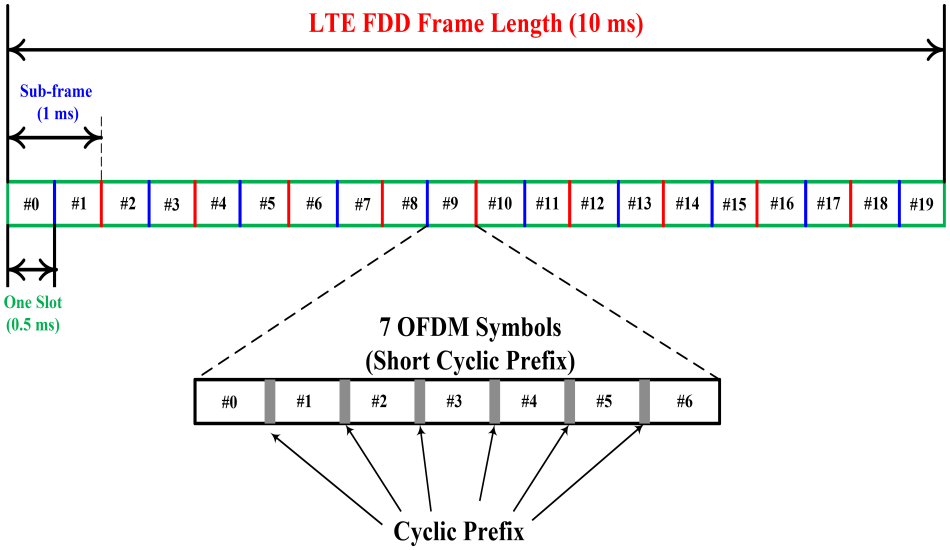

Figure 2.5 Type 1 LTE FDD Frame Structure.

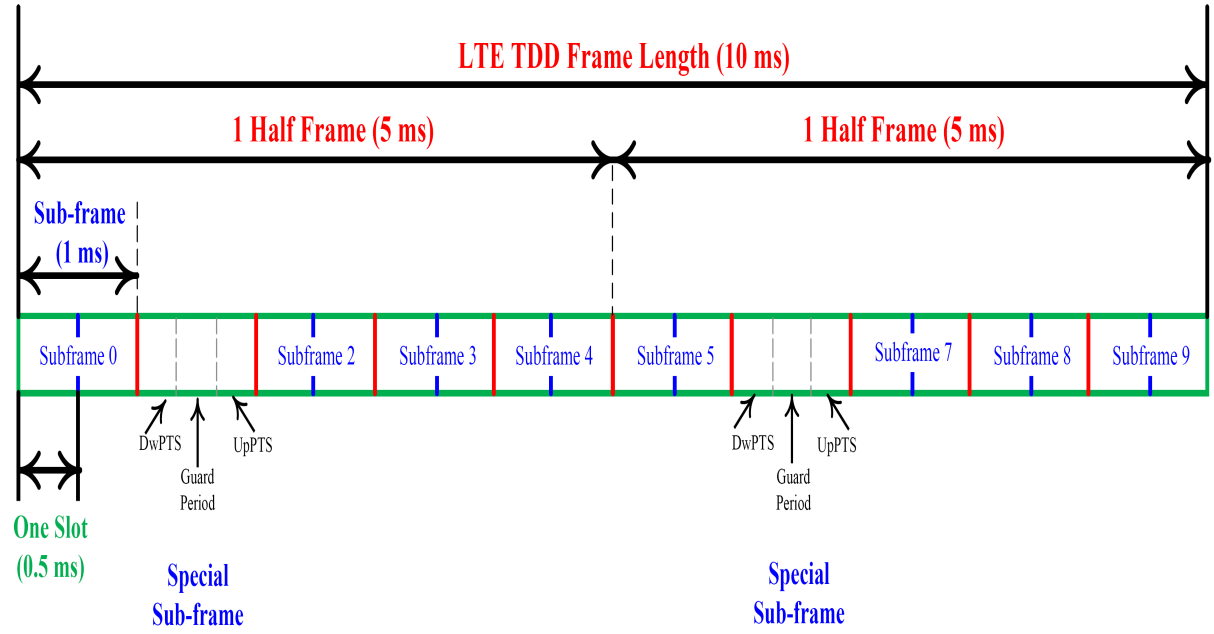

Figure 2.6 Type 2 LTE TDD Frame Structure.

spread. To effectively combat the delay spread of the channel, the duration of the cyclic prefix should be greater than the duration of the multi-path delay spread. At the same time, cyclic prefix also represents an overhead which should be minimized. Two types of CP were specified in LTE, namely the normal CP and the extended CP. The structure of the symbols in a 0.5 ms slot with normal cyclic prefix is shown in Figure 2.7. In normal CP, each slot

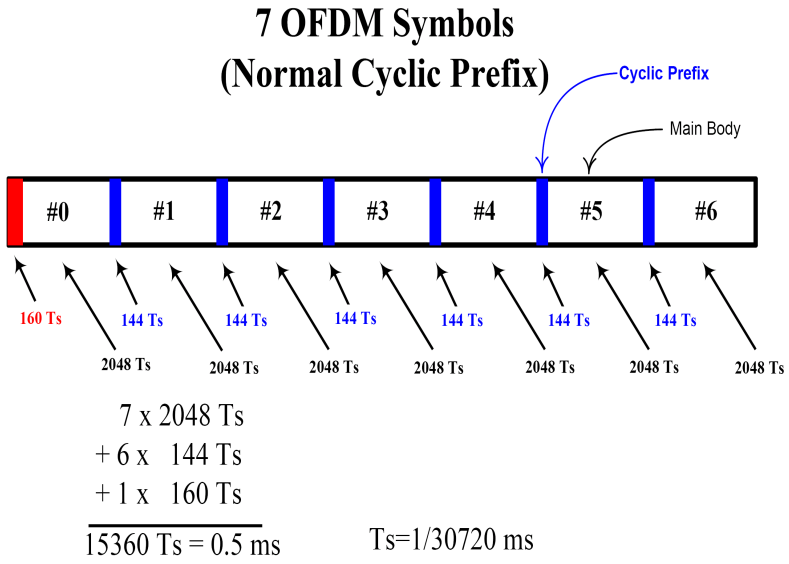

Figure 2.7 Structure of the symbols in one slot with Normal Cyclic Prefix.

consists of 7 OFDM symbols, however, with extended CP (see Figure 2.7) only 6 OFDM symbols constitute one slot as shown in Figure 2.8. The duration of the first cyclic prefix and the subsequent prefixes in terms of sampling time (T_s) are also shown in Figure 2.8. T_s represents the basic time unit and is given by $Ts = 1/(15000 \times 2048)$ seconds. It can be noticed that the duration of the first cyclic prefix is larger than the subsequent cyclic prefixes. For the normal cyclic prefix the duration of the first cyclic prefix is defined as $(160 \times T_s)$, whereas the subsequent cyclic prefixes the duration is only $(144 \times T_s)$. For extended cyclic prefix, all prefixes have the same length which is equal to $512 \times T_s$. The normal cyclic prefix length is proposed to be sufficient for the majority of radio environment scenarios, while the extended cyclic prefix is intended for radio environment with particularly high delay spreads. The cyclic prefix is generated by copying the end of the main body of the OFDM symbol.

Now, we explain how OFDM signal is generated. An OFDM symbol is based on the Inverse Fast Fourier Transform (IFFT), which is an operation of a transformation from frequency domain to time domain. Accordingly, the transmitted signal (the input signal to the OFDM block in Figure 2.4) is defined in the frequency domain. This means that the complex modulated symbols are considered as the coefficients in the frequency domain. The block diagram of an OFDM system is shown in Figure 2.9. The serial input data symbols (modulated synbbols) are firstly converted into a block of parallel complex $\mathbf{S}[k] = [S_0[k],\ S_1[k],\ S_2[k], ...,\ S_{M-1}[k]]^T$ of dimension, where k is the index of an OFDM symbol containing M subcarriers. The M parallel data streams are first independently modulated (e.g. QPSK or M-QAM modulation) to form a vector of complex modulated symbols $\mathbf{X}[k] = [X_0[k],\ X_1[k],\ X_2[k], ...,\ X_{M-1}[k]]^T$.

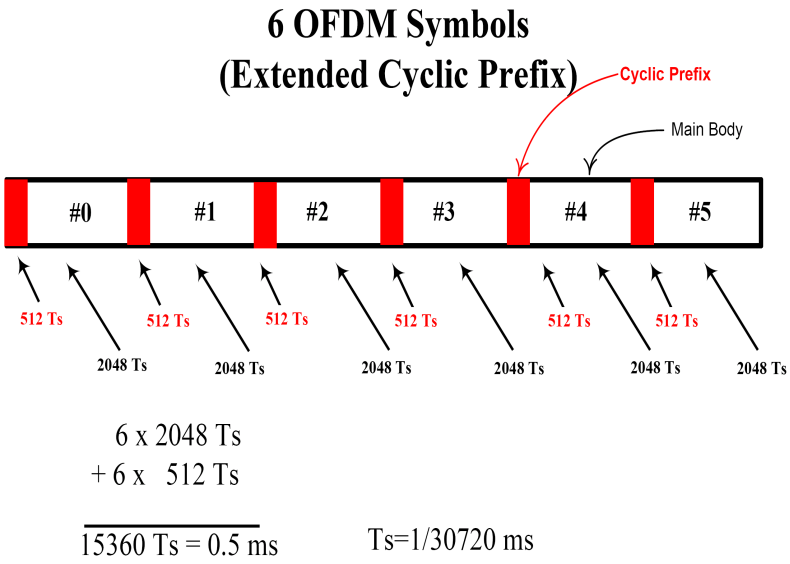

Figure 2.8 Structure of the symbols in one slot with Extended Cyclic Prefix.

The $\mathbf{X}[k]$ vector is then applied to the input of an N-point Inverse Fast Fourier Transform (IFFT). The output of this operation is a set of N complex time-domain samples $\mathbf{x}[k] = [x_o[k],\ x_1[k],\ x_2[k], ...,\ x_{N-1}[k]]^T$. It is worth noting that in practical implementation of an OFDM system, the number of the points used by IFFT (N) is greater than the number of the modulated subcarriers (M) (i.e., $N \geq M$). As shown in Figure 2.9, the un-modulated subcarriers are being padded with zeros. The next important operation in the geenration of an OFDM signal is the creation of a guard period at the beginning of each OFDM symbol $\mathbf{x}$[k] by adding a Cyclic Prefix (CP). This CP is simply generated by taking the last $\mathbf{G}$ samples of the IFFT output and appending them at the beginning of $\mathbf{x}$[k]. This yields the OFDM symbol in time domain as: $[x_{N-G}[k],\ ...,\ x_{N-1}[k],\ x_0[k],\ x_1[k],\ x_2[k], ...,\ x_{N-1}[k]]$ as shown in Figure 2.9. The last step in the OFDM signal generation is the parallel to serial conversion of the IFFT output for transmissions through the radio interface.

The results of the OFDM operation in LTE is that the output signal now possesses two domains; the frequency domain and the time domain. The frequency domain is represented by successive subcarriers and the time domain is represented by successive OFDM symbols. In LTE, the bandwidth of a subcarrier is defined to be 15 KHz or 7.5 KHz. In the frequency domain, resources are grouped in units of 12 subcarriers. Thus, for a subcarrier spacing of 15 KHz, 12 subcarriers occupy a total of 180 KHz. The combination of 12 subcarriers in one slot (7 OFDM symbol) form what is called *Resource Block* (RB). The smallest of resource is called *Resource Element* (RE), which consists of one subcarrier for a duration of one OFDM Symbol. The structure of Resource Block for 15 KHz subcarrier spacing and its constituting

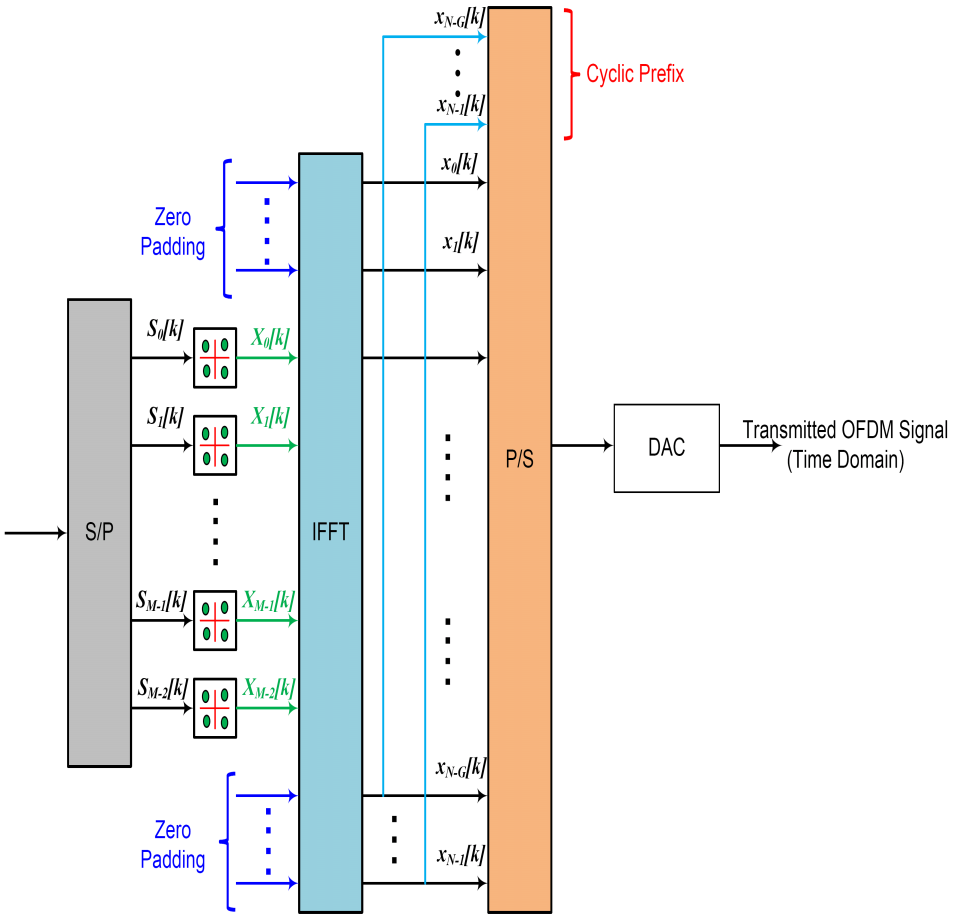

Figure 2.9 OFDM Signal Generation.

REs are shown in Figure 2.10 for illustration.

The number of RB in the frequency domain (N_{DL}^{RB} in Figure 2.10) depends on the transmission bandwidth. LTE is designed as a scalable system where the channel bandwidth is flexible. In fact, the standard defines six channel bandwidths. The possible channel bandwidth as defined in LTE for 15 KHz subcarriers spacing is shown in Table 2.1. The number of IFFT size is also shown in Table 2.1. For example in a 5 MHz bandwitdh, the IFFT size is set to 512 but the number of the used subcarriers is only 300, which represent 25 RB of 12 subcarriers each.

So far, we showed how the signal is generated to be sent over the radio interface. But how the data is organized and what kind of information are transmitted? In LTE, the physical layer receives different data types from the higher layer (MAC layer) which are organized in the form of different channels, called *Transport Channels*. The MAC layer itself receives data from the RLC layer in the form of *Logical channels*. Before sending the transport channels

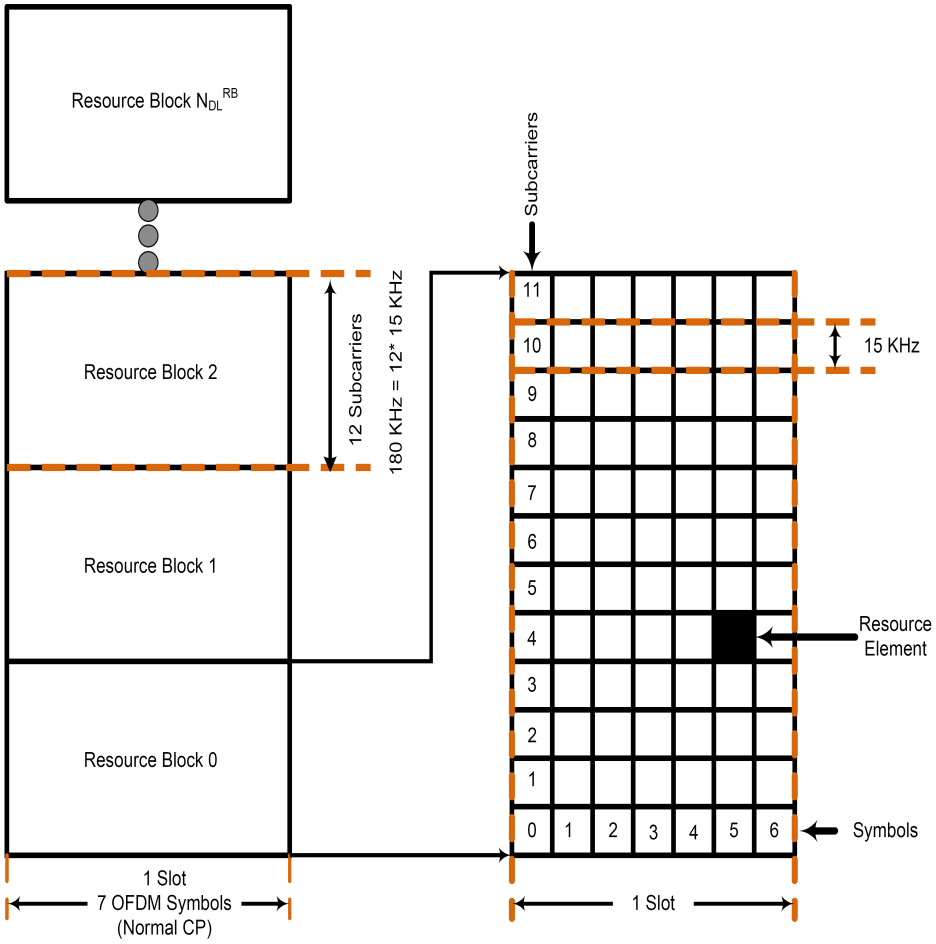

Figure 2.10 LTE Resource Block.

Table 2.1 Resource Block as a function of Channel Bandwidth

Channel Bandwidth	1.4 MHz	3 MHz	5 MHz	10 MHz	15 MHz	20 MHz
Resource Blocks in the frequency domain	6	15	25	50	75	100
FFT Size (N)	128	256	512	1024	1536	2048
Subcarriers in the frequency domain (M)	72	180	300	600	900	1200
Total Subcarriers badwidth (MHz)	1.095	2.715	4.515	9.015	13.515	18.015

into the air, the physical layer process the transport channels to form *Physical Channels*. In addition to the physical channels, the physical layer needs to create its own signals to be sent over the air. The signal generated in the physical layer are called *Physical Signals*. The principle of channels generation and their placement with respect to different layers in LTE is illustrated in Figure 2.11.

As indicated in Figure 2.11, we distinguish three types of physical signals and six types

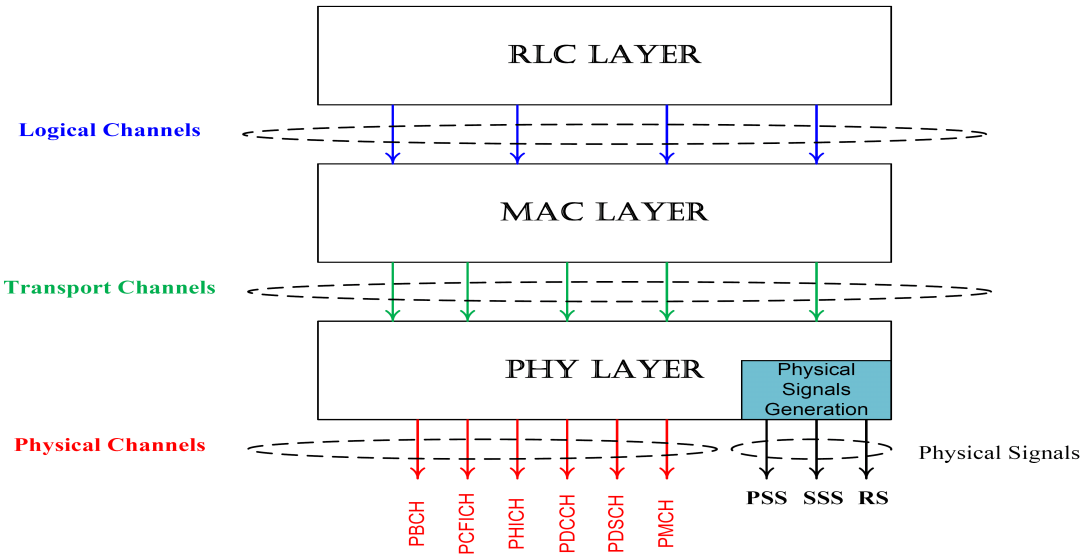

Figure 2.11 Physical Channels and Physical Signals in LTE.

of physical channels in LTE and they are defined as follow:

Downlink Physical Signals: Three different physical signals are generated in the physical layer:

1. Primary Synchronization Signal (PSS)
2. Secondary Synchronization Signal (SSS)
3. Reference Signals (RS)

PSS and SSS are the synchronization signals, used by the UE to achieve radio frame, subframe, slot and symbol synchronization in the time domain as well as the identification of the center of the channel bandwidth in the frequency domain. The reference signals (RS) on the other hand are used for channel estimation purposes and to support channel quality indicator (CQI) reporting and demodulation. They can also be used to support channel quality measurements for handover purposes.

Downlink Physical Channels: To carry the information blocks (data) received from the MAC and higher layers, the number of downlink physical channels are defined in LTE. In total, six physical downlink channels are defined in LTE as follow:

1. Physical Broadcast Channel (PBCH)
2. Physical Control Format Indicator Channel (PCFICH)
3. Physical Hybrid ARQ Indicator Channel (PHICH)

4. Physical Downlink Control Channel (PDCCH)
5. Physical Downlink Shared Channel (PDSCH)
6. Physical Multicast Channel (PMCH)

The PBCH channel is used to broadcast the master information block (MIB) using transport and logical channels from higher layers (MAC and RLC layers). The PBCH is allocated the central 72 subcarriers belonging to the first 4 OFDM symbols of the second time slot of every 10 ms radio frame, which corresponds to 240 resource elements (RE) excluding the resource elements used by the RS $((72\times4)-48)$, where 48 is the number of resource elements allocated to the Reference Signal. The PCFICH is used at the start of each 1 ms downlink subframe to signal the number of symbols used for the PDCCH. The PHICH is used to signal positive or negative acknowledgment for uplink data transferred on the uplink channel. To transfer the downlink control information, LTE uses the PDCCH channel. The PDSCH is the main data downlink channel in LTE. It is used for all user data. In addition to the user data, the system information and paging can also be sent with PDSCH channel. Finally, the PMCH is used to transfer the multimedia broadcast multicast service application data. More details about the use of each physical channel is given in [26] and [44]

2.4 MIMO-OFDM Schemes in LTE

Before explaining the MIMO-OFDM schemes as defined in LTE, we provide a brief theoretical background of the advantages promised by multiple antenna techniques in wireless communication systems. In this context, the first part of this section covers the different configurations of using multiple antennas and their corresponding advantages from theoretical point of view. In the second part, the MIMO schemes as defined in LTE will be explained and the practical issues that cause the gap between the theoretical predictions and practical performances of such systems will be discussed.

Traditional wireless communications systems with one antenna at the transmitter and one antenna at the receiver (Single-Input Single-Output (SISO)) exploit time and/or frequency domains pre-processing the transmitted signal and decode the received data. Adding additional antennas either at the transmitter or at the receiver creates an extra spatial dimension for signal coding and decoding processes. Hence, new areas of processing have emerged such as Space Time and Space frequency processing. Depending on the availability of additional antennas at the transmitter and/or at the receiver, such techniques are classified as Single Input Multi Output (SIMO), Multi Input Single Output (MISO) or Multi-Input Multi-output (MIMO). Thus, in the case of having multiple antenna at the base station and only one antenna at the user's equipment, the uplink (from user equipment to base station) is referred

to SIMO and the downlink (from base station to user equipment) is referred to MISO. It is worth noting that the term MIMO is sometimes also used in its widest sense, thus including SIMO and MISO as special cases.

When multiple antennas are available they can be used in different modes. Essentially, we can distinguish three different modes for multiple antennas, namely *beam-forming* mode, *diversity* mode (receive and transmit) and *multiplexing* mode. In beam-forming mode the advantage of using multiple antennas is evaluated by the so called Array gain. For diversity mode, the diversity gain is usually used to evaluate the advantage of this mode. Finally, the multiplexing gain is the benefit of using multiplexing mode. The principles of each mode and their advantages are described and explained in the following subsection:

2.4.1 Array Gain

The first approach of using multiple antennas is to send or to receive the same signals on all the antennas. In case of multiple receive antennas, a coherent combining techniques can be realized through spatial processing at the receive antennas side. In case of multiple transmit antennas, the coherent combining can be realized through spatial processing at the transmit antennas side. An example of receive coherent combining is the Maximum Ratio Combining (MRC) method and an example of transmit coherent combining is the concentration of energy in one or more directions, the so called beam-forming. In both cases, the results of combining will be reflected in an improvement of average SNR which is represented by an Array gain, also known as beam-forming gain. The array gain can be defined as the increase of the average SNR. In case of MRC, it can be shown that the array gain is constant and is equal to the number of antennas. To illustrate this, we should determine the combined SNR for a MRC system. To this end, let‘s suppose a MRC system with N_r branches (from one transmit antenna to N_r receive antennas).

2.4.2 Diversity Gain

For improving the communication reliability and reducing the sensitivity to the fading channel, we can send or receive the same signal on different antennas. By increasing the number of independent copies of the transmitted signal, the probabilities that at least one of the signals is not experiencing a deep fade increase and hence improving the quality and reliability of reception. This kind of transmissions is known as *Diversity Mode* and the associated gain is known as *Diversity Gain*. In other words, diversity gain corresponds to the mitigation of the effects of multipath fading, by means of transmitting or receiving over multiple antennas in which the fading is sufficiently de-correlated. The Diversity Gain can

be described either in terms of order, which represents the number of effective independently diversity branches or in terms of the slope of the Bit Error Rate curve as a function of the signal to noise ratio at high SNRs.

2.4.3 Multiplexing Gain

Multiple antennas can be used to send different signals on different antennas. The original high data rate signal is first divided into two low data rate signals and each signal is sent from different antennas. In the receiver side, the different signals are processed separately and multiplexed to recover the original high data rate signal. This method is known as Multiplexing mode and the associated gain is the Spatial Multiplexing gain. To evaluate this multiplexing gain, we use to the basics of shannon theory of capacity and spectral efficiency calculations. To this end, in the case of single antenna system (SISO), the data rate calculation is related to the Shannon capacity formula which yields the maximum achievable data rate of a single communication link in Additive White Gaussian Noise (AWGN) channel as [7]:

$$C = B \log_2(1 + \gamma) \tag{2.1}$$

where C is the capacity, or maximum error free data rate; B is the bandwidth of the channel; and γ is the channel SNR. Since antennas diversity can increase the SNR linearly, diversity techniques can increase the capacity but in a *logarithmic* way with respect to the number of antennas. In other words, as the number of antennas increases, the data rate improvement rapidly diminishes. However, it can be concluded from the above equation that when the SNR is low, the capacity can increase linearly with SNR, since $\log(1 + x) \approx x$ for small x [7]. The goal of multiplexing mode is to get more substantial data rate increase at high SNRs and to achieve this goal, the multiple antennas are used to send multiple independent signals. Therefore, the multiplexing mode has the ability to achieve a linear increase in the data rate with the number of antennas at moderate to high SNRs through the use of sophisticated signal processing algorithms. Specifically, it is shown that the capacity can be increased as a multiple of $min(N_t, N_r)$ [7]. The capacity improvement is limited by the minimum of the number of antennas at either the transmitter or the receiver. As an example, a single user MIMO communications between a base station with four antennas and a user equipment with two antennas can support multiplexing of two data signals (also called data stream), and therefore doubling the data rate of the user equipment compared with a single antenna case. To achieve this maximum multiplexing gain, the different subchannels should experience different and de-correlated responses. In ideal case, in high SNR regions and in

rich scattering environments, the multiplexing gain will be equal to two. However in a real environment, a lower value of multiplexing gain can be observed.

Before describing the multiple antenna schemes in LTE, some terminology should be explained. Especially, four main terminologies have been introduced and are widely used in LTE, namely the *Antenna ports*; *spatial layer*; the *rank* and the *codeword*.

– *Antenna ports*: In LTE, the concept of antenna ports is used and should not be confused with the physical antenna elements. In fact, antenna ports are mapped into physical antenna elements. A downlink antenna port is defined by its associated Reference Signal. For example, antenna port 0 is associated with a cell specific Reference Signal, whereas antenna port 6 is associated with a positioning Reference Signal. The complete set of downlink antenna ports and their associated Reference Signals can be found in the Table 2.2:

Table 2.2 Antenna ports and their associated Reference Signals

Antenna Port	3GPP Release	Reference Signal
0 to 3	8	Cell Specific Reference Signal
4	8	MBSFN Reference Signal
5	8	UE Specific Reference Signal
6	9	Positioning Reference Signal
7 to 8	9	UE Specific Reference Signals
9 to 14	10	UE Specific Reference Signals
15 to 22	10	CSI Reference Signals

– *Spatial Layer*: In LTE, this term is used for one of different streams generated by spatial multiplexing. A layer can be described as a mapping of symbols into the transmit antenna ports. This operation is known as layer mapping where the modulated symbols are mapped into a number of layers where the number of layers are equal to the number of antenna ports.
– The *Rank* of the transmission is equal to the number of transmitted layers
– A *CodeWord* (CW) corresponds to a single Transport Block (TB) and it is an independently encoded data block delivered from the Medium Access (MAC) layer, and protected by a CRC.

Note that the number of codewords is always less than or equal to the number of layers, which in turn is always less than or equal to the number of antenna ports. For a rank greater than one, two codewords can be transmitted.

Based on the above mentioned theoretical background and terminologies, the MIMO schemes adopted for LTE Release 8 and 9 can be reviewed and explained. These schemes

relate to the downlink unless otherwise stated.

2.4.4 Diversity Schemes in LTE

In LTE, two main transmit diversity schemes are employed; the first one with 2 transmit antennas and the second one with 4 transmit antennas. Both schemes use only one data stream (one signal). In LTE, one data signal (also called data *stream*) is referred as one *codeword* because only one transport block (TB) is used per data stream. The transport block itself is defined as the unit of transmitted data and it corresponds to the Medium Access Control (MAC) layer Protocol Data Unit (PDU). The Transport Block unit can be passed from the MAC layer to the physical layer once per Transmission Time Interval (TTI), where a TTI is fixed to 1 ms, corresponding to the duration of one subframe as described in the LTE frame structure section. In order to ensure uncorrelated channels between different antennas and hence maximizing the diversity gain, the antennas should be well separated relative to the wavelength. The use of different antenna polarization is another approach that has demonstrate its efficiency in order to guarantee uncorrelated antennas. If a physical channel in LTE is configured for transmit diversity operation using two eNodeB antennas, the diversity scheme is called Space Frequency Block Codes (SFBC). The principle of operation of SFBC transmission is shown in Figure 2.12. As can be seen from Figure 2.12, the SFBC

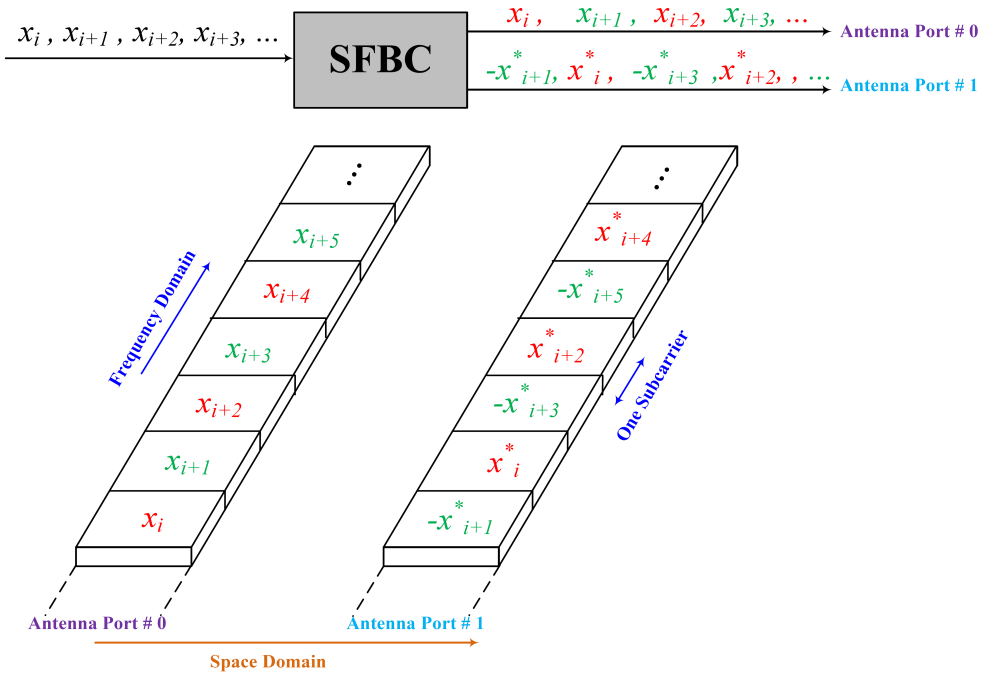

Figure 2.12 Space Frequency Block Coding (SFBC) Scheme in LTE

diversity scheme is, in fact, exactly the frequency domain of the well known Space Time Block Codes (STBC), developed by Alamouti [5]. The fundamental characteristic of this family of code is that the transmitted diversity streams are orthogonal and they can be simply decoded using a linear receiver. It is worth noting that the STBC is already used in UMTS and it operates on pairs of adjacent symbols in the time domain. In LTE, however, the number of available OFDM symbols in a subframe is often an odd number, and hence the application of STBC is therefore not straight forward for LTE. Instead of adjacent symbols in the time domain, in LTE the diversity scheme operates on pairs of adjacent subcarriers, leading to a SFBC.

For SFBC transmission, the transmitted symbols from two eNodeB antenna ports on each pair of adjacent subcarriers are defined as follow [44]:

$$\begin{bmatrix} y^{(0)}(1) & y^{(0)}(2) \\ y^{(1)}(1) & y^{(1)}(2) \end{bmatrix} = \begin{bmatrix} x_1 & x_2 \\ -x_2^* & x_1^* \end{bmatrix} \tag{2.2}$$

where $y^{(p)}(k)$ denotes the symbols transmitted on the k^{th} subcarrier from antenna port p.

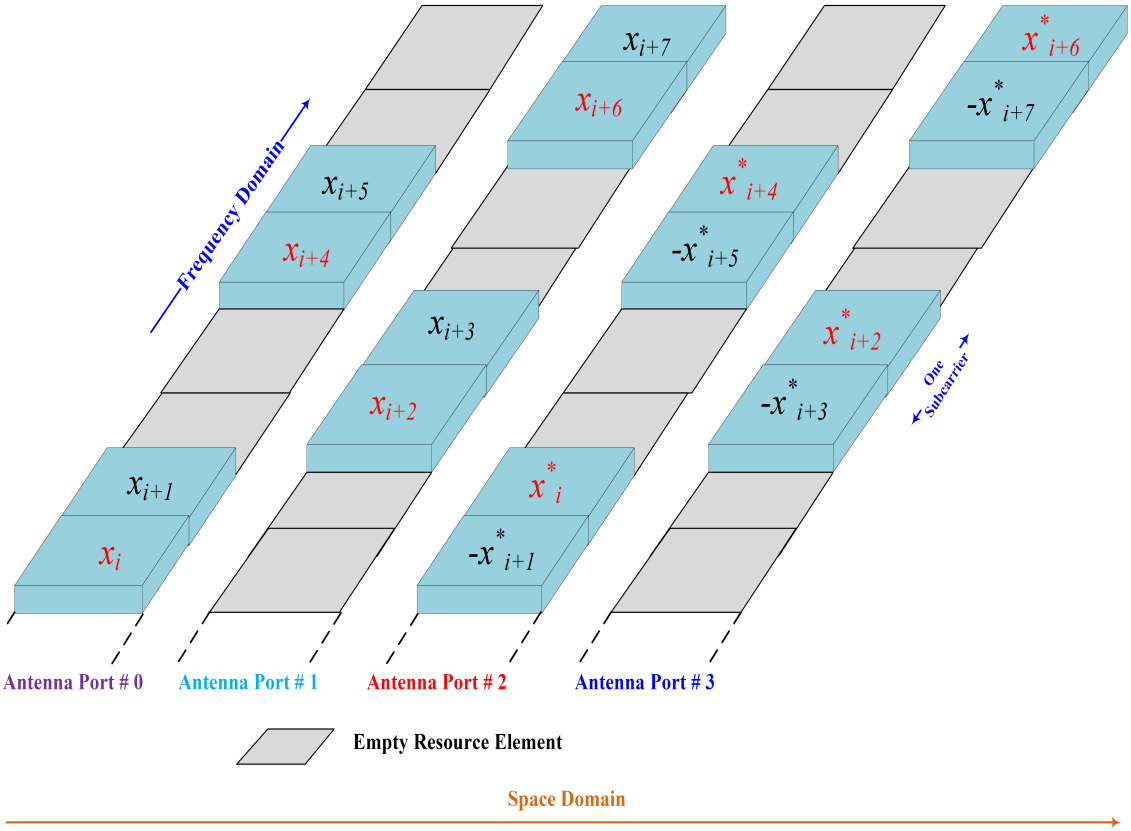

Figure 2.13 Frequency Switched Transmit Diversity (FSTD) Scheme in LTE

In matrix form, the transmitted space frequency block matrix can be generated as follows:

$$\begin{bmatrix} y^{(0)}(1) \\ y^{(0)}(2) \\ y^{(1)}(1) \\ y^{(1)}(2) \end{bmatrix} = \frac{1}{\sqrt{2}} \begin{bmatrix} 1 & 0 & i & 0 \\ 0 & 1 & 0 & i \\ 0 & -1 & 0 & i \\ 1 & 0 & -i & 0 \end{bmatrix} \begin{bmatrix} \Re\{x_1\} \\ \Re\{x_2\} \\ \Im\{x_1\} \\ \Im\{x_2\} \end{bmatrix} \tag{2.3}$$

In case of four transmit antennas (antennas port 0 to 3) and in order to keep the orthogonality of the code, the diversity scheme is simply a combination of SFBC scheme and Frequency Switched Transmit Diversity (FSTD) [44]. FSTD implies that a pair of modulated symbols are transmitted using SFBC scheme with two antennas whereas the other two antennas are not transmitting. In other words, in FSTD, the transmission is alternated between a pair of transmit antennas. This means that the first two symbols are transmitted on the antennas 0 and antenna 2, whereas nothing is transmitted on antennas ports 1 and 3. For the next two symbols, the antennas port 1 and 3 are used for transmission whereas antenna port 0 and 2 are not transmitting. The principle of FSTD diversity scheme is shown in Figure 2.13.The transmission matrix of the FSTD scheme can be then described as follow:

$$\begin{bmatrix} y^{(0)}(1) & y^{(0)}(2) & y^{(0)}(3) & y^{(0)}(4) \\ y^{(1)}(1) & y^{(1)}(2) & y^{(1)}(3) & y^{(1)}(4) \\ y^{(2)}(1) & y^{(2)}(2) & y^{(2)}(3) & y^{(2)}(4) \\ y^{(3)}(1) & y^{(3)}(2) & y^{(3)}(3) & y^{(3)}(4) \end{bmatrix} = \begin{bmatrix} x_1 & x_2 & 0 & 0 \\ 0 & 0 & x_3 & x_4 \\ -x_2^* & x_1^* & 0 & 0 \\ 0 & 0 & -x_4^* & x_3^* \end{bmatrix} \tag{2.4}$$

where, as previously, $y^{(p)}(k)$ denotes the symbols transmitted on the k^{th} subcarrier from antenna port p. This space frequency code is known as Frequency Switched Transmit Diversity (FSTD). It can be noticed form the code matrix that on each subcarrier slot, only two antennas are transmitting. For the first subcarrier slot, the antennas ports 1 and 2 are not transmitting any signals. We will show in the performance analysis in Chapter 3 that this scheme is equivalent to the 2×2 scheme.

2.4.5 Spatial Multiplexing Schemes in LTE

In LTE, a spatial multiplexing mode can either use a single codeword mapped to all the available layers, or two codewords each mapped to one or more different layers. The main advantage of using only one codeword is a decrease in the amount of control signaling required, both for Channel Quality Indicator (CQI) reporting and for HARQ ACK/NACK feedback. In fact, in case of one single codeword, a single value of CQI is needed for all layers

and only one ACK/NACK would have to be signaled per subframe per user equipment (UE). In the case of using two codewords, more control signaling will be required but the advantage of such mapping is that significant multiplexing gain can be possible by using Minimum Mean Square Error and Successive Interference Cancelation (MMSE-SIC) receiver. The codeword to layer mapping are shown in the Table 2.3 [44]:

Table 2.3 Codewords-to-layer Mapping in LTE

Transmission Rank	Codeword 1	Codeword 2
Rank 1	Layer 1	
Rank 2	Layer 1	Layer 2
Rank 3	Layer 1	Layer 2 and Layer 3
Rank 4	Layer 1 and layer 2	Layer 3 and layer 4

Depending on the availability of feed back from the user equipment, two modes of spatial multiplexing were defined in LTE, namely the open loop spatial multiplexing and the closed loop spatial multiplexing modes. The open loop spatial multiplexing mode was introduced in release 8 version of the 3GPP specification and it has not changed within the release 9 and 10 versions of specification. In open loop approach, the UE provides feedback to eNodeB in terms of Rank Indicator (RI) and Channel Quality Indicator (CQI). The RI feedback provides information about the suggested number of layers whereas the CQI provides information about the transport block size. In addition to the RI and CQI feedback, the closed loop spatial multiplexing provides an additional feedback in terms of Precoding Matrix Indicator. The precoding matrix, selected from a defined codebook, is used to form the transmitted layers. Each codebook consists of a set of predefined precoding matrices, with the size of the set being a tradeoff between the number of signaling bits required to indicate a particular matrix in the code book and the suitability of the resulting transmitted beam direction. The difference between open loop and closed loop is that in open loop the UE does not provide any information about the precoding matrix and it is generated independently, whereas in closed loop the precoding matrix is suggested by the UE. In case of two antenna ports, the 2×2 spatial multiplexing always transfers 2 codewords using 2 layers during each subframe see Table 2.4 [26].

For the case of 4 antennas ports, one or two codewords can be transferred during each subframe. Table 2.5 summarizes the number of codewords and layers which are supported by a 4×4 open loop spatial multiplexing.

Table 2.4 Codewords, layers and antenna ports for 2×2 open loop spatial multiplexing.

Number of Codewords	Number of Layers	Number of Antenna Ports
2	2	2

Table 2.5 Codewords, layers and antenna ports for 4x4 open loop spatial multiplexing.

Number of Codewords	Number of Layers	Number of antennas ports
1	2	4
2	2	
	3	
	4	

In open loop spatial multiplexing, instead of sending only two different signals, an additional precoding operation is applied to the transmitted signals before being transmitted onto the radio interface. The precoding scheme adopted for LTE is the so-called Large Delay Cyclic Delay Diversity (CDD). It should be noted that CDD is not used in LTE as an exact diversity scheme, as its name stipulate, but rather as a precoding scheme for spatial multiplexing mode and that is why it was not introduced in the diversity schemes section. This CDD precoding is defined using the following equation [26]:

$$\begin{bmatrix} y^{(0)}(i) \\ . \\ . \\ . \\ y^{(P-1)}(i) \end{bmatrix} = W(i) \times D(i) \times U \times \begin{bmatrix} x^{(0)}(i) \\ . \\ . \\ . \\ x^{(v-1)}(i) \end{bmatrix} \tag{2.5}$$

where P is the number of output antenna ports, i is the sample number and v is the number of input layers. It is worth noting that the precoding multiplication is a function of the sample number 'i' but only the elements within the matrix U are not a function of the sample number 'i'. To illustrate the principle of coding, let's have a closed look to the case of two transmit antennas and two receive antennas as shown in Figure 2.14. For 2×2 open loop spatial multiplexing, 3GPP specifies the $W(i)$; $D(i)$ and U matrix as [26]:

$$W(i) = \frac{1}{\sqrt{2}} \begin{bmatrix} 1 & 0 \\ 0 & 1 \end{bmatrix} \tag{2.6}$$

$$D(i) = \begin{bmatrix} 1 & 0 \\ 0 & e^{-j(\pi)i} \end{bmatrix} \tag{2.7}$$

$$U = \frac{1}{\sqrt{2}} \begin{bmatrix} 1 & 0 \\ 1 & e^{-j(\pi)} \end{bmatrix} \tag{2.8}$$

It can be noticed that the matrix W in case of 2×2 open loop scheme is fixed and is not actually a function of 'i'. The transmitted signal is then obtained by the product of $W(i)$, $D(i)$ and U as [26]:

$$W(i) \times D(i) \times U = \frac{1}{\sqrt{2}} \begin{bmatrix} 1 & 0 \\ 0 & 1 \end{bmatrix} \times \begin{bmatrix} 1 & 0 \\ 0 & e^{-j(\pi)i} \end{bmatrix} \times \frac{1}{\sqrt{2}} \begin{bmatrix} 1 & 0 \\ 1 & e^{-j(\pi)} \end{bmatrix} \tag{2.9}$$

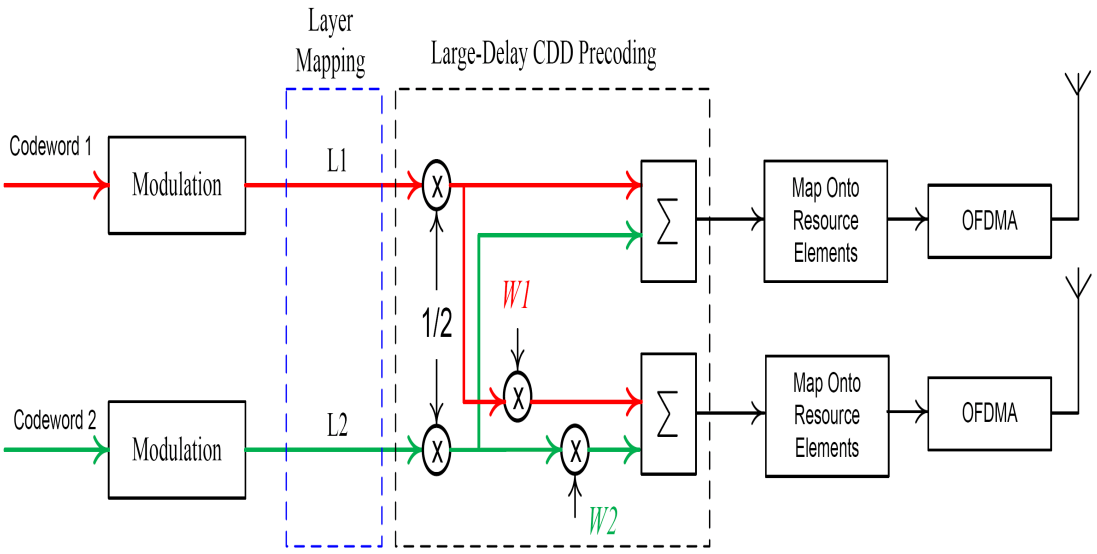

Figure 2.14 2×2 Open Loop Spatial Multiplexing with Large-Delay CDD Precoding.

The results of 2.9 depends on the indices 'i' of transmitted symbols and hence two different results are possible, one for odd number and one for even number. For the odd number of 'i', is then:

$$W(i) \times D(i) \times U = \frac{1}{2} \begin{bmatrix} 1 & 1 \\ 1 & -1 \end{bmatrix} \tag{2.10}$$

For even number of 'i', the results is found to be:

$$W(i) \times D(i) \times U = \frac{1}{2} \begin{bmatrix} 1 & 1 \\ -1 & 1 \end{bmatrix} \tag{2.11}$$

The summary of the described layer mapping and precoding for the 2×2 open loop spatial multiplexing with two codewords is shown in Figure 2.14:

CHAPTER 3

PERFORMANCE EVALUATION OF MIMO SYSTEMS IN LTE

3.1 Introduction

Two main and fundamental key performance indicators which have bee used to evaluate the performance of the wireless communication systems are the Bit Error Rate (BER)[39], and the data throughput or its related channel capacity bound. For a system using one antenna at the transmitter and one antenna at the receiver and in non fading AWGN channel, the evaluation of the BER for most of the known modulation schemes is well known [39]. Using more antennas at the transmitter and at the receiver and also in more realistic fading channel models, such as Rayleigh, Rician and Nakagami, the evaluation becomes more complex and necessitates the use and the development of advanced mathematical tools. In this context, the theory of BER evaluation had experienced an important evolution during the past decade. Initially, the evaluation of the BER performance was based on a classical approach where the Gaussian Q-function (also known as Gaussian Probability Integral) was used (Chapter 4 in [6]). However, this classical approach suffers from two main disadvantages when extended to more general complex channels especially those experiencing fading. The first disadvantage is related to the upper infinite limit where it requires a truncation in case of numerical evaluation. The second and more significant disadvantage is related to the presence of the argument of the function as the lower limit of the integral. In general case, the lower limit in the integral depends on other random parameters and this dependency requires statistical averaging over their probability distribution which poses analytical difficulties. In other words, to evaluate the average error probability in the presence of fading channels, the Gaussian Q-function should be averaged over the fading amplitude distribution. To overcome the mentioned disadvantages, an alternative representation of the Gaussian Q-function has been developed and since then widely used for the evaluation of the BER (See Appendice B). In the alternative representation of the Q-function, the argument of the function is neither the upper nor the lower limit of the integral. Using the alternative representation of the Gaussian Q-function, the evaluation of the average error probability becomes a problem of evaluation of the integral of the Laplace transform of the probability density function of the SNR distribution, which represents the Moment Generation Function (MGF). This new approach of representation of the Q-function is particularly effective for evaluation of the average error probability of MIMO schemes where the probability density function of

the SNR has more complicated form like the N order Chi-squared distribution. In [29], the method of MGF was used to evaluate the BER of three phase relaying wireless system using the Alamouti STBC code [5]. Instead of using the alternative representation of the Gaussian Q-function, in [30], the Marcum Q-function was used to derive an approximate expression of BER analysis of Alamouti-MRC scheme with imperfect channel state information in Rician fading channel. In LTE the BER is mainly evaluated by simulation and to the best of our knowledge, the BER analysis is rarely treated in the literature. One of our goal is to develop in this thesis some closed form expressions of the BER for the main MIMO schemes as used in LTE.

To study the performance of LTE systems, a MATLAB based downlink physical layer simulator (Appendice C) for Link Level Simulation (LLS) has been developed in [32] [36]. A System Level Simulation of the Simulator is also available [25]. The main goal in developing the LTE simulator was to facilitate comparison with the work of different research groups and it became publicly available for free under academic non-commercial use license [36]. The main features of the simulator are adaptive coding and modulation, MIMO transmission and scheduling. As the simulator includes many physical layer features, it can be used for different applications in research [25]. In [47], the simulator was used to study the channel estimation of OFDM systems and the performance evaluation of a fast fading channel estimator was presented. In [42] and [41], a method for calculating the Precoding Matrix Indicator (PMI), the Rank Indicator (RI), and the Channel Quality Indicator (CQI) were studied and analyzed with the simulator.

The remainder of this chapter is organized in two main parts. The first part (i.e., section 3.2) is dedicated to the analysis of BER of the major MIMO schemes included in LTE. In subsection 3.2.1, we set up the system and channel model used in the simulation. In subsection 3.2.2, we present a performance analysis for the average BER of SFBC and FSTD MIMO schemes. The numerical and simulation results and discussions are presented in subsection 3.2.3. The second part of this chapter (i.e., section 3.3 and section 3.4) considers the capacity and data throughput evaluation. The capacity analysis is presented in section 3.3.2 followed by the data throughput evaluation in Section 3.4. The simulations results as well as the discussions of the obtained results are presented in subsection 3.4.1.

3.2 BER Analysis of LTE MIMO Schemes

3.2.1 System Model

In a MIMO system with N_r receive antennas and N_t transmit antennas, the relation between the received and the transmitted signals on OFDM subcarrier frequency k ($k \in 1, ..., N$), at sampling instant time n is given by

$$\mathbf{y}_{k,n} = \mathbf{H}_{k,n}\mathbf{x}_{k,n} + \mathbf{n}_{k,n} \tag{3.1}$$

where $\mathbf{y}_{k,n} \in C_{N_r \times 1}$ is the received output vector, $\mathbf{H}_{k,n} \in C_{N_r \times N_t}$ represents the channel matrix on subcarrier k at instant time n, $\mathbf{x}_{k,n} \in C_{N_t \times 1}$ is the transmit symbol vector and $\mathbf{n}_{k,n} \sim \mathcal{CN}(0, \sigma_n^2.\mathbf{I})$ is a white, complex valued Gaussian noise vector with variance σ_n^2 and $\mathbf{I}$ is an $N_r \times N_r$ identity matrix. Assuming perfect channel estimation, the channel matrix and noise variance are considered to be known at the receiver. A linear equalizer filter given by a matrix $\mathbf{F}_{k,n} \in C_{N_r \times N_r}$ is applied on the received symbol vector $\mathbf{y}_{k,n}$ to determine the post-equalization symbol vector $\mathbf{r}_{k,n}$ as follows [41]

$$\mathbf{r}_{k,n} = \mathbf{F}_{k,n}\mathbf{y}_{k,n} = \mathbf{F}_{k,n}\mathbf{H}_{k,n}\mathbf{x}_{k,n} + \mathbf{F}_{k,n}\mathbf{n}_{k,n}. \tag{3.2}$$

The Zero Forcing (ZF) or Minimum Mean Square Error (MMSE) design criterion are typically used for the linear receiver and the input signal vector is normalized to unit power [53]. In MIMO-OFDM systems, the key factor of link error prediction and performances is the signal to noise ratio (SNR) which represents the measurement for the channel quality information. In this study, the SNR is defined as follows [32]:

$$\gamma_{k,n} = \frac{\|\mathbf{H}_{k,n}\mathbf{x}_{k,n}\|_{\mathrm{F}}^2}{N_t\sigma_n^2} \tag{3.3}$$

where $\mathbf{x}_{k,n}$ is the transmitted symbol vector, $\|.\|_F^2$ is the squared Frobenius norm of a matrix.

3.2.2 Average BER Performance analysis for several M-QAM Schemes

In this section, a Bit Error Rate (BER) analysis is presented for Multiple-Input Multiple-Output (MIMO) schemes in the 3GPP Long Term Evolution (LTE) system. Analytical expressions for the average BER of the system are derived over flat Rayleigh fading channels for two different MIMO schemes as defined in LTE, assuming M-ary quadrature amplitude modulation (M-QAM) schemes and are evaluated numerically. The analysis is based on the probability density function of the instantaneous Signal to Noise Ratio and the Moment

generating function (Appendice C).

Analysis for 2×1 SFBC-OFDM Scheme

As described in Chapter 2, in LTE, the transmit diversity techniques are defined only for 2 and 4 transmit antennas and one data stream. When two eNodeB antennas are available for transmit diversity operation, the Space Frequency Block Code (SFBC) is used [43]. SFBC is based on the well known Space Time Block Code (STBC), derived by Alamouti for two transmit antennas [5]. STBC is employed with the UMTS and it operates on pairs of adjacent symbols in the time domain. Since the signal in LTE is a two dimensional signal (in time and frequency domains) and the number of available OFDM symbols in a subframe is not always an even number, the direct application of STBC is not straightforward. In LTE, for SFBC transmission, the symbols are transmitted from two eNodeB antenna ports on each pair of adjacent subcarriers as follows [43]:

$$\begin{bmatrix} y^{(0)}(1) & y^{(0)}(2) \\ y^{(1)}(1) & y^{(1)}(2) \end{bmatrix} = \begin{bmatrix} x_1 & x_2 \\ -x_2^* & x_1^* \end{bmatrix} \tag{3.4}$$

where $y^{(p)}(k)$ denotes the symbols transmitted on the k^{th} subcarrier from antenna port p. An important characteristic of such codes is that the transmitted signal streams are orthogonal and a simple linear receiver is required for optimal performance.

Since OFDM converts the multipath channel into N frequency-flat fading channel, we first derive the BER expressions over flat Rayleigh fading channels, given by $P_b(E)$. Then, the overall average BER over N subcarriers, in each case can be calculated from

$$BER = \frac{1}{N} \sum_{k=1}^{N} P_{b,k}(E) \tag{3.5}$$

where the index k (subcarrier index) is ignored for the sake of brevity. In addition, the impact of cyclic prefix in OFDM is assumed to be negligible.

For the 2×1 SFBC MIMO scheme, the probability density function of the SNR for each subcarrier is given by a chi-square distribution function as follows [52]:

$$f(\gamma) = \frac{2}{\bar{\gamma}^2} \gamma e^{-\frac{2}{\bar{\gamma}}\gamma} \tag{3.6}$$

where $\bar{\gamma}$ is the average SNR per symbol given by $\bar{\gamma} = E_s/N_0$.

To derive the BER, we follow the unified approach to the performance analysis of digital

communication systems over generalized fading channel [48]. To this end, we first derive the expression of Moment Generating Function (MGF) of the derived probability density function of the instantaneous SNR as [6]:

$$M_{\bar{\gamma}}(s) = \int_0^{\infty} e^{-s\gamma} f(\gamma) d\gamma. \tag{3.7}$$

Inserting (3.6) into (3.7) and solving the integral, the MGF yields:

$$M_{\bar{\gamma}}(s) = \frac{4}{\bar{\gamma}^2 (s + \frac{2}{\bar{\gamma}})^2}. \tag{3.8}$$

The average BER expression for M-QAM modulation scheme can be obtained from [6] (Equation 8.111; Page 255) as:

$$P_b(E) \cong B \sum_{i=1}^{\sqrt{M}/2} \frac{1}{\pi} \int_0^{\pi/2} M_{\bar{\gamma}}(A_{i,\theta})\, d\theta \tag{3.9}$$

where $A_{i,\theta} = \frac{(2i-1)^2}{2\sin^2\theta} \frac{3}{(M-1)}$ and B is defined by

$$B = 4 \left(\frac{\sqrt{M}-1}{\sqrt{M}} \right) \left(\frac{1}{\log_2 M} \right). \tag{3.10}$$

Then, using the MGF expression in (3.8), the associated MGF becomes:

$$M_{\bar{\gamma}}(A_{i,\theta}) = \frac{4}{\bar{\gamma}^2 \left(\left[\frac{(2i-1)^2}{2\sin^2\theta} \frac{3}{(M-1)} \right] + \frac{2}{\bar{\gamma}} \right)^2}. \tag{3.11}$$

The BER expression is then obtained by substituting (3.11) into (3.9). After some manipulations, we obtain:

$$P_b(E) \cong B \sum_{i=1}^{\sqrt{M}/2} \frac{1}{\pi} \int_0^{\pi/2} \left(\frac{\sin^2\theta}{\sin^2\theta + c_i} \right)^2 d\theta \tag{3.12}$$

where $c_i = \frac{3(2i-1)^2}{2(M-1)} \frac{\bar{\gamma}}{2}$.

Equation (3.12) represents the average BER performance as a function of $\bar{\gamma} = E_s/N_0$ and

it can be evaluated by numerical evaluation of the integral in (3.12) for M-QAM modulation schemes. Alternatively, the integral in Equation (3.12) can be solved analytically using [6], which give us a closed-form expression for the average BER of M-QAM modulation as follows:

$$P_b\left(E\right) \cong B \sum_{i=1}^{\sqrt{M}/2} \mathcal{I}_2\left(\pi/2, c_i\right) \tag{3.13}$$

where the closed-form expression for $\mathcal{I}_2(.,.)$ can be obtained from [6] (Eq.5A.24) as follows:

$$\begin{aligned}
\mathcal{I}_n\left(\phi, D\right) &= \frac{1}{\pi}\int_0^{\phi}\left(\frac{\sin^2\theta}{\sin^2\theta + D}\right)^n d\theta, \qquad -\pi \le \phi \le \pi \\
&= \frac{\phi}{\pi} - \frac{\beta}{\pi}\left\{\left(\frac{\pi}{2} + \tan^{-1}\alpha\right)\sum_{q=0}^{n-1}\begin{pmatrix} 2q \\ q \end{pmatrix}\frac{1}{\left(4\left(1+D\right)\right)^q}\right. \\
&\quad \left. + \sin\left(\tan^{-1}\alpha\right)\sum_{q=1}^{n-1}\sum_{p=1}^{q}\frac{T_{p\,q}}{\left(1+D\right)^q}\left[\cos\left(\tan^{-1}\alpha\right)\right]^{2(q-p)+1}\right\}
\end{aligned} \tag{3.14}$$

where $T_{p\,q} = \begin{pmatrix} 2q \\ q \end{pmatrix}\left[\begin{pmatrix} 2(q-p) \\ q-p \end{pmatrix} 4^p\left[2(q-p)+1\right]\right]^{-1}$, $\beta = \sqrt{\frac{D}{1+D}}\,\mathrm{sgn}\phi$, and $\alpha = -\beta\cot\phi$.

This concludes our analysis of the 2×1 SFBC scheme in LTE. In the next section, we will follow the same approach to derive the BER of the 4×2 FSTD scheme.

Analysis for the 4×2 FSTD-OFDM Scheme

In LTE, the frequency space code, designed for 4 transmit antennas is defined as follows:

$$\begin{bmatrix} y^{(0)}(1) & y^{(0)}(2) & y^{(0)}(3) & y^{(0)}(4) \\ y^{(1)}(1) & y^{(1)}(2) & y^{(1)}(3) & y^{(1)}(4) \\ y^{(2)}(1) & y^{(2)}(2) & y^{(2)}(3) & y^{(2)}(4) \\ y^{(3)}(1) & y^{(3)}(2) & y^{(3)}(3) & y^{(3)}(4) \end{bmatrix} =$$

$$\begin{bmatrix} x_1 & x_2 & 0 & 0 \\ 0 & 0 & x_3 & x_4 \\ -x_2^* & x_1^* & 0 & 0 \\ 0 & 0 & -x_4^* & x_3^* \end{bmatrix}. \tag{3.15}$$

where $y^{(p)}(k)$ denotes the symbols transmitted on the k^{th} subcarrier from antenna port p. For the 4×2 FSTD MIMO scheme, we can show that the instantaneous SNR of the system,

for k-th subcarrier, is equivalent to that for a 2×2 STBC MIMO system. Therefore, the probability density function of the SNR is given by a chi-square distribution function as follows [52]:

$$f(\gamma) = \frac{8}{3\bar{\gamma}^4}\gamma^3 e^{-\frac{2}{\bar{\gamma}}\gamma}. \tag{3.16}$$

In this case, the MGF expression can be obtained by substituting (3.16) into (3.7), which yields

$$M_{\bar{\gamma}}(s) = \frac{16}{\bar{\gamma}^4(s+\frac{2}{\bar{\gamma}})^4}. \tag{3.17}$$

Similarly to the SFBC case discussed in previous Section, inserting (3.17) into (3.9), the average BER expression with M-QAM modulation for FTSD can be written as

$$P_b(E) \cong B \sum_{i=1}^{\sqrt{M}/2} \frac{1}{\pi} \int_0^{\pi/2} \left(\frac{\sin^2\theta}{\sin^2\theta + c_i} \right)^4 d\theta \tag{3.18}$$

where $c_i = \frac{3(2i-1)^2}{2(M-1)}\frac{\bar{\gamma}}{2}$, an integral which can be calculated numerically. Alternatively, the integral in (3.18) can be solved analytically, which yields a closed-form expression for the average BER of M-QAM modulation as follows:

$$P_b(E) \cong B \sum_{i=1}^{\sqrt{M}/2} \mathcal{I}_4(\pi/2, c_i) \tag{3.19}$$

where the closed-form expression for $\mathcal{I}_4(.,.)$ can be obtained from (3.14). Finally, for the sake of comparison, we can express the average BER for the SISO case, that has been derived for Rayleigh fading channels and M-QAM signals by [6] (Eq. 8.112; Page 256):

$$P_b(E) \cong B/2 \sum_{i=1}^{\sqrt{M}/2} \left(1 - \sqrt{\frac{1.5(2i-1)^2\overline{\gamma}\log_2 M}{M-1+1.5(2i-1)^2\overline{\gamma}\log_2 M}} \right) \tag{3.20}$$

where B is defined in Equation (3.10). This concludes our BER analysis of 2×1 SFBC and 4×2 FSTD schemes in LTE. To verify our analysis, the numerical results of our analysis as well as the results of Monte-Carlo simulation will be provided in subsection 3.2.3.

3.2.3 Numerical results and discussions for the average BER

In this section, we present and discuss the results obtained from the mathematical expressions derived in the previous section 3.2.2 of this chapter. Monte-Carlo simulation results, using the Link Level LTE Simulator, are also provided to prove the accuracy of the analy-

sis. The common settings for Monte-Carlo simulations are summarized in Table 3.1. The average BER performance as a function of $\overline{\gamma} = Es/N_0$ for SISO, 2×1 SFBC and 4×2 FSTD MIMO schemes and different modulation modes have beenconsidered. The results obtained for QPSK modulation appear in Figure 3.1. Figure 3.2 and Figure 3.3 show the results for 16-QAM modulation and 64-QAM modulation respectively. In each Figure, the BER of SISO scheme as well as the BER of sSFBC and FSTD diversity schemes are shown. It can be seen that the average BER of QPSK, 16-QAM and 64-QAM schemes at high SNRs decrease by factors $\overline{\gamma}^1$, $\overline{\gamma}^2$, and $\overline{\gamma}^4$, for SISO, 2×1, and 4×2 cases, respectively. Thus, the corresponding diversity order (slope of the curves) is 1, 2 and 4 for SISO, 2×1 SFBC and 4×2 FSTD schemes, respectively. Since as stated earlier for the 4×2 FSTD scheme, for each time-slot/frequency-slot 2 out of 4 transmit antennas are in use, therefore the diversity order must be $2 \times 2 = 4$. In fact, the corresponding average BER curve for 4×2 FSTD is somehow like the classical 2×2 STBC system, when the channel is not time-varying. In all cases it is clear that the BER performance improves as the number of transmit or receive antennas increases, as expected. More specifically, if we consider Figure 3.1, a BER of 10^{-5} for SISO scheme is achieved with an SNR of 48 dB. For the 2×1 SFBC scheme, the same level of BER (i.e., 10^{-5}) is achieved in SNR = 27 dB, which represents a 21 dB improvement compared to the SISO scheme. The 4×2 FSTD scheme performs even more efficiently since an improvement of 32 dB is observed at the same BER level of 10^{-5}, as the required SNR is found to be 16 dB. Hence, the SNR gain of the 4×2 FSTD scheme compared to the 2×1 SFBC scheme is about 11dB (27 dB - 16 dB). Analogous observations can be made for the 16-QAM modulation order (Figure 3.2). For this modulation scheme, a BER of 10^{-4} for SISO scheme is obtained with an SNR of almost 43 dB. For the 2×1 SFBC scheme only an SNR of 29 dB is needed to reach the 10^{-4} level of BER, which represents an improvement in SNR of 14 dB. The SNR improvement gain of the 4×2 FSTD with respect to SISO scheme is almost 23 dB as the required SNR to achieve 10^{-4} with 4×2 FSTD scheme is found to be 20 dB. The SNR gain of 4×2 FSTD with respect to 2×1 SFBC is only 9 dB (29 dB - 20 dB). For 64-QAM

Table 3.1 Simulation Settings

Parameter	Setting
Transmission Schemes	SISO; 2×1 SFBC; 4×2 FSTD
Bandwidth	5 MHz
Simulation length	5000 subframes
Channel Type	Flat Rayleigh
Channel knowledge	Perfect
CQI	6 (QPSK); 9 (16-QAM) and 16 (64-QAM)

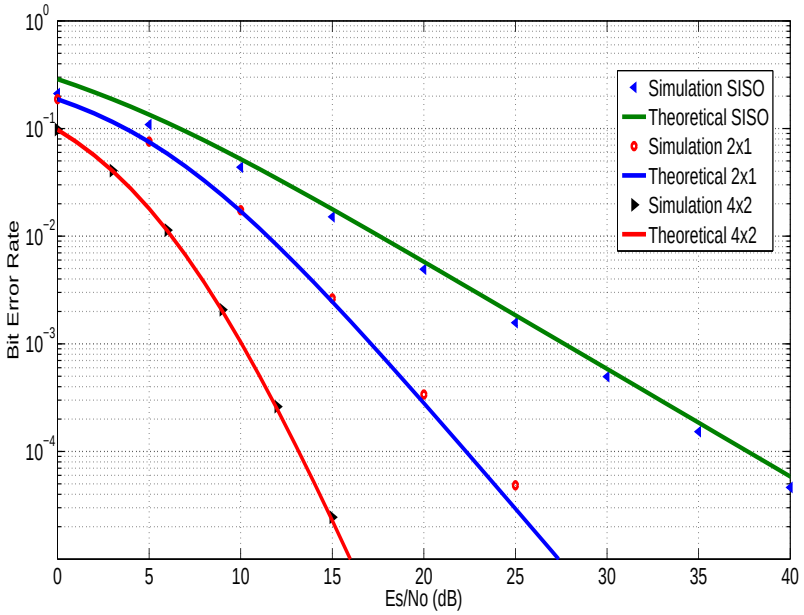

Figure 3.1 Numerical Evaluation and Monte-Carlo Simulations of the average BER for QPSK modulation.

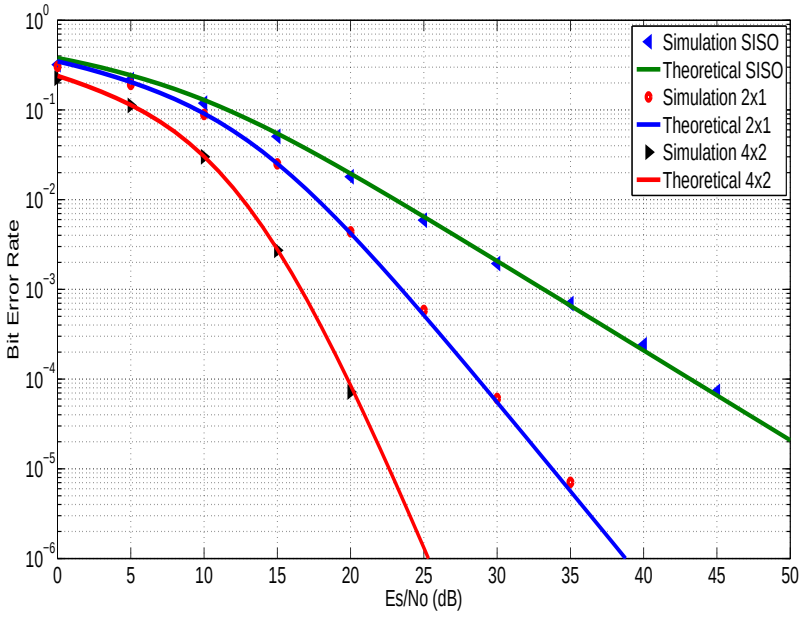

Figure 3.2 Numerical Evaluation and Monte-Carlo Simulations of the average BER for 16-QAM modulation.

modulation (Figure 3.3), the 2x1 SFBC scheme shows a SNR improvement of almost 14 dB compared to the SISO scheme at 10^{-4} BER level. The 4×2 FSTD scheme however has a 22 dB SNR gain compared to SISO scheme at the same BER level (10^{-4}). In addition to the previous observations, the comparison of the results with respect to modulation order are as expected. In fact, at 10^{-4} BER level, the required SNRs for SISO scheme are found to be 38 dB; 43 dB and 48 dB for QPSK; 16-QAM and 64-QAM, respectively. This means that to reach the 10^{-4} BER level the 64-QAM requires 10 dB higher SNR compared to QPSK modulation, which is in compliance with the theory of performance of high order modulations. Finally, it can be observed from Figure 3.1, Figure 3.2 and Figure 3.3 that numerical evaluation results obtained from BER formulas match closely to the BER results obtained from Monte-Carlo simulations. This verifies the accuracy of our mathematical analysis.

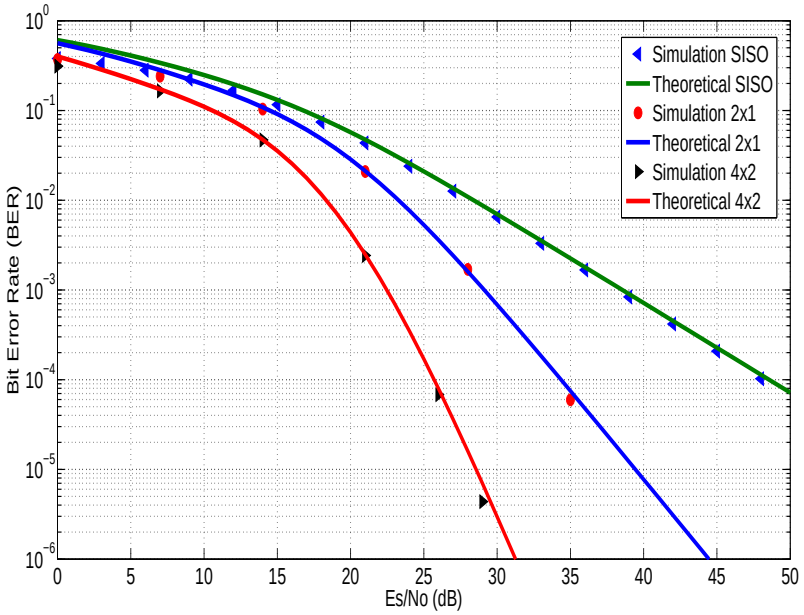

Figure 3.3 Numerical Evaluation and Monte-Carlo Simulations of the average BER for 64-QAM modulation.

3.3 Channel Capacity Analysis for LTE systems

In the previous section, we presented the average BER performance of LTE's MIMO diversity schemes (SFBC and FSTD). In this section, the performances in terms of capacity are investigated and evaluated. The channel capacity of SISO systems is described by the information theory based on the mathematical frame work introduced by Shannon [45]. In fact, it is through the theory of information that communication systems have evolved to their

present form. MIMO systems are no exception to this rule since Telatar [51] has extended the work of Shannon to the case of multiple antennas and non OFDM case. As an application of the theory, we will consider first the channel capacity for the spatial multiplexing MIMO scheme followed by the channel capacity of the different diversity schemes. In a second step, the data throughput analysis for M-QAM modulation schemes of the diversity MIMO schemes in LTE will be provided.

3.3.1 Channel Model and Channel Capacity of Spatial Multiplexing Scheme

Telatar's work [51] on MIMO channel capacity for single carrier system and in Rayleigh channel, is considered as the pioneering work that triggered research in multi antenna systems. Since the detailed explanation and development of Telatar work is not the subject of this thesis, we will simply recapitulate the most important results based on his work. In Telatar's work, the following vector transmission model with N_t transmit antennas and N_r receive antennas is used [51]:

$$\mathbf{y} = \sqrt{\frac{\varrho}{N_t}}\mathbf{H}\mathbf{s} + \mathbf{n} \tag{3.21}$$

In the above model, ϱ is the average signal to noise ratio and $\mathbf{y}$ represents the received vector of size N_r x 1 and $\mathbf{s}$ represents the transmitted vector of size N_t x 1. The MIMO channel is represented by the $\mathbf{H}$ matrix of size $N_r \times N_t$ whereas the noise is represented by the vector $\mathbf{n}$ of size $N_r \times 1$. The fundamental outcome of Telatar's work was the development of the mutual information between the transmitted signal and the received signal, $I(\mathbf{s};\mathbf{y})$ when the channel matrix $\mathbf{H}$ is deterministic and is known to the receiver which is given as [51]:

$$I(\mathbf{s};\mathbf{y}) = \log_2\left[\det\left(\mathbf{I}_{N_r} + \frac{\varrho}{N_t}\mathbf{H}\mathbf{C}_\mathbf{s}\mathbf{H}^H\right)\right] \qquad \text{[bps/Hz]} \tag{3.22}$$

where $\mathbf{C}_\mathbf{s}$ is the covariance matrix of transmitted signal vector $\mathbf{s}$ and $\mathbf{I}$ is the identity matrix with dimension N_r. ϱ is the average signal to noise ratio. By definition, the channel capacity is the maximum of the mutual information where the maximization is taken over all possible covariance matrix $\mathbf{C}_\mathbf{s}$ and hence the deterministic MIMO channel capacity can be written as [55] [51]:

$$C(\mathbf{H}) = \max_{p(\mathbf{s})} I(\mathbf{s};\mathbf{y}) \qquad \text{[bps/Hz]} \tag{3.23}$$

$$C(\mathbf{H}) = \max_{tr\,\mathbf{C}_\mathbf{s}=N_t} \log_2\left[\det\left(\mathbf{I}_{N_r} + \frac{\varrho}{N_t}\mathbf{H}\mathbf{C}_\mathbf{s}\mathbf{H}^H\right)\right] \qquad \text{[bps/Hz]} \tag{3.24}$$

The above equation is known as the "log-det" formula and is considered as the pioneering work that triggered research in multi antennas systems. For fading channel, the channel matrix $\mathbf{H}$ is a random matrix and hence the associated channel capacity is also a random variable. To deal with the random behaviour of the channel, the average of the above equation over the distribution of $\mathbf{H}$ with the given name of ergodic MIMO channel capacity can be defined as [51]:

$$C_E = E\left\{\max_{tr\,\mathbf{C_s}=N_t} \log_2\left[\det\left(\mathbf{I}_{N_r} + \frac{\varrho}{N_t}\mathbf{H}\mathbf{C_s}\mathbf{H}^H\right)\right]\right\} \qquad \text{[bps/Hz]} \tag{3.25}$$

It is worth noting that the above derivation of the ergodic MIMO channel capacity does not tell us how to choose the covariance matrix of $\mathbf{s}$ ($\mathbf{C_s}$) to get the maximum mutual information. To be able to compute the maximization, it should be clarified if the transmitter, the receiver, or both have perfect knowledge of the channel state information (CSI).

If the channel matrix $\mathbf{H}$ is known at the transmitter, the transmit covariance matrix ($\mathbf{C_s}$) can be chosen to maximize the channel capacity for a given realization of the channel. The main tool for performing this maximization is a technique known as water filling which we will not consider in this thesis. If the channel matrix $\mathbf{H}$ is, however, known at the receiver, Telatar showed that the optimal signal covariance matrix has to be chosen according to:

$$\mathbf{C_s} = \mathbf{I} \tag{3.26}$$

This means that the antennas should transmit uncorrelated streams with the same average power. With such covariance matrix, the ergodic MIMO channel capacity becomes [51]:

$$C_E = \mathbf{E}\left\{\log_2 \det\left(\mathbf{I}_{N_r} + \frac{\varrho}{N_t}\mathbf{H}\mathbf{H}^H\right)\right\} \qquad \text{[bps/Hz]}. \tag{3.27}$$

3.3.2 Channel Model and Channel Capacity of Diversity Schemes

The ergodic channel capacity in (3.27) is valid for channel matrix where different signals are transmitted independently and hence cannot be applied directly to the space time block coding where the signals are transmitted in the form of space block codes. In fact, a STBC scheme with N_t transmit antennas and N_r receive antennas is generally characterized by the

transmission matrix which has general form [49]:

$$G = \begin{pmatrix} g_{11} & g_{21} & \cdots & g_{N_t 1} \\ g_{12} & g_{22} & \cdots & g_{N_t 2} \\ . & . & ... & . \\ . & . & ... & . \\ g_{1T} & g_{2T} & \cdots & g_{N_t T} \end{pmatrix} \tag{3.28}$$

where g_{ij} represents a linear combination of the signal constellation components and their conjugates. g_{ij} is transmitted from the ith transmit antenna in the jth time slot for $i = 1, ..., N_t$ and $j = 1, ..., T$. T represents the number of time slots used to transmit S symbols. For such STBC, it has been found that the equivalent AWGN scaled channel is given by [59]:

$$\mathbf{y_{nT}} = \frac{1}{R_c}\|\mathbf{H}\|_F^2 \mathbf{x_{nT}} + \mathbf{w_{nT}} \tag{3.29}$$

where $\mathbf{y_{nT}}$ is the $S \times 1$ complex matrix after STBC decoding and S represents the number of transmitted symbols. $\mathbf{x_{nT}}$ is the transmitted $S \times 1$ complex vector with each entry having energy E_s/N_t, E_s is the maximum total transmitted energy on the N_t transmit antennas per symbol time, and $\mathbf{w_{nT}}$ is complex Gaussian noise with zero mean and variance $N_0/2$ in each dimension. $\|\mathbf{H}\|_F^2 = \sum_{i=1}^{N}\sum_{j=1}^{M}\|h_{ij}\|^2$ is the squared Frobenius norm of $\mathbf{H}$, h_{ij} is the channel gain from the ith transmit antenna to the jth receive antenna. R_c is the code rate of the STBC and defined as S/T, where T is the number of time slots to transmit one block code. From the equivalent AWGN channel in (3.29), it was shown that the effective instantaneous SNR at the receiver denoted as γ is given as [59]:

$$\gamma = \frac{E_s}{N_t R_c N_0}\|\mathbf{H}\|_F^2 \tag{3.30}$$

which means that the channel matrix is converted into a scalar channel [40] [31] [12] [59] and hence the ergodic capacity of the equivalent STBC channel in (3.29) is given by [40] and [12] as:

$$\overline{C} = E\left[R_c \log_2(1+\gamma)\right] \qquad \text{(b/s/Hz)} \tag{3.31}$$

or equivalently, by inserting (3.30) into (3.31):

$$\overline{C} = E\left[R_c \log_2\left(1 + \frac{E_s}{N_t R_c N_0}\|\mathbf{H}\|_F^2\right)\right] \qquad \text{(b/s/Hz)} \tag{3.32}$$

If the probability density function of the instantaneous SNR $p(\gamma_s)$ is known, the ergodic

capacity of the equivalent STBC can be evaluated using the following integral equation [40]:

$$\overline{C} = R_c \int_0^{\infty} \log_2 (1+\gamma)\, p(\gamma_s) d\gamma_s \qquad \text{(b/s/Hz)} \tag{3.33}$$

Equation (3.33) represents the fundamental formula for capacity evaluation of any diversity STBC scheme. This is through this equation that we will present our capacity analysis of SFBC-OFDM and FSTD-OFDM diversity schemes in LTE environment.

SFBC Channel Capacity Analysis

Since OFDM system converts the multipath channel into N frequency flat-fading subchannels, the average capacity over flat-fading subchannel that is defined by $\overline{C}_k$ is determined first. Then, the overall average channel capacity over N can be found as:

$$\overline{C}^{\chi} = \frac{1}{N} \sum_{k=1}^{N} \overline{C}_k^{\chi} \tag{3.34}$$

where k represents the subcarrier index and $\chi \in \{SFBC, FSTD\}$. The average capacity achieved by a SFBC-OFDM scheme is calculated using the probability density function of the instantaneous SNR [52]:

$$\overline{C}_k^{SFBC} = \int_0^{\infty} R_c \log_2\ (1+\gamma) f_{\gamma}^{SFBC}(\gamma) d\gamma \tag{3.35}$$

where $f_{\gamma}^{SFBC}(\gamma)$ is defined as

$$f_{\gamma}^{SFBC}(\gamma) = \frac{2}{\bar{\gamma}^2} \gamma e^{-\frac{2}{\bar{\gamma}}\gamma} \tag{3.36}$$

Substituting the PDF in the equation of average capacity, we obtain:

$$\overline{C}_k^{SFBC} = \int_0^{\infty} R_c \log_2\ (1+\gamma) \frac{2}{\bar{\gamma}^2} \gamma e^{-\frac{2}{\bar{\gamma}}\gamma} d\gamma \tag{3.37}$$

After some manipulation, the equation of the $\overline{C}_k^{SFBC}$ can be written as:

$$\overline{C}_k^{SFBC} = A\mu \int_0^{\infty} \ln\ (1+\gamma)(\mu\gamma)^{\eta-1} e^{-\mu\gamma} d\gamma \tag{3.38}$$

where

$$A = \frac{R_c \times \log_2(10) \times \log_{10}(e)}{2};\ \mu = \frac{2}{\overline{\gamma}};\ \eta = 2 \tag{3.39}$$

The integral in equation (3.38) can be evaluated using the following results [22]:

$$\frac{\mu}{(\eta-1)!}\int_0^\infty \ln(1+x)(\mu x)^{\eta-1}e^{-\mu x}dx = \mathcal{P}_\eta(-\mu)E_1(\mu) + \Sigma_{q=1}^{\eta-1}\frac{1}{q}\mathcal{P}_q(\mu)\mathcal{P}_{\eta-q}(-\mu) \tag{3.40}$$

where $\mathcal{P}_q(.)$ and $E_1(x)$ represent respectively the Poisson distribution and the exponential integral of first order which are given as [22]

$$\mathcal{P}_q(x) = \Sigma_{v=0}^{q-1}(\frac{x^v}{v!})e^{-x} \tag{3.41}$$

$$E_1(x) = \int_x^\infty t^{-1}e^{-t}dt \qquad \text{for} \qquad x>0 \tag{3.42}$$

Using (3.40), the closed form of (3.38) becomes

$$\overline{C}_k^{SFBC} = A\{\mathcal{P}_2(-\mu)E_1(\mu) + \mathcal{P}_1(\mu)\mathcal{P}_1(-\mu)\} \tag{3.43}$$

This concludes our analysis for the 2×1 SFBC scheme.

FSTD Channel Capacity Analysis

Following the same approach adopted for the analysis of 2×1 SFBC scheme, we can determine the average channel capacity for the (4×2) FSTD scheme. To this end, we use the expression for the kth OFDM subcarrier $\overline{C}_k^{FSTD}$ [52]:

$$\overline{C}_k^{FSTD} = \int_0^\infty R_c \log_2(1+\gamma) f_\gamma^{FSTD}(\gamma)d\gamma \tag{3.44}$$

where $f_\gamma^{FSTD}(\gamma)$ is defined by:

$$f_\gamma^{FSTD}(\gamma) = \frac{8}{3\bar{\gamma}^4}\gamma^3 e^{-\frac{2}{\bar{\gamma}}\gamma}. \tag{3.45}$$

Substituting (3.45) in (3.44), we obtain:

$$\overline{C}_k^{FSTD} = \int_0^\infty R_c \log_2(1+\gamma)\frac{8}{3\bar{\gamma}^4}\gamma^3 e^{-\frac{2}{\bar{\gamma}}\gamma}d\gamma \tag{3.46}$$

which after some manipulation, becomes:

$$\overline{C}_k^{FSTD} = \frac{A\mu}{3}\int_0^\infty \ln(1+\gamma)(\mu\gamma)^{\eta-1}e^{-\mu\gamma}d\gamma \tag{3.47}$$

where A and μ are as defined in (3.39) and $\eta = 4$. Using (3.40), a closed form can be found

as:

$$\overline{C}_k^{FSTD} = 2A\left[\mathcal{P}_4(-\mu)E_1(\mu) + \Sigma_{q=1}^{3}\frac{1}{q}\mathcal{P}_q(\mu)\mathcal{P}_{\eta-q}(-\mu)\right] \tag{3.48}$$

This concludes our analysis of 4×2 FSTD MIMO scheme in LTE. The numerical results in terms of bits/s/Hz are shown in Figure 3.4. To verify our analysis, the results of Monte-

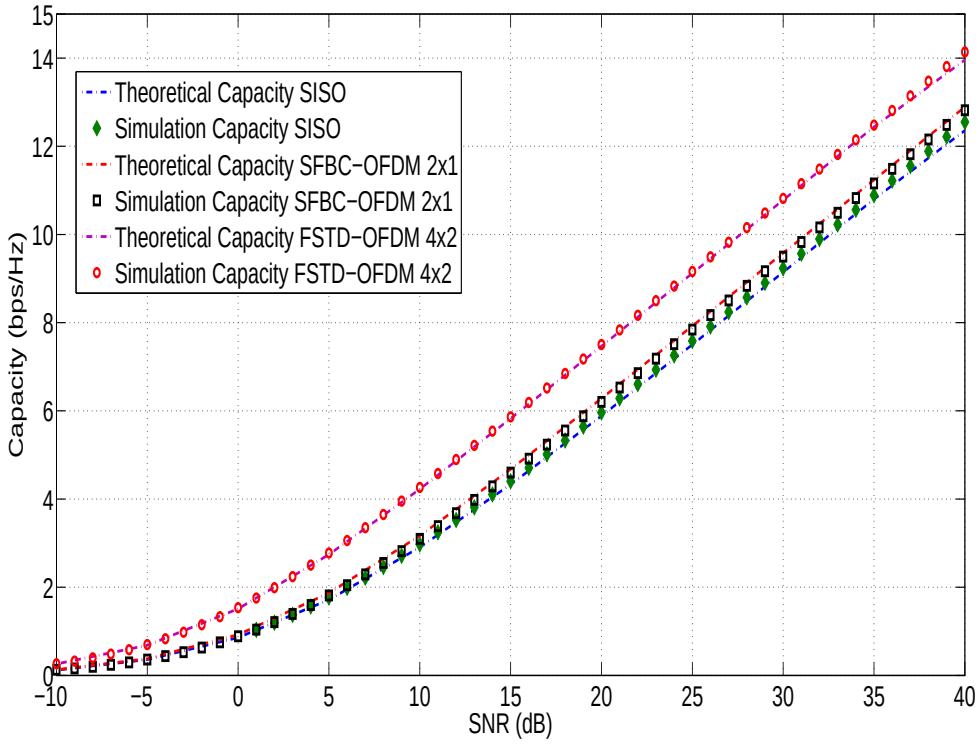

Figure 3.4 Capacity for SISO, SFBC-OFDM and FSTD-OFDM Schemes

Carlo simulation of channel capacity of the two studied diversity schemes as well as the SISO case are also included. The dashed line curve in Figure 3.4 represents the channel capacity of SISO scheme using our analysis. The diamond shaped points represents the SISO capacity obtained with Monte-Carlo simulation. The theoretical channel capacity of 2×1 STBC is shown by the red curve in Figure 3.4, whereas the black square line represent the capacity obtained by Monte-Carlo simulation. As expected, in the high SNR regions, only a small improvement of the channel capacity of the 2×1 SBC with respect to the SISO case is observed. Specifically, for SNR = 34 dB the improvement of 2×1 STBC is about 0.5 bits/s/Hz with respect to SISO. For low SNR regions, the channel capacity of the SISO case and the 2×1 STBC is almost the same. The theoretical channel capacity of the 2×2 STBC

scheme is shown by the purple dashed line in Figure 3.4. The improvement with respect to the SISO case is more important. In fact, for the same SNR = 34 dB, the improvement is about 1.6 bits/s/Hz. Finally, it can be observed from Figure 3.4 that numerical evaluation results obtained from capacity analysis match closely to the capacity results obtained from Monte-Carlo simulations, which comforts us in the accuracy of our mathematical analysis.

3.4 Data Throughput Performance Evaluation for M-QAM Modulation Schemes

In SISO OFDM systems, the maximal data throughput depends on the available bandwidth and the parameters associated with the OFDM signal, such as the number of subcarriers and the modulation order (QPSK, 16-QAM, 64-QAM). For a given frequency bandwidth (B) the maximal coded data throughput in bits per second can be approximated by the following simple equation [32]:

$$CodedThroughput(bps) = \frac{N_{FB}.N_{SC}.N_{OFDM}.N_b.ECR}{T_{sub}} \tag{3.49}$$

where N_{FB} is the number of Frequency Blocks in the given frequency bandwidth (B), N_{SC} is the number of subcarriers in one Frequency Block, N_{OFDM} is the number of OFDM symbols in one subframe, N_b is the number of bits in one subcarrier; ECR is the Effective Code Rate, and T_{sub} is the duration of one subframe that is equal to 1 ms. In LTE, N_{SC} and N_{OFDM} are fixed with values 12 and 14 respectively [4]. For 5 MHz ($N_{FB} = 25$) bandwidth LTE system with 64-QAM Modulation ($N_b = 6$) and ECR = 0.9, the maximal data throughput that can be supported by the system is then 22.68 Mbps. The uncoded data throughput can be found by excluding the effective code rate (ECR) from the equation (3.49). This yields:

$$UncodedThroughput(bps) = \frac{N_{FB}.N_{SC}.N_{OFDM}.N_b}{T_{sub}} \tag{3.50}$$

The throughput results can be compared to the system capacity $\overline{C}_B^{\chi}$ ($\chi \in \{SFBC, FSTD\}$) of a flat fading channel as developed in Section 3.3 but adjusted by the inherent system losses. In this case, the system capacity is simply given as [32]:

$$\overline{C}_B^{\chi} = \mathcal{F} \times \mathcal{B} \times \overline{C}^{\chi}. \tag{3.51}$$

where $\mathcal{F}$ and $\mathcal{B}$ are two correcting factors. The correcting factor $\mathcal{B}$ can be calculated as [32]:

$$\mathcal{B} = \frac{N_{SC}.N_{OFDM}.N_{FB}}{T_{sub}} \tag{3.52}$$

where N_{SC} is the number of subcarriers in one Resource Block and is equal to 12, N_{OFDM} represents the number of OFDM symbols in one subframe and for normal cyclic prefix it is equal to 14. N_{FB} is the number of resource blocks (RB) that fit into the selected bandwidth (for example in 5 MHz bandwidth we found 25 Resource Blocks). The values of N_{FB} corresponding to the selected bandwidth (B) are shown in Table 3.2.

Finally, T_{sub} is the duration of one subframe and is equal to 1 ms. To take into account the losses due to the added cyclic prefix and reference symbols, a correction factor $\mathcal{F}$ is introduced in the calculation of the system capacity and is given by [32]:

$$\mathcal{F} = \frac{T_{\text{frame}} - T_{cp}}{T_{\text{frame}}} \times \frac{N_{sc} \times N_{OFDM}/2 - 4}{N_{sc} \times N_{OFDM}/2} \tag{3.53}$$

where T_{frame} is the fixed duration frame and is equal to 10 ms. T_{cp} represents the total Cyclic Prefix time of all OFDM symbols within one frame and is given by:

$$T_{cp} = (T_{cp1} + 6 \times T_{cp2}) \times N_{slot} \tag{3.54}$$

where T_{cp1} is the duration of the first cyclic prefix of the first OFDM symbol in one slot and is equal to $5.2\mu s$. T_{cp2} is the duration of the cyclic prefix of the next six OFDM symbols in one slot as shown in Figure 2.7 and is equal to $4.7\mu s$. Finally, N_{slot} is the number of slots within the duration of one frame and is equal to 20. The results of calculation of the system capacity based on Equation 3.51 for different bandwidth values are shown in Figure 3.5.

$$\overline{C}_B = \mathcal{F} \times \mathcal{B} \times \log_2(1 + \gamma). \tag{3.55}$$

The results in Figure 3.5 represent the limit of channel capacity of a system with continuous valued inputs and continuous valued outputs of complex signals for different channel bandwidth (B) as defined in LTE (Table 3.2). These limits can be considered as an upper

Table 3.2 Number of Resource Blocks

B (MHz)	N_{FB}
1.4	6
5	25
10	50
15	75
20	100

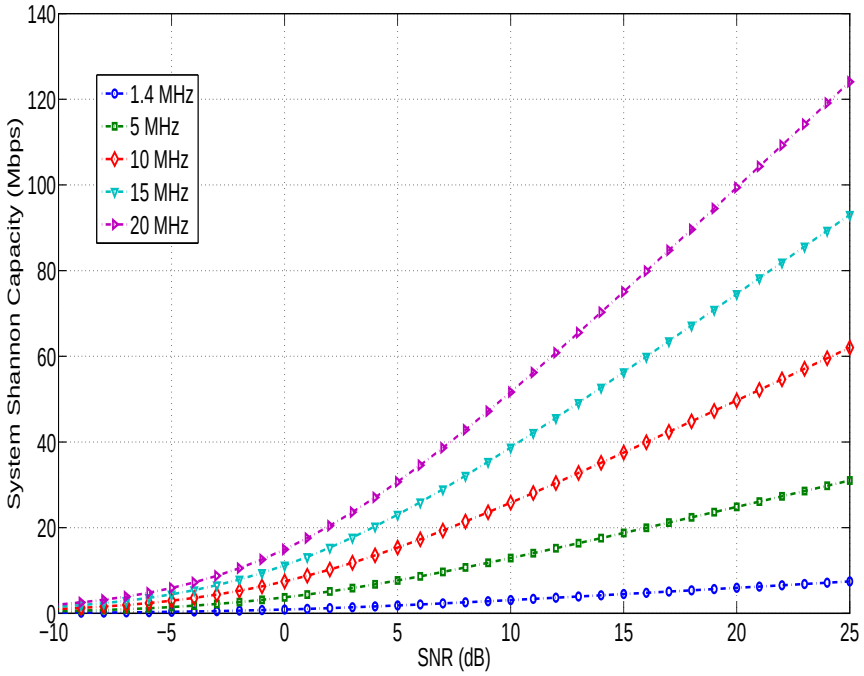

Figure 3.5 System Capacity as a function of SNR for different Bandwidth settings

bound of real data throughput of a system with discrete valued multilevel/phase inputs. It can also be noticed from the Figure how the Shannon capacity increases as the bandwidth increases. The results relative to real data throughput and their respective limit will be shown in the next section.

Table 3.3 ECR and Modulation Order for CQI

CQI	Modulation	ECR	ECR x 1024[6]
1	4QAM	0.0762	78
2	4QAM	0.1172	120
3	4QAM	0.1885	193
4	4QAM	0.3008	308
5	4QAM	0.4385	449
6	4QAM	0.5879	602
7	16QAM	0.3691	378
8	16QAM	0.4785	490
9	16QAM	0.6016	616
10	64QAM	0.4551	466
11	64QAM	0.5537	567
12	64QAM	0.6504	666
13	64QAM	0.7539	772
14	64QAM	0.8525	873
15	64QAM	0.9258	948

Table 3.4 SISO Generated Data

Modulation Scheme		QPSK		
MIMO Configuration		SISO	2×1 SFBC	4×2 FSTD
ECR		0.5879	0.6016	0.9258
Max Possible Data (Bits/SubFrame)		8400	8400	8400
Tx Data bits	1^{st} SubFrame	4512	4372	4136
	2^{nd} to 5^{th} SubFrames	4680	4456	4220
Tx Coded Bits	1^{st} SubFrame	7712	7456	7056
	2^{nd} to 5^{th} SubFrames	8000	7600	7200
Tx User Symbols	1^{st} SubFrame	3856	3728	3528
	2^{nd} to 5^{th} SubFrames	4000	3800	3600
Expected Data Throughput (Bits/Subframe)		8000	7600	7200
Calculated ECR		0.5850	0.5863	0.5861

3.4.1 Numerical Results and Discussion for System Throughput

In this section, we present numerical results of the data throughput results of SFBC-OFDM and FSTD-OFDM MIMO schemes for different M-QAM modulation schemes using the LTE simulator [36]. The LTE simulator allows the calculation of coded and uncoded data throughput. For coded calculations, the transmitted signal is coded using the Turbo Code as defined in LTE. The overall effective code rates for different modulation schemes are defined in LTE and are given in Table 3.3. The Monte-Carlo simulation results are presented in the Figure 3.6; 3.7 and 3.8, where they are compared to coded and un-coded data throughput for the SISO configuration. Figure 3.6 represents the results for QPSK modulation. The results of 16-QAM are presented in Figure 3.7 while those relative to 64-QAM modulation appear in Figure 3.8.

For QPSK modulation, the un-coded data throughput of SISO configuration is shown by the ball blue curve. It can be observed that as the SNR increases the data throughput increases and it reaches its maximum at an SNR of almost 48 dB. The coded data throughput of the same modulation (QPSK) and represented by the blue curve in Figure 3.6 reaches its maximum with only 10 dB. As expected from the coding process, the coded data throughput is less than the un-coded data throughput. In fact, the coded and un-coded data throughputs are related by the effective code rate used for channel coding. As shown in Table 3.3, the ECR for QPSK (CQI = 6) is equal to 0.5879, which represents the ratio of the useful transmitted data rate to the overall coded data after channel coding. An ECR of 0.5879 means that only 0.5879 of the transmitted data are useful data. The remaining data are used only for error protection and detection. This principle is well represented in the results of Figure 3.6, where the coded data throughput is found to be 4.9 Mbps whereas the un-coded data throughput is 8.3 Mbps, which represents, effectively and as expected, a code rate of 0.5879. The benefits of using the channel coding (Turbo coding in LTE)is clearly shown in Figure

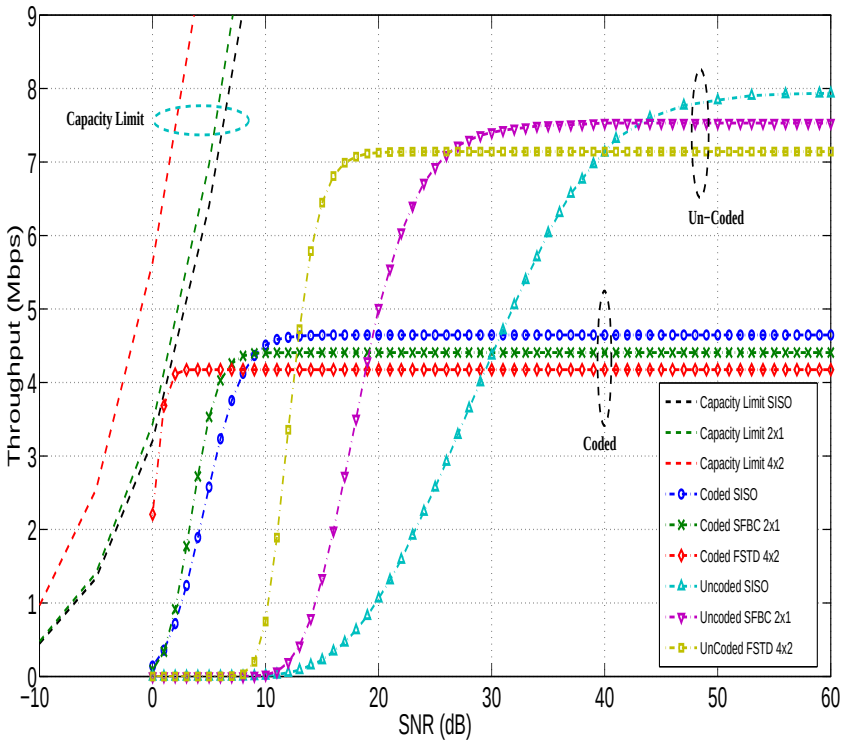

Figure 3.6 Data Throughput for QPSK Modulation

3.6, where the data throughput of coded scheme is much closer to the channel capacity limit. The coded and un-coded data throughput of the 2×1 SFBC are represented by the green and purple curves respectively. In case of un-coded scheme, the improvement with respect to the SISO case is more significant and substantial as shown in Figure 3.6. However, for coded case, there is no big difference between SISO and 2×1 scheme and the improvement is less significant. One last interesting observation from the results in Figure 3.6 is the fact that at high SNRs the SISO data throughput is greater than the data throughput for 2×1 and 4×2 diversity schemes. This result is explained by the fact that more overhead data is transmitted in case of diversity schemes as shown in Table 3.4. Specifically, for SISO scheme the symbol rate is 4000 per subframe (1 ms) whereas with 2×1 SFBC case, the symbol rate is 3800 per subframe. The symbol rate of 4×2 FSTD is the smallest one and is found to be 3600 per subframe and that is why the data throughput of 4×2 FSTD is the smallest one at the high SNR region as shown in Figure 3.6. This observation is valid for both coded and un-coded data throughput. The red and citrine curves represent the coded and un-coded data throughput respectively for the 4×2 FSTD diversity scheme. Same observations as for 2×1 SFBC scheme can be made here. The theoretical channel capacity limits for SISO, 2×1

SFBC and 4×2 FSTD in a Rayleigh channel are also shown in Figure 3.6 for illustration and to show the effect of channel coding. It is clearly perceptible that the data throughput comes closer to the capacity limit with using channel coding.

For 16-QAM modulation (Figure 3.7), which corresponds to a CQI of 9, the code rate

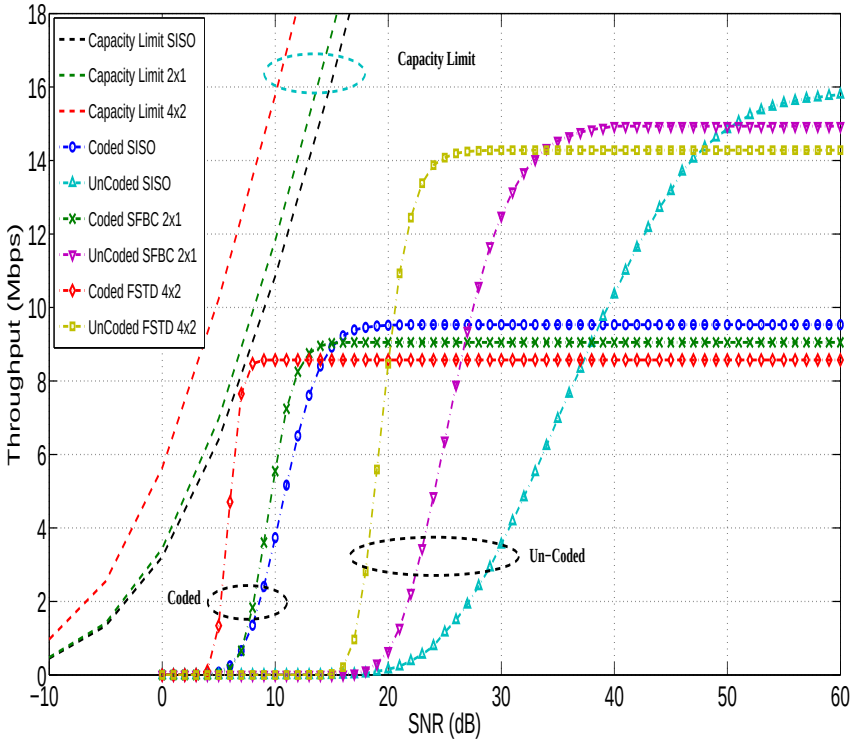

Figure 3.7 Data Throughput for 16QAM Modulation

is 0.6016 (Table 3.3) and hence the un-coded data throughput is higher than the coded data throughput. For SISO scheme, the maximum un-coded and coded data throughput, represented by the ball blue and blue curves in Figure 3.7, are found to be 15.8 Mbps and 9.5 Mbps respectively, which corresponds as expected to a 0.6 (9.5/15.8) code rate. The maximum data throughput is achieved with a SNR of 60 dB in case of un-coded scheme whereas only 20 dB is needed to achieve the maximum of data throughput for coded scheme. It can be observed from Figure 3.7 that the best performance in terms of data throughput is achieved with the 4×2 FSTD scheme where the maximum data throughput is reached at SNR = 10 dB. To attain the maximum in 2×1 SFBC scheme an SNR of 16 dB is required. For SISO scheme an SNR of 20 dB is needed to achieve the maximum data throughput. These results demonstrate the benefits of the diversity schemes. The code rate for CQI 15 (64-QAM Modulation) is 0.9258 which is close to 1. The maximum un-coded and coded

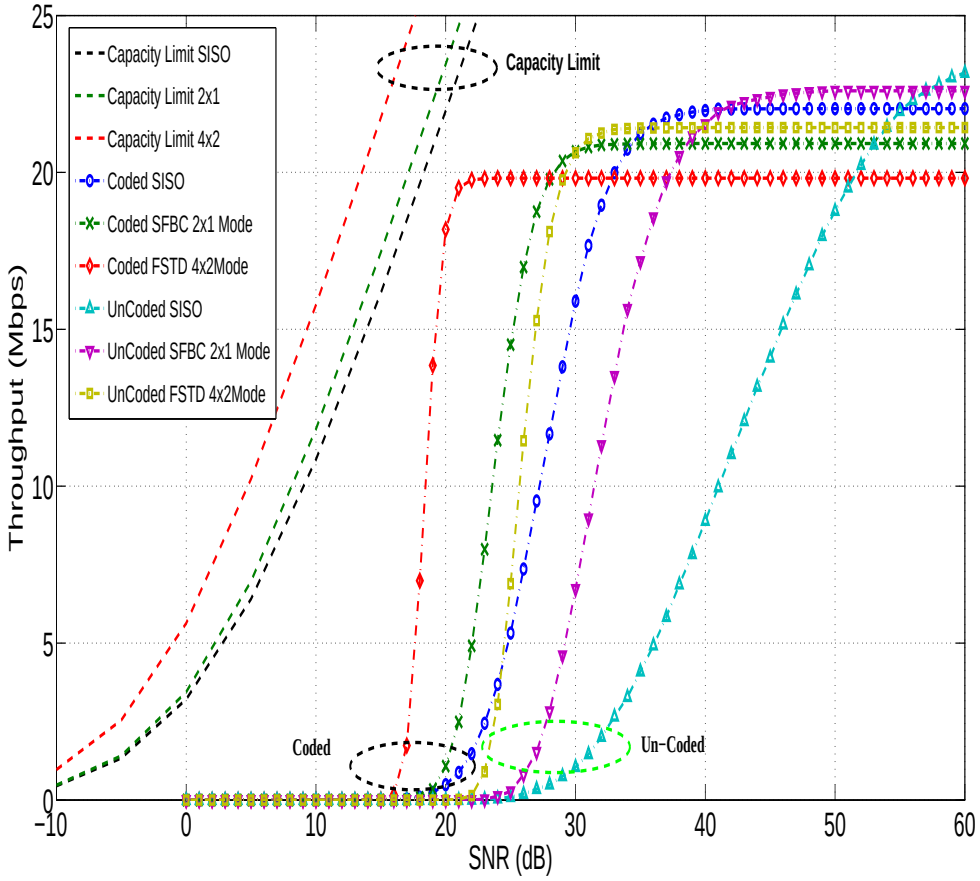

Figure 3.8 Data Throughput for 64QAM Modulation

data throughputs are found to be 23.5 Mbps and 22 Mbps respectively, which correspond to a code rate of 0.9258. The effectiveness of the the FSTD scheme is clearly observed in Figure 3.8 where the maximum data throughput is achieved with 23 dB compared to 32 dB with 2×1 SFBC and 41 dB with SISO. The theoretical channel capacity limit is also shown in the Figure. To compare the coded data throughput with the theoretical limit of channel capacity, the coded data throughput of all modulation schemes ad diversity schemes are made in Figure 3.9, where the coded data throughput for QPSK, 16-QAM and 64-QAM and for SFBC and FSTD MIMO schemes are plotted. It can be observed from Figure 3.8 the benefit of using higher order modulation in high SNR regions.

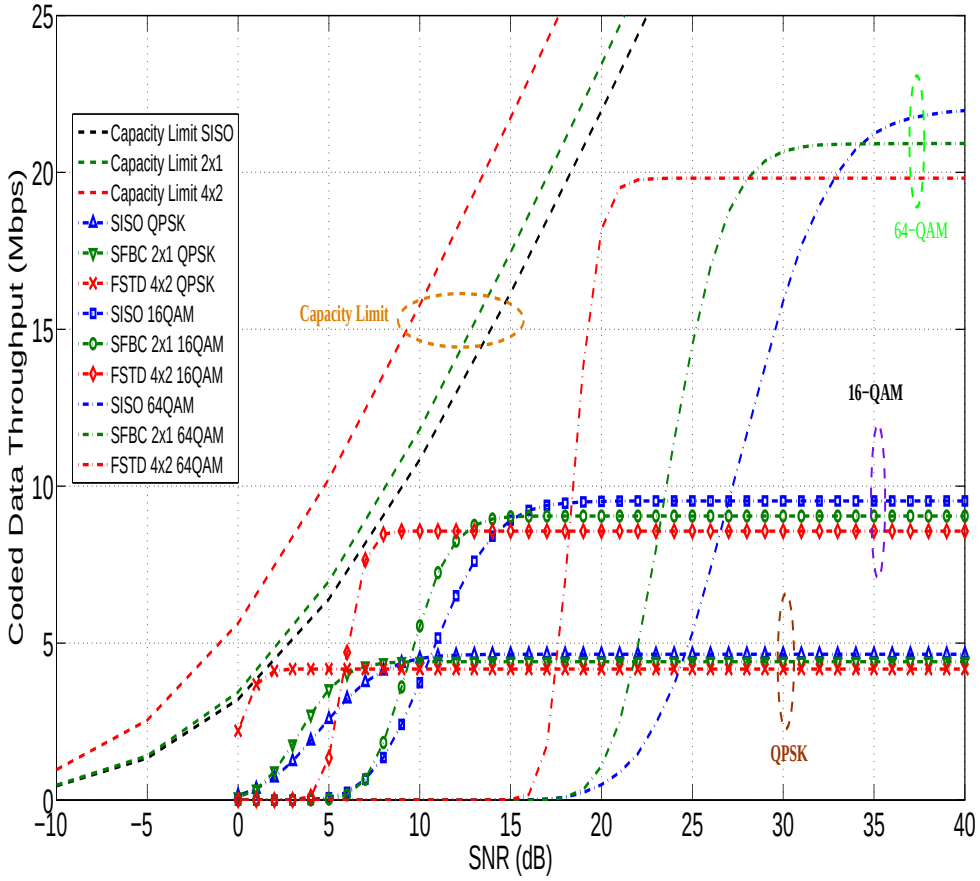

Figure 3.9 Coded Data Throughput for M-QAM Modulation

CHAPTER 4

ANTENNA SELECTION IN MIMO SYSTEMS

As discussed in Chapter 3, the MIMO systems using multiple antennas at the transmitter and multiple antennas at the receiver can improve significantly the system data rates and reliability. The data rate improvement is achieved by the simultaneous transmission of multiple streams of data using spatial multiplexing techniques. For channels with no spatial correlation, the data rate can increase linearly with the minimum number of transmit and receive antennas (min (N_r, N_t). A popular example of spatial multiplexing technique is the V-BLAST suggested by Foschini [15]. The improvement in reliability is achieved through the use of space diversity to significantly reduce the deep fades probability of a channel. In 1998, Alamouti has designed a simple transmit diversity scheme with two transmit antennas [5]. Alamouti's method provides a full diversity and requires simple linear operations both at the transmit and receive sides. The processes of coding and decoding are performed in blocks of transmitted symbols. Using the theory of orthogonal designs, the simple transmit diversity technique of Alamouti has been generalized for a number of transmit antennas greater than two [50] to a family of transmit diversity schemes known as Orthogonal Space-Time Block Codes (OSTBC). As a different approach, Space-Time Trellis Codes (STTC) are also used as transmit diversity schemes in MIMO systems. Also, OSTBC are the simplest space-time codes that exploit the diversity offered by multiple antennas MIMO systems.

Besides the above mentioned advantages, MIMO systems have also some drawbacks. One of the main drawback in the developments of MIMO systems is the increased cost caused by the implementation of multiple Radio Frequency (RF) chains. For example, a $N_r \times N_t$ MIMO system requires on the receiver side N_r low noise amplifiers, N_r analog to digital converters as well as N_r RF to Intermediate Frequency (IF) converters and N_t digital to analog converters, and on the transmitter side N_t RF amplifiers and N_t IF to RF converters to be implemented which leads to high costs for the implementation of MIMO systems. To remedy this problem, MIMO systems with antenna selection have been proposed, where the number of available antennas at the receiver (N_r) is greater than the number of implemented RF chains (L_r). The antenna selection scheme has been studied and used for a long time in the context of radio links at the receiver with a single antenna at the transmitters. In the literature, this technique is known as *Selection Combining* (SC) and *Hybrid Selection*/MRC (H-S/MRC). In the SC technique, one receive antenna is selected out of N_r antennas whereas in HS/MRC L_r

antennas are selected from N_r receive antennas. For the case of a MIMO system in general, the use of the antenna selection technique is known as the *Hybrid Selection*/MIMO (HS/MIMO). Using a predefined selection criterion, several ($L_r \leq N_r$) among the N_r receive antennas can be selected. Thus, one can use a limited number of RF chains which are allocated to the best L_r antennas. Obviously, this significant reduction in the complexity of the implementation is not without price. In fact, it is at the expense of a loss, relatively small, in the system capacity compared to the MIMO system using all antennas.

This chapter is organized as follows. In Section 4.1, we provide a brief literature overview of the theory of antenna selection in MIMO systems and its impact on the performance of these systems and more specifically, the impact on the channel capacity and the Bit Error Rate. A detailed description of main antennas selection algorithms is also provided in this section. In section 4.2, some results of the impact of the implemented Un-Correlated Based Selection (UCBS) algorithms are provided. In section 4.3, we present the analysis of the performance of MIMO systems using antennas selection techniques in non correlated channels. Finally, in section 4.4, we evaluate the impact of antenna correlation on the BER performances of MIMO OSTBC with receive antennas selection.

4.1 Antenna Selection Overview

MIMO systems with antenna selection have been extensively studied in various literatures [17], [9], [18], [34]. In [34], the authors study the capacity upper bound of MIMO systems with antenna selection on the receiver side. In particular they demonstrate that the capacity is very close to that of a system without selection if the number of receive antennas is greater or equal than the number of transmit antennas. The authors in [17] investigate the capacity of MIMO systems with antenna selection in the case when the rank of the channel matrix is low. Based on the minimization of the probability of error per symbol (SER), the authors [9] and [18] present an antenna selection scheme for space-time block coding systems. In [18], the authors study the performances of joint transmit and receive antenna selection for the cases of exact channel knowledge (ECK) and for statistical channel knowledge (SCK). For ECK case, they consider the specific Alamouti code [5], whereas the more general space time coding is considered for the SCK case. In their analysis, they adopt a selection criterion that maximizes the Frobenius norm of the channel and, accordingly, they derive expressions showing improvement in the signal to noise ratio (SNR) and in the outage capacity. They use the outage capacity to affirm that the spatial diversity using the space time block coding is maintained by the antenna selection. This impact is also analyzed in [58]. In their analysis, an upper bound on the performance of BER systems with antenna selection is explicitly

derived. They demonstrate that the diversity order of a system with antenna selection is the same as that of the system using all available antennas. In addition, they derive a tight upper bound for the performance of the bit error rate (BER) for a system with N_r receive antennas N_t transmit antennas and $L_r = 1$. An expression for the BER performance of Alamouti code has also been developed when $L_r = 1$. In [24] , Heath et al. propose a criteria for selecting an optimal antenna of subset that minimize the error rate. In their studies, they use coherent receivers such as liner or maximum likelihood (ML) over a slowly varying channel. Several selection algorithms, geared at maximizing the channel capacity were presented by different authors [19] − [10]. In [27], the authors consider an antenna selection on the transmitter side for OSTBC codes. Through Monte-Carlo simulations, they demonstrate that under the assumption that the number of selected antennas is fixed, the performance is improved when the number of available transmit antennas is increased. [54] consider the selection of antennas for MIMO systems using three transmit antennas and a single receive antenna. They introduce an algorithm to select the two best antennas based on the channel statistics provided by the receiver. A complete review of the literature on antenna selection in MIMO systems can be found in [33].

The optimal choice in antenna selection requires the knowledge and the estimation of the full channel MIMO matrix. To perform the estimation of all antennas, it seems necessary to make available all the N_r RF chains, which goes against the goal of reducing the number of RF chains. However, in an environment that changes sufficiently slowly and with the help of a training sequence, antennas can be multiplexed to different RF chains so that the channel is estimated successively antenna by antenna. Practically a RF receive chain is connected to the first receive antenna during the first part of the training sequence to estimate the channel seen by the first antenna. Then the same chain is connected to the second antenna in the second part of the training sequence to estimate the channel of the second antenna. This procedure is then repeated for all available antennas. This allows the determination of the channel state information (CSI) in all antenna elements (N_r). At the end of the training sequence, the channels of all antennas are estimated and based on that estimation, the best L_r antennas are selected . Therefore, a few more bits of training sequence are needed instead of additional RF channels. In a system with high data rate, such additional bits do not affect the spectral efficiency significantly.

In this chapter, we consider a MIMO system equipped with N_t transmit antennas and N_r receive antennas as shown in Figure 4.1. In addition, we suppose that the transmitter has L_t radio frequency (RF) chains and the receiver has L_r RF chains, where $L_t < N_t$ and $L_r < N_r$,

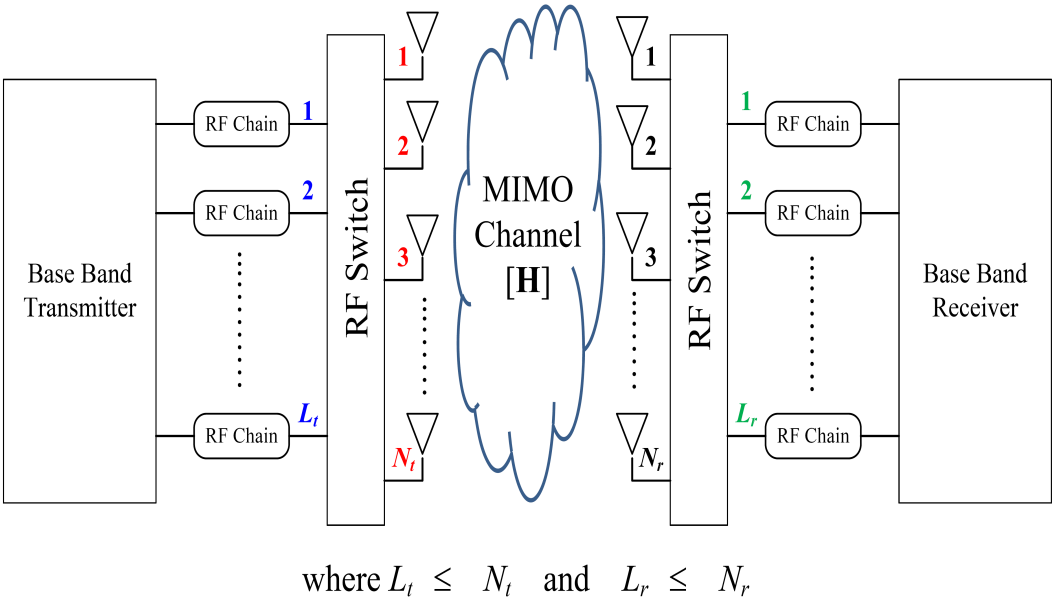

Figure 4.1 MIMO system Model with Antenna Selection

as indicated in Figure 4.1. When there is no antenna selection, $L_t = N_t$ and $L_r = N_r$. Referring to Figure 4.1, we can distinguish three types of antenna selection mechanisms:

1. Receive Antenna Selection (RAS)
2. Transmit Antenna Selection (TAS)
3. Joint Transmit-Receive Antenna Selection (TRAS)

In case of Receive Antenna Selection, we have $L_t = N_t$. The goal of a Receive Antenna selection algorithm is to find the *optimal* subset of receive antennas that maximizes some selection criteria. This is what is called the *optimal* receive antenna selection. The only mechanism for an optimal receive antenna selection is to make an exhaustive search among all possible combinations and find the antennas subset that maximizes the selection criterion. It follows that an optimal receive antenna selection necessitates a prohibiting time of computation for the evaluation of the selection criteria $\binom{N_r}{L_r}$ times. For Transmit Antenna Selection, we have $L_r = N_r$ and the optimal transmit antenna selection necessitate the evaluation of the selection criteria $\binom{N_t}{L_t}$ times. Finally, for joint transmit-receive antenna selection a total of $\binom{N_t}{L_t}\binom{N_r}{L_r}$ evaluation of the selection criteria is needed. Usually, the selection criteria goal is to maximize the channel capacity or minimize the BER.

Based on the system model in Figure 4.1, the received signal at an instant index time n is given by:

$$\mathbf{y}[n] = \mathbf{H}\mathbf{x}[n] + \mathbf{n}[n], \tag{4.1}$$

where $\mathbf{H}$ is a $N_r \times N_t$ matrix

$$\mathbf{H} = \begin{pmatrix} h_{11} & h_{12} & \cdots & h_{1N_t} \\ h_{21} & h_{22} & \cdots & h_{2N_t} \\ \vdots & \vdots & \ddots & \vdots \\ h_{N_r1} & h_{N_r2} & \cdots & h_{N_rN_t} \end{pmatrix}, \tag{4.2}$$

where the element h_{ij} represents the channel transfer coefficient between transmitter j and receiver i. $\mathbf{x}[n]$ is the transmitted vector of size $(N_t \times 1)$ at instant time n and $\mathbf{n}[n]$ represents the vector of additive white gaussian noise (AWGN) of size $N_r \times 1$. The elements h_{ij}, of the matrix $\mathbf{H}$ are complex gaussian random variables with zero mean and 0.5 variance per dimension. The elements of $\mathbf{n}[n]$ are random gaussian variables with zero mean and $N_0/2$ variance per dimension. Only otherwise stated, it is assumed that all the channels are independent and the channel state information (CSI) is perfectly known at the receiver, but not at the transmitter. In a quasi static fading channel, the channel coefficients are considered constant during one frame but they change independently from frame to frame. In a block fading channel, the channel coefficients are considered constant during one block of symbols, but they change independently from one block to another. In both cases, the channel is considered a non-frequency selective channel (Flat-fading channel). This is the case when the coherence bandwidth of the channel is much larger than the bandwidth of the transmitted signal. We consider the following two main selection criteria which maximize the channel capacity and maximize the SNR.

4.1.1 Antenna Selection Scheme based on the Channel Capacity

When the channel state information is not known at the transmitter, which is the case for many situations, the transmitted power should be distributed equally through all transmitted antennas. Hence, the signal to noise ratio (SNR) in each receive antenna is given by [13]:

$$\rho \doteq \frac{P}{N_o B}, \tag{4.3}$$

where P is the total transmitted power and B is the transmitted bandwidth. If we define the ratio $\gamma \doteq E_b/N_o$, where E_b is the average energy per transmitted bit, the relation between ρ and γ is then given by:

$$\gamma = \frac{\rho}{R}, \tag{4.4}$$

where R represents the information transmitted rate in bits/s/Hz. The channel capacity of MIMO system using all antennas at the transmitter and at the receiver sides (no-selection) is given by [13]:

$$C = \log_2 \left[\det \left(I_{N_r} + \frac{\rho}{N_t} \mathbf{H}\mathbf{H}^\dagger \right) \right]. \tag{4.5}$$

.

In [33], it was shown that in receive antenna selection, when the receiver selects the best L_r antennas out of N_r antennas that maximize the channel capacity in (4.5), the channel capacity of the selected channel matrix is upper bounded by:

$$C_{\text{select}} \leq \sum_{i=1}^{L_r} \log_2 \left(1 + \frac{\rho}{N_t} \gamma_i \right), \tag{4.6}$$

where γ_i represents the squared norm of the ith line of the matrix $\mathbf{H}$, after ascending ordering. Hence, γ_i are ordered random variables with a Chi-square distribution. This upper bound is tight enough for $L_r < N_r$. It was also shown that the channel capacity of MIMO systems is maintained provided that the number of selected antennas in one side is at least equal to the number of available antennas at the other side. While the antenna selection maintains the majority of the promised capacity by MIMO systems, the computation level due to the selection algorithm complexity is quite large because there are $\left(\begin{smallmatrix} N_r \\ L_r \end{smallmatrix} \right)$ possibilities for selection from each side. In order to reduce the computation complexity, many sub-optimal antenna selection algorithms have been proposed with no extensive loss in capacity compared to optimal selection [33]. When the transmission data rate is larger than the instantaneous mutual information, an outage event appears. In a quasi static fading chanel, where the channel coefficients are constant during all the frame, it is not possible to quantify with an average measure. In such situation, the Shannon capacity is essentially a random variable. The probability of such event is known as *outage probability*. This probability for high SNR regions, when the best L_r receive antennas are selected, is upper bounded by [46]:

$$\mathcal{P}_{select} \leq k_o \gamma^{-N_t N_r}, \tag{4.7}$$

where

$$k_o = \frac{\left(\frac{2^R - 1}{R} \left(\begin{array}{c} N_r \\ L_r \end{array} \right) N_r N_t \right)^{N_r N_t}}{(N_t N_r)!}, \tag{4.8}$$

We can see from Equation (4.7) that the diversity order, expressed by the N_tN_r exponent, is the same for a MIMO system without antenna selection ($L_r = N_r$) and for a MIMO system with receive antenna selection ($L_r < N_r$), and this is true for any value of N_r, N_t, and L_r. However, this expression cannot be used to quantify the outage probability, simply because the upper bound gap is large. For that reason, the authors of [46] used another expression to quantify the degradation of the SNR (ρ) due to receive antenna selection. This expression is given by [46]:

$$\mathcal{P}_{select} \leq P_r \left(\sum_{i=N_r-L_r+1}^{N_r} X_{i:N_r} \leq \left(2^{R/L_r} - 1\right) \frac{N_t L_r}{\rho} \delta \right), \tag{4.9}$$

where $\delta = 10^{\zeta/10}$, $X_{i:N_r}$ represents the diagonal elements of the matrix $\mathbf{HH}^H$ after ordering (random variables with Chi-Square distribution with $2N$ degrees of freedom) and ζ represents the maximum deviation between the lower bound and the exact value of outage probability. This deviation is expressed by [46]:

$$\zeta = 10 \log_{10} \left[\frac{2^R}{(2^{R/N_r} - 1) N_r} \left(\frac{N_r - 1}{N_r} \right)^{N_r - 1} \right]. \tag{4.10}$$

Equation (4.10) represents an approximation of the degradation of the SNR due to antennas selection.

4.1.2 Antenna Selection Scheme based on the SNR

The antenna selection based on the instantaneous signal to noise ratio (SNR) is more attractive because it is more practical than the one based on the maximization of channel capacity. In the following, we consider the impact of receive antenna selection for MIMO systems using the orthogonal space time block coding (OSTBC). Many upper bounds of the probability of bit error rate (BER) of OSTBC have been derived in [58], for an arbitrary number of transmit antennas and receive antennas as well as arbitrary number of selected antennas. In case of BPSK constellation and Maximum Likelihood Decoding (MLD), the probability of error per bit of a MIMO system without selection, for high SNR, is approximated by [39]:

$$P_b(e) \approx \left(\begin{array}{c} 2N_tN_r - 1 \\ N_tN_r \end{array} \right) \left(4 \frac{E_s}{N_0} \right)^{-N_tN_r}, \tag{4.11}$$

where E_s is the average energy per transmitted symbol, and $N_0/2$ is the variance (per dimension) of the complex additive white Gaussian noise (AWGN). It clearly shows that the

diversity order is $N_t N_r$. In [58], it was shown that when the best L_r antennas were selected among N_r antennas, the probability of error is approximated by:

$$P_b(e) \approx \left(\begin{array}{c} 2N_t N_r - 1 \\ N_t N_r \end{array} \right) \left(4 \frac{L_r}{N_r} \frac{E_s}{N_0} \right)^{-N_t N_r}. \tag{4.12}$$

.

Comparing equation (4.11) with (4.12), we can conclude that, for $L_r < N_r$, the diversity order does not change with antenna selection compared to MIMO system using all the antennas. In addition, it is easy to notice that the SNR reduction due to receive antenna selection is upper bounded by $10\log_{10}(N_r/L_r)$ dB. In [58], an exact bound was derived when the receiver selects the best antennas.

4.1.3 Antenna Selection Algorithms

Many algorithms for antenna selection have been published in the literature [10], [37], [56], which can be classified as receive antennas selection, transmit antenna selection or joint transmit-receive antenna selection. Furthermore as discussed earlier, antenna selection algorithms can also be classified based on the selection criterion such as:

– selection based on the maximization of channel capacity (C)

– selection based on the minimisation of error probability (BER)

Antenna selection algorithms that minimize the bit error probability will necessarily minimize the pairwise error probability (PEP) and the union bound. The minimization of the bit error probability leads necessarily to maximizing the instantaneous signal to noise ratio. On the other hand, maximizing the capacity does not lead to maximizing the signal to noise ratio. Intuitively, maximizing capacity and maximizing the signal to noise ratio appear to be equivalent. But this is not always the case in theory. In fact, antenna selection based on maximizing the SNR does not lead necessarily to channel capacity maximization. This is attributed to the fact that the capacity is much more affected by the phase difference between the antenna elements than the instantaneous signal to noise ratio. On the other hand, maximizing the received SNR leads, necessarily, to the minimization of the BER. It then follows that the algorithms based on the SNR maximizing are equivalent to those based on minimization of the BER. In what follows, we present the different algorithms for antenna selection.

Norm Based Selection Algorithm (NBS)

The simplest algorithm for antenna selection is known as *Norm Based Selection* (NBS) [18]. The principle of the algorithm is to select the receive antennas subset that maximize the Frobenius norm of the channel. This method does not require too much computation, but does not provide a good performance. The algorithm was developed for systems using orthogonal space-time block coding (OSTBC), particularly the Alamouti coding [18]. The choice of the Frobenius norm as a selection criterion is motivated by the fact that the signal to noise ratio and, therefore, the probability of error, depend on the Frobenius norm. In fact, for OSTBC systems, the received signal to noise ratio is given by [5]:

$$\gamma = \gamma_o \|\mathbf{H}\|_F^2, \tag{4.13}$$

where $\gamma_o = E_s/(N_t N_o)$ and $\|\mathbf{H}\|_F^2$ is the Frobenius norm of the matrix $\mathbf{H}$ defined by:

$$\|\mathbf{H}\|_F^2 = \sum_{i=1}^{N_r} \sum_{j=1}^{N_t} |h_{ij}|^2. \tag{4.14}$$

where h_{ij} represents the elements of the channel matrix $\mathbf{H}$ as defined in section 4.1. The symbol probability error P_e is then upper bounded by [18]:

$$P_e \ \leq \ e^{-d\gamma_o \|\mathbf{H}\|_F^2}, \tag{4.15}$$

where d is a constant that depends on the modulation order. From equations (4.15) and (4.13), it is clear that maximizing the Frobenius norm inevitably leads to maximizing the SNR and at the same time minimizing the instantaneous probability of error. For this algorithm, two analyzes have been developed to quantify the performance [18]. The first analysis is based on the average signal to noise ratio. This analysis is general and can be applied to any orthogonal space time block codes. The second analysis focuses on the *outage probability*. The capacity analysis is limited to the case of a transmit selection with Alamouti coding. Following this analysis, the antenna selection gain in terms of the average signal to noise ratio is expressed by [18]:

$$g = \log_{10}\left(\frac{\mathcal{E}\{\gamma\}}{\gamma_o L_r L_t}\right) = \log_{10}\left(\frac{\mathcal{E}\{\sum_{i=1\ldots L_t} {T_{n_i}}^2\}}{L_r L_t}\right), \tag{4.16}$$

where $\gamma_o L_r L_t$ is the signal to noise ratio (SNR) for the orthogonal space time codes without antennas selection and $\mathcal{E}\{\gamma\}$ is the average signal to noise ratio for orthogonal space time codes with antenna selection given by [18]:

$$\mathcal{E}\{\gamma\} = \gamma_o \mathcal{E}\{\|\mathbf{H}\|_F^2\} = \gamma_o \sum_{i=1}^{N_t} \mathcal{E}\{T_{n_i}^2\}, \tag{4.17}$$

where T_k $(k = 1, 2, ..., N_t)$ is the Frobenius norm of the N_t columns of the channel matrix $\mathbf{H}$. In [18], the gain (Equation (4.16)), g, is found to be substantial.

Correlation Based selection Algorithm (CBS)

Although the NBS algorithm is simple and straightforward to implement, its major drawback is that it does not provide a good performance. An alternative to this algorithm has been proposed in [10]. This method is based on the correlation between the lines of the channel matrix. The method is to find two lines with a strong correlation and then delete the one having low power. This process is repeated until $(N_r - L_r)$ lines are eliminated. With this algorithm, it is possible to get L_r lines with a minimum of correlation and maximum power.

Optimal Selection

The capacity of a $(N_t \times N_r)$ MIMO system using all antennas is given by [10]:

$$C_{\text{full}} = \log_2 \left[\det \left(I_{N_r} + \frac{\bar{\Gamma}}{N_t} \mathbf{H}\mathbf{H}^\dagger \right) \right], \tag{4.18}$$

where I_{N_r} is the identity matrix of size $(N_r \times N_r)$, $\bar{\Gamma}$ is the signal to noise ratio per MIMO branch and the sign † indicate the Hermitian transpose. After receive antenna selection of L_r antennas that maximize the channel capacity, the equation in 4.18 becomes:

$$C_{\text{select}} = \max_{S(\mathbf{H}_{\text{W}})} \left(\log_2 \left[\det \left(I_{L_r} + \frac{\bar{\Gamma}}{N_t} \mathbf{H}_{\text{W}} \mathbf{H}_{\text{W}}^\dagger \right) \right] \right), \tag{4.19}$$

where $\mathbf{H}_{\text{W}}$ is obtained by deleting $(N_r - L_r)$ rows of the original matrix $\mathbf{H}$ and $S(\mathbf{H}_{\text{W}})$ represents the set of all possible $\mathbf{H}_{\text{W}}$. The optimal antenna selection necessitates the calculation of $\binom{N_r}{L_r}$ determinants, which is time consuming. For this reason, authors presented a

sub-optimal algorithm allowing the reduction of complexity calculation [10].

Sub-Optimal Selection

The sub-optimal algorithm proposed by the authors [10] is based on the following equality:

$$\det\left(I_{L_r}+\frac{\bar{\Gamma}}{N_t}\mathbf{H}_{\mathrm{W}}\mathbf{H}_{\mathrm{W}}^{\dagger}\right)=\prod_{k=1}^{r}\left(1+\frac{\bar{\Gamma}}{N_t}{\lambda_k}^2\right), \tag{4.20}$$

where r represents the rank of the channel matrix and λ_k are the singular values of $\mathbf{H}_{\mathrm{W}}$. The rank and the singular values should then be maximised in order to maximize the capacity. When two rows (h_k and h_l) of the matrix $\mathbf{H}$ are identical, one of these two rows can be eliminated. The power of each row ($\|h_k\|^2$) is also calculated in order to select the row with highest power. If two rows have different powers, the row with the highest power is selected and the other is rejected. Where there are no identical rows in the matrix, the rows with high correlation are deleted. In this manner, we obtain a matrix $\mathbf{H}_{\mathrm{W}}$ having low correlated rows and with higher power.

The algorithm from [10] is the following:

1. The channel vector h_k is defined as the $k-th$ row of the matrix $\mathbf{H}$, where k is an element of the set $X=\{1,2,....,N_r\}$.
2. for all k and l $(k,l\in X)$, $k>l$, calculate the correlation $\Xi(k,l)$. The correlation $\Xi(k,l)$ is defined as $\Xi(k,l)=|\langle h_k,h_l\rangle|$.
3. Loop

   a) Choose the l (with $k,l\in X, k>l$) that give the largest correlation $\Xi(k,l)$.

   b) if $\|h_k\|^2>\|h_l\|^2$, eliminate h_l, otherwise, eliminate h_k. Delete l (or k) from X.

   c) repeat steps a) and b) until N_r-L_r rows are eliminated.

Un-Correlated Based Selection Algorithm (UCBS)

One of the disadvantages of the CBS algorithm is that it requires the computation of the correlation of all the rows of the channel matrix. In addition, it creates a lot of loss in capacity compared to the optimal selection. To overcome these drawbacks, the authors of [37] presented a new algorithm and made changes to the CBS algorithm to improve its performance in terms of capacity.

The UCBS algorithm is intended only for the receive antenna selection. The receiver has L_r receive antennas and N_r RF receive chains, where $L_R < N_r$. At the transmitter side, the number of antennas and RF chains are equal ($N_t = L_t$). The goal of the UCBS algorithm is to maximize the channel capacity. It is an algorithm that is based on the norm and the non-correlation between the rows of channel matrix. The algorithm considers a MIMO system equipped with N_t antennas at the transmitter and N_r antennas at the receiver. The channel is assumed to be quasi-static with a non-frequency selective Rayleigh fading. In this case, the input-output relationship of the MIMO system can be expressed as [37]:

$$\mathbf{y} = \sqrt{\frac{\rho}{N_t}}\mathbf{H}\mathbf{x} + \mathbf{n}, \tag{4.21}$$

where $\mathbf{y}$ is an $(N_r \times 1)$ received vector, $\mathbf{x}$ represents the transmitted vector of size $(N_t \times 1)$, $\mathbf{n}$ is an additive white gaussian noise (AWGN) with $(N_o/2)$ per dimension, ρ is the average signal to noise ration at each receive antenna and $\mathbf{H}$ is the MIMO channel matrix of size $(N_r \times N_t)$. The channel is supposed to be perfectly known at the receiver but not at the transmitter side. The expression of the MIMO channel capacity when the channel state information is not available at the transmitter can be given by [51]:

$$C(\mathbf{H}) = \log_2 \left[\det \left(\mathbf{I}_{N_t} + \frac{\rho}{N_t}\mathbf{H}^{\dagger}\mathbf{H} \right) \right], \tag{4.22}$$

$$C(\mathbf{H}) = \log_2 \left[\det \left(\mathbf{I}_{N_r} + \frac{\rho}{N_t}\mathbf{H}\mathbf{H}^{\dagger} \right) \right], \tag{4.23}$$

where $\mathbf{I}_{N_r}$ is the $N_r \times N_r$ identity matrix, $(.)^{\dagger}$ represents the Hermitian transpose, and det(.) is the matrix determinant.

The principle of the selection algorithm is to select the best L_r receive antennas among N_r available based on the capacity maximization. We denote by $\mathbf{w}$ the subset of indices of selected antennas (Example: $\mathbf{w} = \{2, 3, 5\}$ means that the second, third and fifth antennas have been selected). The channel matrix corresponding to the selected antennas $\mathbf{w}$ is denoted by $\mathbf{H}_{\mathrm{W}}$. With these notations, the channel capacity is determined by:

$$C(\mathbf{H}_{\mathbf{w}}) = \log_2 \left[det \left(\mathbf{I}_{L_r} + \frac{\rho}{N_t}\mathbf{H}_{\mathbf{w}}\mathbf{H}_{\mathbf{w}}^{\dagger} \right) \right], \tag{4.24}$$

The purpose of selection algorithm is to find the matrix $\mathbf{H_w}$ that maximizes the channel capacity $C(\mathbf{H_w})$. The optimal selection method is an exhaustive search of all possible combinations to find the antennas set that provides the maximum channel capacity. However, this requires the computation of $\left(\begin{smallmatrix} N_r \\ L_r \end{smallmatrix} \right)$ determinants for each channel realization. To illustrate this method, consider the case of a system where we want to select two antennas among the eight available antennas. In this case, the optimal method requires computation of:

$$\left(\begin{array}{c} N_r \\ L_r \end{array} \right) = \left(\begin{array}{c} 8 \\ 2 \end{array} \right) = \frac{8!}{2! \,.\, (8-2)!} = 28 \tag{4.25}$$

determinants. It is clear that the computational complexity becomes very large. This is the reason for the interest in the development of sub-optimal antenna selection algorithms. The idea behind the UCBS algorithm is to determine the matrix $\mathbf{H_w}$ by providing easier computations than the required determinants. To this end, the matrix $\mathbf{H_w}$ is decomposed into singular values (SVD). The channel capacity in terms of singular values decomposition is then given by [37]:

$$C(\mathbf{H_w}) = \sum_{j=1}^{r} \log_2 \left[det \left(\mathbf{I}_{L_r} + \frac{\rho}{N_t} |\lambda_j \left(\mathbf{H_w} \right)|^2 \right) \right], \tag{4.26}$$

where r is the rank of the channel matrix $\mathbf{H_w}$ and $\lambda_j \left(\mathbf{H_w} \right)$ represents the jth singular value of the matrix $(\mathbf{H_w})$. Based on Equation (4.26), we can notice that to maximize the channel capacity $C(\mathbf{H_w})$, it is imperative to maximize the singular values (λ_j) and the rank (r) of the matrix $\mathbf{H_w}$. The problem becomes then to find the matrix $\mathbf{H}_\mathrm{W}$ that has un-correlated rows and maximum norm.

The UCBS algorithm is based on two parameters, namely $\alpha_{i,j}$ and $\beta_{i,j}$, defined in the following way [37]:

$$\alpha_{i,j} = \frac{|\mathbf{h}_i \mathbf{h}_j{}^\dagger|}{\|\mathbf{h}_i\| \|\mathbf{h}_j\|}, \tag{4.27}$$

$$\beta_{i,j} = \sqrt{1 - {\alpha_{i,j}}^2}, \tag{4.28}$$

where $\mathbf{h}_i$ represents the ith row of the channel matrix $\mathbf{H}$ et $\|.\|$ is the vector Euclidian norm. The value of $\alpha_{i,j}$ represents the correlation between the ith and jth rows of the channel matrix $\mathbf{H}$. Consequently, $\beta_{i,j}$ corresponds to the non-correlation between ith row and jth row of the channel matrix $\mathbf{H}$. The proposed selection algorithm adopts an incremental procedure. The

procedure begins with an empty set of selected antennas. In each step of the algorithm, one antenna is added to this set. Thereby, as the first step, the row with high Euclidian Norm is selected. In the next step, the two parameters in equations (4.27) and (4.28) are calculated with respect to the selected antenna in the first step for all remaining antennas. The antenna that maximize a cost function $f_{n,j}$ is then selected and added to the selected antenna in the first step. The cost function of the jth row is defined as follow:

$$f_{n,j} = \begin{cases} \|\mathbf{h}_j\|^2, & \text{if} \quad n = 1 \\ \|\mathbf{h}_j\|^2 \sum_{m=1}^{n-1} {\beta^2}_{w_m,j} & \text{if} \quad n \geq 2 \end{cases} \tag{4.29}$$

where w_m is the mth selected antenna index. Hence, at each step, the selection rule is to find the index w_m of the receive antenna that maximizes the cost function $f_{n,j}$, i.e.

$$w_n = \arg \max_{j \in S_n} f_{n,j}, \tag{4.30}$$

where S_n is the set of indices of receiving antennas which have not been selected in the previous step. The procedure ends when all necessary antennas are chosen. Thus, the proposed algorithm provides L_r receive antennas corresponding to the rows with a minimum of correlation between them and having the maximum power.

Selection of two Rx antennas:

We Consider the specific case of selecting two antennas ($L_r = 2$). The $\hat{\mathbf{H}}_{\mathrm{W}}$ channel matrix that maximize the channel capacity is found as follows:

$$\begin{aligned} \hat{\mathbf{H}}_{\mathrm{W}} &= \arg \max_{\mathbf{H}_{\mathrm{W}}} \left[\log_2 \left[\det \left(\mathbf{I}_{Lr} + \frac{\rho}{N_t} \mathbf{H}_{\mathrm{W}} {\mathbf{H}_{\mathrm{W}}}^{\dagger} \right) \right] \right] \\ &= \arg \max_{\mathbf{H}_{\mathrm{W}}} \left[\det \left(\mathbf{I}_{Lr} + \frac{\rho}{N_t} \mathbf{H}_{\mathrm{W}} {\mathbf{H}_{\mathrm{W}}}^{\dagger} \right) \right]. \end{aligned} \tag{4.31}$$

For high SNR values, the equation (4.31) can be approximated by:

$$\begin{aligned} \hat{\mathbf{H}}_{\mathrm{W}} &\approx \arg \max_{\mathbf{H}_{\mathrm{W}}} \left[\det \left(\frac{\rho}{N_t} \mathbf{H}_{\mathrm{W}} {\mathbf{H}_{\mathrm{W}}}^{\dagger} \right) \right] \\ &= \arg \max_{\mathbf{H}_{\mathrm{W}}} \left[\det \left(\mathbf{H}_{\mathrm{W}} {\mathbf{H}_{\mathrm{W}}}^{\dagger} \right) \right]. \end{aligned} \tag{4.32}$$

.

Table 4.1 UCBS Selection Algorithm

1	$S = \{1, 2, 3, ..., Nr\}$
2	for $j = 1$ to Nr
3	$\quad {\beta_j}^2 = 0$
4	$\quad \gamma_j = \|\mathbf{h}_j\|$
5	end
6	$w = \arg\max {\gamma_j}^2$
7	for $n = 2$ to L_r
8	$\quad S = S - \{w\}$
9	$\quad$ for all $j \in S$
10	$\quad\quad \alpha_j = \frac{\|\mathbf{h}_w {\mathbf{h}_j}^H\|}{\gamma_w \gamma_j}$
11	$\quad\quad {\beta_j}^2 = {\beta_j}^2 + (1 - {\alpha_j}^2)$
12	$\quad\quad {f_j} = {\gamma_j}^2 {\beta_j}^2$
13	$\quad$ end
14	$\quad w = \arg\max {f_j}^2$
15	end
16	return $\{1, 2, 3, ..., N_r\} - S$

In the first step, the index w_1 of the row with high Euclidian Norm is found. By taking into account the index w_1 of the first selected antenna, the determinant term in Equation (4.32) can be developed as follows:

$$\begin{aligned}
\det(\mathbf{H}_{\mathrm{W}}\mathbf{H}_{\mathrm{W}}{}^{\dagger}) &= \det\left(\begin{bmatrix}\mathbf{h}_{w1}\\ \mathbf{h}_j\end{bmatrix}\begin{bmatrix}\mathbf{h}_{w1}{}^{\dagger} & \mathbf{h}_j{}^{\dagger}\end{bmatrix}\right)\\
&= \det\left(\begin{bmatrix}\|\mathbf{h}_{w1}\|^2 & \mathbf{h}_{w1}\mathbf{h}_j{}^{\dagger}\\ \mathbf{h}_j\mathbf{h}_{w1}{}^{\dagger} & \|\mathbf{h}_j\|^2\end{bmatrix}\right)\\
&= \|\mathbf{h}_{w1}\|^2\|\mathbf{h}_j\|^2 - (\mathbf{h}_{w1}\mathbf{h}_j{}^{\dagger})(\mathbf{h}_j\mathbf{h}_{w1}{}^{\dagger})\\
&= \|\mathbf{h}_{w1}\|^2\|\mathbf{h}_j\|^2 - |\mathbf{h}_{w1}\mathbf{h}_j{}^{\dagger}|^2\\
&= \|\mathbf{h}_{w1}\|^2\|\mathbf{h}_j\|^2\left(1 - \left(\frac{|\mathbf{h}_{w1}\mathbf{h}_j{}^{\dagger}|}{\|\mathbf{h}_{w1}\|\|\mathbf{h}_j\|}\right)^2\right)\\
&= \|\mathbf{h}_{w1}\|^2\|\mathbf{h}_j\|^2(1 - \alpha_{w1,j}^2)\\
&= \|\mathbf{h}_{w1}\|^2\|\mathbf{h}_j\|^2\beta_{w1,j}^2
\end{aligned} \tag{4.33}$$

$$\hat{\mathbf{H}}_{\mathrm{W}} = \arg\max_{\mathbf{H}_{\mathrm{W}}}\left[\|\mathbf{h}_{w1}\|^2\|\mathbf{h}_j\|^2\beta_{w1,j}^2\right] \tag{4.34}$$

.

The antenna index, w_2, that has to be selected in the second step is therefore given by:

$$w_2 = \arg\max_{j \in S_2} \left[\|\mathbf{h}_j\|^2 \beta_{w1,j}^2 \right] \tag{4.35}$$

where S_2 is the set of receive antennas indices except the index w_1. The detailed algorithm is summarized in Table 4.1.

Modified UCBS Algorithm (MUCBS)

In the previously introduced algorithms, the aim of the antenna selection was either to maximize capacity or minimize error probability. For example, the goal of the algorithm UCBS was only to maximize capacity. The performance of this algorithm in terms of error probability have not been discussed. The same observation can be made for the CBS algorithm. The NBS algorithm maximizes only the signal to noise ratio. In the MUCBS algorithm [56], the possibility of selecting antennas has been developed by maximizing channel capacity and minimizing the probability of error at the same time. The goal of the MUCBS algorithm is to select antennas so as to both maximize the capacity and minimize the probability of error. The algorithm uses based on the same principle as the UCBS algorithm but with some modifications in order to minimize the probability of error as well as maximizing the channel capacity. Hence the name of Modified UCBS algorithm (MUCBS). The MUCBS algorithm is intended only for the selection of receiver antennas. In a system with a total of N_r antennas, the selection of L_r ($L_r < N_r$) antennas is performed in two main steps. The first step selects L_c antennas that maximize capacity. In the second step, L_e new antennas are selected among the $(N_r - L_c)$ remaining antennas. The selection of L_e antennas in the second step is based on the fact that the entire L_s ($L_s = L_c + L_e$) antennas possess a minimum pairwise error probability (PEP). The the channel capacity maximization is identical to that used in UCBS algorithm. The details of this maximization were already provided in the previous section. In what follows, we present only the minimization of pairwise error probability (PEP).

Once the new L_e antennas are selected, L_s antennas are determined. The channel matrix corresponds corresponding to $(L_S \times N_t)$ antennas is then denoted by $\mathbf{H}_s$. Performing the singular value decomposition of the matrix $\mathbf{H}_s$, we get:

$$\mathbf{H}_s = \mathbf{U}\mathbf{\Delta}\mathbf{V}^H \tag{4.36}$$

where $\mathbf{U}$ and $\mathbf{V}$ are unitary matrices, and $\mathbf{\Delta}$ is the diagonal matrix of singular values specified by $\mathbf{\Delta} = \{\lambda_1, \lambda_2, ..., \lambda_{L_s}\}$. These $\lambda_i (i = 1, 2, ..., L_s)$ represent the singular values of $\mathbf{H}_s$

and $\lambda_1 \geq \lambda_2 \geq ..... \geq \lambda_{L_s}$.

For MUCBS algorithm, the rule of selection based on minimisation of PEP is to find the index $\mathbf{w}_s$ of the receive antenna that maximizes the minimum eigenvalue of $\mathbf{H}_s$ as follows [56]:

$$\mathbf{w}_s = \arg \max_{\mathrm{W}_s \in S} \lambda_{L_s}(\mathbf{H}_s), \tag{4.37}$$

where S is the set of the remaining antennas indices that has not be selected in the previous step.

4.2 Performance Evaluation of UCBS Antenna Selection Algorithm

In this section, we present an evaluation of the performance of antenna selection in MIMO systems using the UCBS algorithm through MATLAB simulations. In a first step, the impact of this algorithm on the capacity has been obtained. Subsequently, we applied the UCBS algorithm for a system using Alamouti space-time coding and its performance in terms of bit error rate was evaluated.

4.2.1 Impact of the UCBS Algorithm on the capacity of MIMO systems

The system which is considered is a MIMO system with two transmit antennas and eight receiving antennas ($N_t = 2, N_r = 8$). For Monte-Carlo simulations, we generated random realisation of the channel matrix $\mathbf{H}$. For an exhaustive research, we have created a complete set $S(\mathbf{H}_{\mathrm{W}})$ of all possible matrices $\mathbf{H}_{\mathrm{W}}$ by eliminating all possible permutations $(N_r - L_r)$ rows of the matrix realisation $\mathbf{H}$. The size of the matrix $\mathbf{H}_{\mathrm{W}}$ is (2×2), because we have to select two antennas elements ($L_r = 2$) among eight available antennas. For each element of the set S, we have computed the capacity using equation (4.5) and selected the element that has the largest value of capacity. The results of this calculation correspond to the capacity of a (2×2) system with the selection of two optimal antennas among eight available antennas. The cumulative distribution function of this capacity is represented by the red curve in Figure 4.2. The capacity of a (2×2) MIMO system without antenna selection is obtained by randomly eliminating $(N_r - L_r)$ rows of the realisation matrix $\mathbf{H}$. The cumulative distribution function of the capacity is represented by the blue curve in Figure 4.2. The channel capacity of a system with selection, using the UCBS algorithm is obtained as follows. For each realization of the channel, $\mathbf{H}$, we apply the UCBS algorithm to determine the selected rows of the matrix $\mathbf{H}$. For each of these sub-matrices $\mathbf{H}_{\mathrm{W}}$, we evaluate the channel capacity. The result of this calculation corresponds to the capacity of a MIMO system (2×2) with antenna selection. The cumulative distribution functions of the channel capacity with antenna selection using UCBS

algorithm and with optimal selection (2×2) are represented in Figure 4.2. To compare the

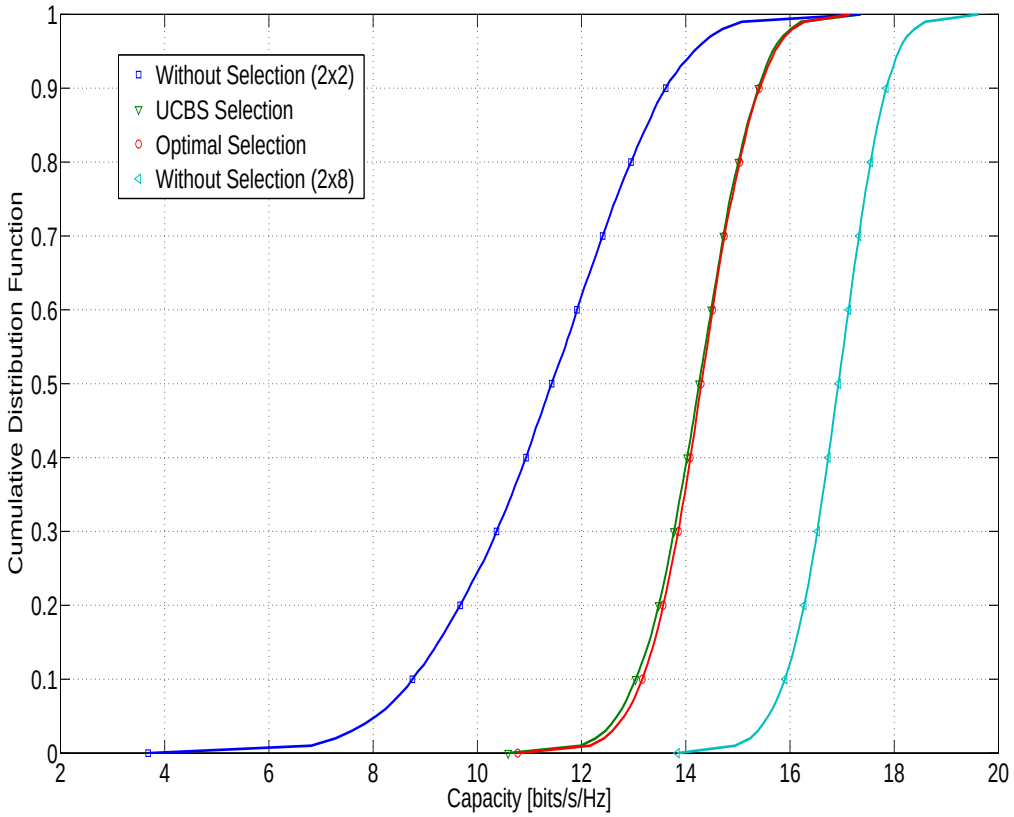

Figure 4.2 MIMO Capacity with Antennas Selection, $N_t = 2, N_r = 8, L_r = 2$ and SNR = 20 dB

results with a complex system, the capacity of a (2×8) MIMO system was also calculated. The cumulative distribution function of this capability is represented by the right curve in Figure 4.2. All of cumulative distributions functions(cdf) of the channel capacity were obtained for a signal to noise ratio equal to 20dB. We notice the antenna selection technique increases considerably the capacity relative to a system without antenna selection. Selecting two out of eight receive antennas leads to about 3 bits/s/Hz gain in terms of ergodic capacity as compared to the (2×2) system without selection. However, compared to the complex system (2×8), the system with a selection represents a loss of nearly 2.5 bits/s/Hz. More importantly, we see that the capacity obtained by UCBS algorithm is very close to that obtained by the optimal selection procedure.

4.3 BER Analysis of the MIMO STBC System using Receive Antenna Selection

In this section, we present an analytical performance evaluation of the 2×2 wireless MIMO Alamouti coding scheme using receive antenna selection. Complete knowledge of the Channel State Information (CSI) at the receiver, i.e., perfect knowledge of both the symbol synchronisation and the channel gains, and a MIMO model of uncorrelated Rayleigh fading subchannels are assumed. A receive selection algorithm based on the maximizing SNR is used to select two antennas. Under these assumptions, we derive the exact average BER for Binary Phase Shift Keying (BPSK) modulation using the Moment Generating Function (MGF) and the order statistics associated with the instantaneous SNR at the two selected receive antennas. We consider a wireless communication system with 2 transmit antennas and $N_r \geq 2$ receive antennas (Figure 4.1). It is assumed that the amplitudes of fading from each transmit antenna to each receive antenna are mutually uncorrelated Rayleigh distributed. We also assume that CSI is known at the receiver [14]. At each time the two transmit antennas send Alamouti coded blocks and two receive antennas are selected according to the best and next best SNR. Let $\mathbf{H} = [h_{i,j}]$ denote the $N_r \times 2$ MIMO channel matrix, where $h_{i,j}$ is the fading coefficient between transmit and receive antenna, $j = 1, 2$, $i = 1, 2, ..., N_r$ respectively, a sample of independent complex Gaussian random variables with zero mean and variance $1/2$ per dimension. For decoding purposes, a 2×2 matrix $\widetilde{\mathbf{H}}$, a subset of $\mathbf{H}$, is used to denote the channel between the two selected receive antennas. The corresponding receiver SNR for the Alamouti scheme [5] is then given by [18]:

$$\gamma = \frac{\gamma_0}{2} \left\| \widetilde{\mathbf{H}} \right\|_F^2 \tag{4.38}$$

where $\|.\|_F^2$ denote the Frobenius norm, $\gamma_0 = E_b/N_0$ is the average total energy per bit at the transmitter and N_0 the one-sided power spectral density of the additive white Gaussian noise (AWGN). For a BPSK modulation scheme, the instantaneous BER of a SISO system for coherent demodulation is given as [39]

$$P_e = \frac{1}{2} erfc(\sqrt{\gamma}) \tag{4.39}$$

where γ is the instantaneous SNR at the receiver.

In the selection process, we choose the two receive antennas $i(1), i(2)$ such that

$$\widetilde{\mathbf{H}} = \begin{bmatrix} h_{i(1),1} & h_{i(1),2} \\ h_{i(2),1} & h_{i(2),2} \end{bmatrix} \tag{4.40}$$

where

$$i(1) = \arg \max_{i \in \{1,2...N_r\}} \{|h_{i,1}|^2 + |h_{i,2}|^2\} \quad (4.41)$$

$$i(2) = \arg \max_{\substack{i \in \{1,2...N_r\} \\ i \neq i(1)}} \{|h_{i,1}|^2 + |h_{i,2}|^2\} \quad (4.42)$$

.

To derive an expression of the average BER, we must determine the joint probability density function of $i(1)$ and $i(2)$. This is done in the forthcoming section.

4.3.1 Error analysis of the receive antenna selection scheme

In this section, we derive the exact BER expression for the proposed selection scheme over quasi-static flat Rayleigh fading channels for any $N_r \geq 2$. Let $Y_i = |h_{i,1}|^2 + |h_{i,2}|^2$ be the instantaneous normalized channel power received at antenna i. It is known [39] that the Y_i , $i = 1, 2, ..., N_r$, are i.i.d. chi-squared random variables with 4 degrees of freedom and with probability density [39]

$$f_Y(x) = \begin{cases} xe^{-x} & if\ x \geq 0 \\ \\ 0 & otherwise \end{cases} \quad (4.43)$$

and a cumulative distribution function

$$F_Y(x) = \begin{cases} 1 - e^{-x}(1+x) & if\ x \geq 0 \\ \\ 0 & otherwise \end{cases} \quad (4.44)$$

Rearranging the random variables Y_i in descending order as $\{ Y_{i(1)}, Y_{i(2)}...Y_{i(N_r)} \}$ where $Y_{i(1)} \geq Y_{i(2)} \geq ... \geq Y_{i(N_r)}$, the joint probability density of the largest $\{Z_1 = Y_{i(1)}\}$ and the second largest $\{Z_2 = Y_{i(2)}\}$ variables is given as [11], [8]

$$f_{Z_1,Z_2}(x,y) = \begin{cases} N_r(N_r-1)f_Y(x)f_Y(y)F_Y(y)^{N_r-2} & if\ 0 \leq x \leq y < \infty \\ \\ 0 & otherwise \end{cases} \quad (4.45)$$

Finally, the random variable $\rho = Z_1 + Z_2$ represents the total instantaneous normalized channel power received by the 2×2 selection scheme and its probability density is readily obtained as [11]

$$f_\rho(x) = \begin{cases} \int_0^{x/2} f_{Z_1,Z_2}(x-u,u)du \quad if\ x \geq 0 \\ \\ 0 \qquad\qquad otherwise \end{cases} \tag{4.46}$$

Using (4.45), (4.44) and (4.43), the expression of (4.46) can be explicitly written as

$$f_\rho(x) = \begin{cases} N_r(N_r-1)\int_0^{x/2} G(x,u)du \quad if\ x \geq 0 \\ \\ 0 \qquad\qquad otherwise \end{cases} \tag{4.47}$$

where

$$G(x,u) = (x-u)ue^{-x}\left[1-e^{-u}(1+u)\right]^{N_r-2} \tag{4.48}$$

Straightforward but lengthly computations allow us to write $f_\rho(x)$ for $x \geq 0$ as

$$f_\rho(x) = \begin{cases} \frac{x^3}{6}e^{-x} \qquad\qquad\qquad if\ N_r = 2 \\ \\ N_r(N_r-1)e^{-x}(\frac{x^3}{12} + Ax + B + \sum_{j=1}^{N_r-2} e^{-j\frac{x}{2}} \\ \times \sum_{m=0}^{j+2} \alpha_{j,m}x^m) \qquad if\ N_r > 2 \end{cases} \tag{4.49}$$

Where the coefficients A,B, α are given by

$$\begin{aligned} A &= \sum_{j=1}^{N_r-2}(-1)^j \frac{(N_r-2)!}{(N_r-2-j)!}\sum_{i=0}^{j}\frac{(i+1)}{(j-i)!j^{i+2}} \\ B &= -\sum_{j=1}^{N_r-2}(-1)^j \frac{(N_r-2)!}{(N_r-2-j)!}\sum_{i=0}^{j}\frac{(i+1)(i+2)}{(j-i)!j^{i+3}} \\ for\ j &= 1,2...N_r-2 \\ \alpha_{j,0} &= (-1)^j \frac{(N_r-2)!}{(N_r-2-j)!}\sum_{i=0}^{j}\frac{(i+1)(i+2)}{(j-i)!j^{i+3}} \\ \alpha_{j,1} &= (-1)^j \frac{(N_r-2)!}{2(N_r-2-j)!}\sum_{i=0}^{j}\frac{i(i+1)}{(j-i)!j^{i+2}} \\ \alpha_{j,2} &= (-1)^j \frac{(N_r-2)!}{8(N_r-2-j)!}\sum_{i=0}^{j}\frac{(i+1)(i-2)}{(j-i)!j^{i+1}} \end{aligned}$$

$$for\ m = 3, 4...j+2$$

$$\begin{aligned}\alpha_{j,m} &= (-1)^j \frac{j^m (N_r-2)!}{2^m m!(N_r-2-j)!} \\ &\times \sum_{i=m-2}^{j} \frac{(i+1)(i+2-2m)}{(j-i)!j^{i+3}}\end{aligned}$$

Using the expression of (4.49), the moment generating function (MGF) of $\gamma = \frac{\gamma_0}{2}\rho$ can be obtained as [6]

$$\Phi_\gamma(s,\gamma_0) = \int_0^\infty e^{-s\frac{\gamma_o \rho}{2}} f_\rho(\rho) d\rho \tag{4.50}$$

Substituting (4.49) in (4.50), we obtain the expression of the MGF as

$$\Phi_\gamma(s,\gamma_0) = \begin{cases} \frac{16}{(s\gamma_0+2)^4} & if\ N_r = 2 \\ N_r(N_r-1)(\frac{8}{(s\gamma_0+2)^4} + \frac{4A}{(s\gamma_0+2)^2} + \frac{2B}{(s\gamma_0+2)} & \\ + \sum_{j=1}^{N_r-2} \sum_{m=0}^{j+2} \frac{\alpha_{j,m} m! 2^{m+1}}{(s\gamma_0+2+j)^{m+1}}) & if\ N_r > 2 \end{cases} \tag{4.51}$$

Finally, the BER for coherent binary signals is given by [6]

$$P_e(\gamma_0) = \frac{1}{\pi} \int_0^{\pi/2} \Phi_\gamma(\frac{1}{\sin(\theta)^2}, \gamma_o) d\theta \tag{4.52}$$

substituting (4.51) in (4.52) the BER can be obtained as:

$$P_e(\gamma_0) = \begin{cases} 16I(\gamma_0,0,4) & if\ N_r = 2 \\ N_r(N_r-1)[2^3 I(\gamma_0,0,4) & \\ +4.A.I(\gamma_0,0,2) + 2.B.I(\gamma_0,0,1) & \\ + \sum_{j=1}^{N_r-2} \sum_{m=0}^{j+2} \alpha_{j,m}.m!.2^{m+1} I(\gamma_0,j,m+1)] & \\ & if\ N_r > 2 \end{cases} \tag{4.53}$$

where

$$I(\gamma_0,j,k) = \frac{1}{\pi} \int_0^{\pi/2} \frac{1}{(\frac{\gamma_0}{\sin(\theta)^2} + 2 + j)^k} d\theta \tag{4.54}$$

is an auxiliary integral [21] which can be expressed in terms of known analytically defined functions as [21]

$$\begin{aligned} I(\gamma_0, j, k) &= \frac{1}{2\pi(\gamma_0 + j + 2)} B(\frac{1}{2}, k + \frac{1}{2}) \\ &\quad \times {}_2F_1\left(k, \frac{1}{2}, k+1; \frac{2+j}{\gamma_0 + j + 2}\right) \end{aligned} \tag{4.55}$$

where B(x,y) is the incomplete beta function [21] defined as

$$B(x, y) = \frac{\Gamma(x)\Gamma(y)}{\Gamma(x+y)} \int_0^1 u^{x-1}(1-u)^{y-1} du \tag{4.56}$$

and ${}_2F_1(\alpha, \beta, \gamma; z)$ is the Gauss Hypergeometric function [21]. Note that the Beta function $B(x, y)$ and the Gauss hypergeometric function ${}_2F_1(\alpha, \beta, \gamma; z)$ are provided for common mathematical software such as MATLAB, MAPLE and MATHEMATICA.

Numerical Results

In this section, we illustrate the analytical and simulation performance for the Alamouti scheme with receive antennas selection over un-correlated Rayleigh fading channels. The one rate Alamouti code is used. At a given symbol period, two signals are simultaneously transmitted from the two antennas. The signal transmitted from the first antenna is denoted by x_1 and from the second antenna by x_2. During the next symbol period signal $-{x_2}^*$ is transmitted from the first antenna, and signal ${x_1}^*$ is transmitted from the second antenna, where * is the complex conjugate operation [5].

$$\begin{bmatrix} x_1 & x_2 \\ -{x_2}^* & {x_1}^* \end{bmatrix} \tag{4.57}$$

It is assumed that the channel state information is exactly known at the receiver, such as on a static channel, where the channel gains can be obtained by sending a pilot sequence used for channel estimation [16]. In the simulations, we consider a (2×2) MIMO system with space-time block coding (Alamouti) and we evaluate the impact of antenna selection on the performance in terms of bit error rate. The BPSK modulation scheme is used. The number of RF chains is fixed ($L_r = 2$) but the number of available antennas ($N_r = 2, 3, 4, 6$) is variable. In a first step, we evaluate the performance of bit error rate for the case of $N_r = 2$ and $L_r = 2$. This case corresponds to the classical Alamouti system (2×2) without antenna selection. Thereafter, $N_r = 3$) is considered and $L_r = 2$ antennas are selected from $N_r = 3$ using UCBS algorithm. For this configuration, the BER performance is evaluated. The same

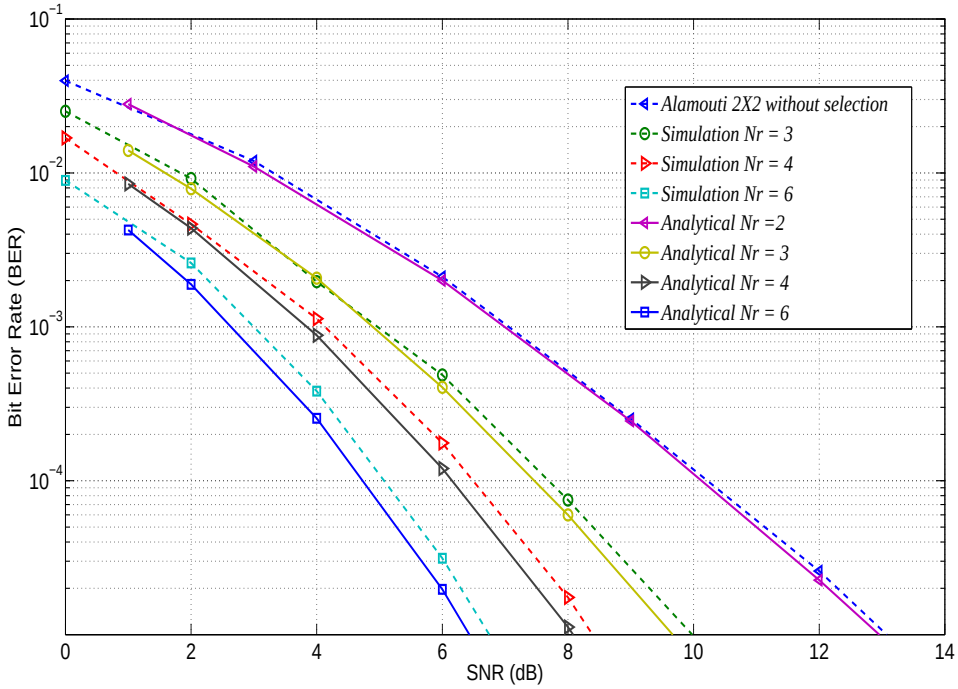

Figure 4.3 Comparison of Simulation Results and Analytical expressions for $N_r = 2, 3, 4, 6$

evaluation is repeated for $N_r = 4, 5, 6$. The simulation results are shown in Figure 4.3. In the case of $L_r = 2$ without antenna selection, the results correspond to those shown in [5]. When $N_r = 3$ the SNR gain about 3 dB for BER of 10^{-5} can be observed. For the same BER, the gain becomes almost 7 dB when $N_r = 6$ is considered. From the curves in Figure 4.3, it is easy to notice that the more the number of available receive antennas, provides a better BER performance. BER expression results match closely to the simulations for SNR between 0 dB and 12 dB and the expression for the case of $N_r = 2$ correspond to the exact BER performance of the 2×2 Alamouti Scheme without selection.

4.4 Effect of Antenna Correlation on Receive Antenna Selection

In Section 4.3, we assumed that the coefficients of the fading channels corresponding to each transmit and receive antennas were mutually uncorrelated Rayleigh distributed implying that the elements h_{ij} of the $\mathbf{H}$ matrix are uncorrelated. However, since spatial correlation is an important factor in MIMO performance, we set our goal to evaluate through simulations the impact of spatial correlation between antennas on the performance of the MIMO systems using receive antenna selections in flat fading channels. As a performances metric, we consider the Bit Error Rate (BER) for Orthogonal Space Time Block Coding (OSTBC) using receive

antenna selection. The UCBS algorithm, discussed in section 4.1.3 will be used as the receive antenna selection algorithm. For simplicity, it is assumed that all antennas have the same radiation pattern and furthermore the spatial correlation is independent of the position of an antenna in the array.

4.4.1 System and Channel Model

We consider the MIMO system model as shown in Figure 4.1 where $L_t = N_t = 2$. We consider $N_r > L_r$ available receive antennas where $L_r = 2$ receive antennas are selected out of N_r antennas. The relation between the transmitted signal and the received signal is given by

$$\mathbf{y}[n] = \mathbf{H}\mathbf{x}[n] + \mathbf{n}[n], \tag{4.58}$$

where the channel matrix $\mathbf{H}$ is defined as

$$\mathbf{H} = \begin{bmatrix} h_{11} & h_{12} \\ h_{21} & h_{22} \\ . & . \\ . & . \\ . & . \\ h_{N_r1} & h_{N_r2} \end{bmatrix} \tag{4.59}$$

$$\mathbf{H} = \begin{bmatrix} h_{11} & h_{12} \\ h_{21} & h_{22} \\ h_{31} & h_{32} \\ h_{41} & h_{42} \\ . & . \\ . & . \\ . & . \\ h_{N_r1} & h_{N_r2} \end{bmatrix} \tag{4.60}$$

where $h_{i,j}$ is the fading coefficient between transmit antenna j and receive antenna i, ($j = 1, 2$, $i = 1, 2, ..., N_r$). $h_{i,j}$ is a sample of independent complex Gaussian random variables with zero mean and variance $1/2$ per dimension. $\mathbf{x}[n]$ is the transmitted vector of size (2×1) at instant time n and $\mathbf{n}[n]$ represents the vector of additive white gaussian noise (AWGN) of size $N_r \times 1$. The elements of $\mathbf{n}[n]$ are random gaussian variables with zero mean and $N_0/2$ variance per dimension. To introduce the correlation effect in the channel model, we assume that the correlation matrix of the MIMO channel is the Kronecker product of the receive and

transmit correlation matrices [28]

$$R_{MIMO} = R_{rx} \otimes R_{tx} \tag{4.61}$$

where R_{rx} and R_{tx} represent respectively the receive and transmit correlation matrices defined as

$$R_{tx} = \begin{bmatrix} 1 & \rho_{12}^{tx} & \dots & \rho_{1N_t}^{tx} \\ \rho_{21}^{tx} & 1 & \dots & \rho_{2N_t}^{tx} \\ . & . & \dots & . \\ \rho_{N_t1}^{tx} & \rho_{N_t2}^{tx} & \dots & 1 \end{bmatrix}_{N_t \times N_t} \tag{4.62}$$

and

$$R_{rx} = \begin{bmatrix} 1 & \rho_{12}^{rx} & \dots & \rho_{1N_r}^{rx} \\ \rho_{21}^{rx} & 1 & \dots & \rho_{2N_r}^{rx} \\ . & . & \dots & . \\ \rho_{N_r1}^{rx} & \rho_{N_r2}^{rx} & \dots & 1 \end{bmatrix}_{N_r \times N_r} \tag{4.63}$$

The correlated MIMO channel matrix, $\mathbf{H}_c$, is then obtained as:

$$\mathbf{vec}(\mathbf{H}_c) = C\ \mathbf{vec}(\mathbf{H}) \tag{4.64}$$

where C is the result of the Cholesky decomposition of R_{MIMO}, $\mathbf{H}$ is the fading MIMO channel matrix defined in (4.59)

$$R_{MIMO} = CC^T \tag{4.65}$$

4.4.2 Simulations Results and Discussion

Using the system and channel model considered in section 4.4.1, we performed Monte-Carlo simulations to evaluate the performances of receive antenna selection with spatial correlation between the elements h_{ij} of the channel matrix $\mathbf{H}$. BPSK modulation and 2×2 Alamouti coding as OSTBC are in effect in the simulations. For receive antenna selection, the UCBS receive selection algorithm described in section 4.1.3 is used. For a fixed value of N_r, a $N_r \times 2$ correlated Rayleigh fading channel matrix is generated and only 2×2 rayleigh channel matrix is selected using the UCBS algorithm so that the two best receive antennas are chosen out of N_r available receive antennas. Based on the selected 2×2 channel, the performance of the Alamouti code in terms of BER is evaluated. The simulation results for

different number of available receive antennas, i.e., $N_r = \{3, 4, 6, 8\}$ are shown in Figures 4.4; 4.5; 4.6 and 4.7. In each case, several values for spatial correlation coefficient values are assumed $\{0.5; 0.7; 0.9; 0.997\}$. The correlation coefficient is applied for both receive and transmit side and we consider a uniform correlation between antennas, i.e., $\rho_{ij}^{tx} = \rho_{ij}^{rx} = \rho$ which implies that the same correlation coefficient is applied to all pairs of antennas. The results for $N_r = 3$, where two receive antennas are selected out from 3 receive available antennas, are shown in Figure 4.4. In this Figure, the BER performance in terms of SNR for different values of correlation coefficients, ρ, are shown. The degradation effect of the spatial

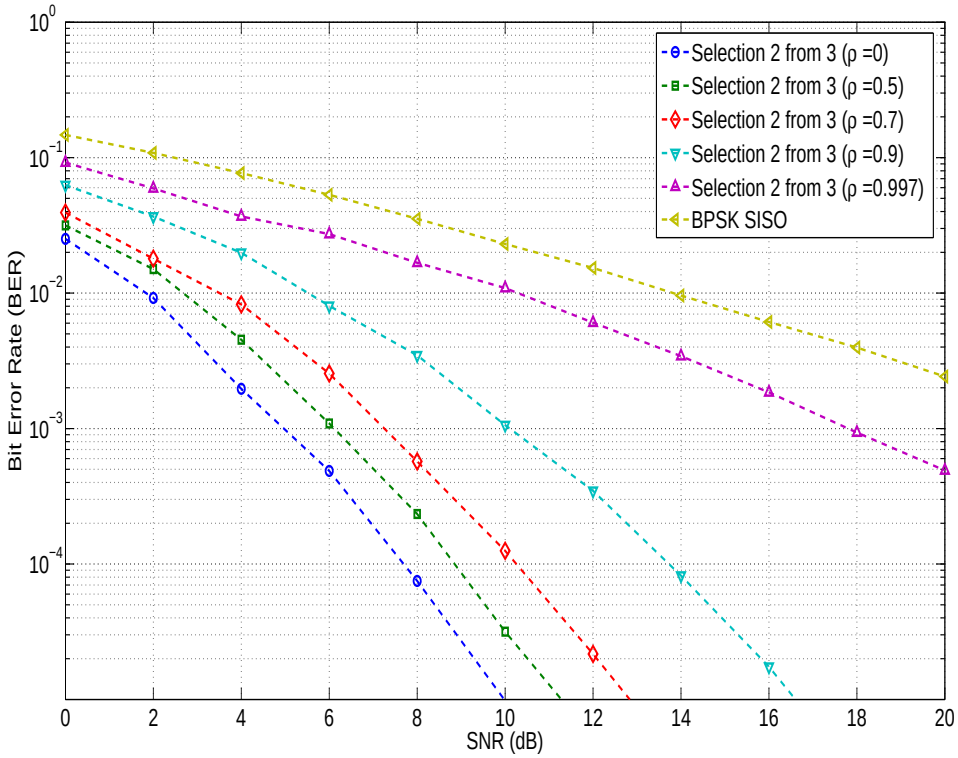

Figure 4.4 Receive Antenna Selection With mixed Correlation ($L_r = 2; N_r = 3$)

correlation on the BER performance is clearly observed in the Figure. For a BER = 10^{-3}, a difference of 13 dB can be observed between un-correlated ($\rho = 0$) and a highly correlated channel ($\rho = 0.997$). In fact, to achieve a BER = 10^{-3}, the SNR is found to be 5 dB for un-correlated channel whereas an SNR of 18 dB is needed to achieve the same BER with highly correlated channel ($\rho = 0.997$). We can also notice that the slope of the BER curves for correlations coefficient of up to 0.7 are almost the same and corresponds to the diversity order of 6, which corresponds to $N_r \times N_t 3 \times 2 = 6$. However, the slope of the BER curve for correlation coefficient equal to 0.9999 changes dramatically. In fact, the slope goes to 1

for highly correlated channel (0.997), which is the same as the slope of the SISO curve. This indicates that when the Rx antennas are fully correlated the diversity order of the system will be equal to 1, which is the diversity order of SISO case. However, it can be observed that in that case, the BER of the MIMO 2x2 system is still about 3 dB better compared to SISO case (i.e. a gain). This is due to the fact that 2 antennas (even though they are fully correlated) are in use and twice SNR (i.e., 3 dB) are received at the receiver side, compared to SISO. Similar results about the BER for $N_r = 4, 6$ and 8 are shown in Figures 4.5, 4.6, 4.7. In Figure 4.5, where $N_r = 4$, a difference of about 14 dB is observed between un-correlated channel ($\rho = 0$) and highly correlated channel ($\rho = 0.997$) at a BER level equal to 10^{-3}. In fact, the SNR is found to be 4 dB for 10^{-3} BER, whereas an SNR of 18 dB is needed to achieve the same level of BER (10^{-3}).

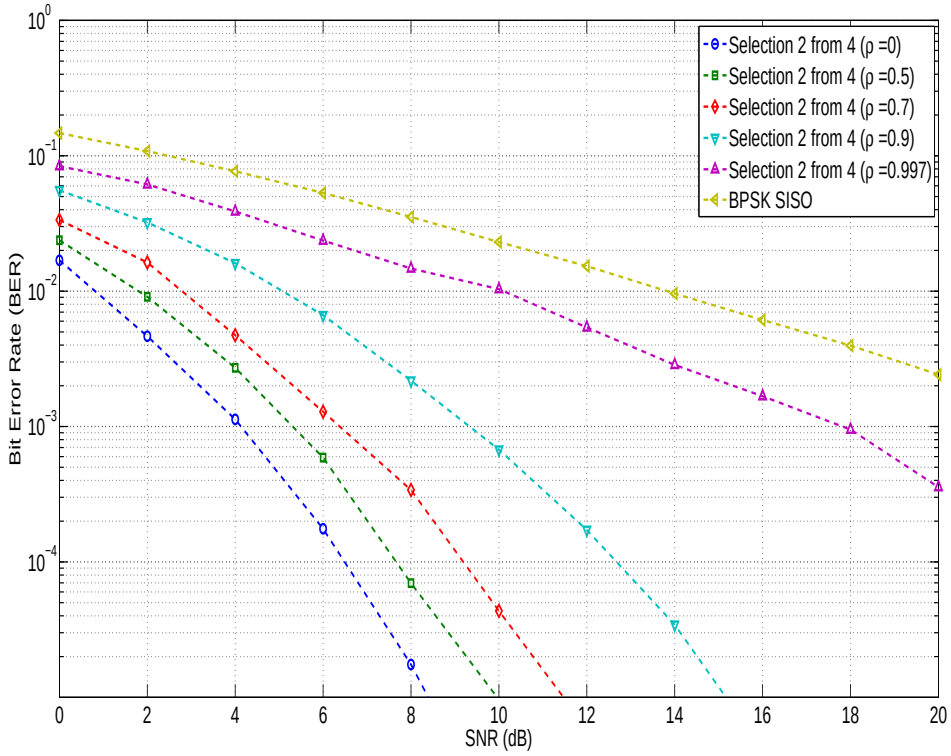

Figure 4.5 Receive Antenna Selection With mixed Correlation ($L_r = 2; N_r = 4$)

Again for correlation coefficients other than approximately equal to 1 (i.e. 0.5 and 0.7), the slope of the curve corresponds to the diversity order of 8 ($N_r \times 2$). This means that the diversity order ($N_r \times N_t$) is maintained for correlation coefficient not equal to 1. A similar conclusion can be made when we consider Figures 4.6 and 4.7. Finally, to compare the results of receive antenna selection with no selection, we plotted in Figure 4.8 presents the

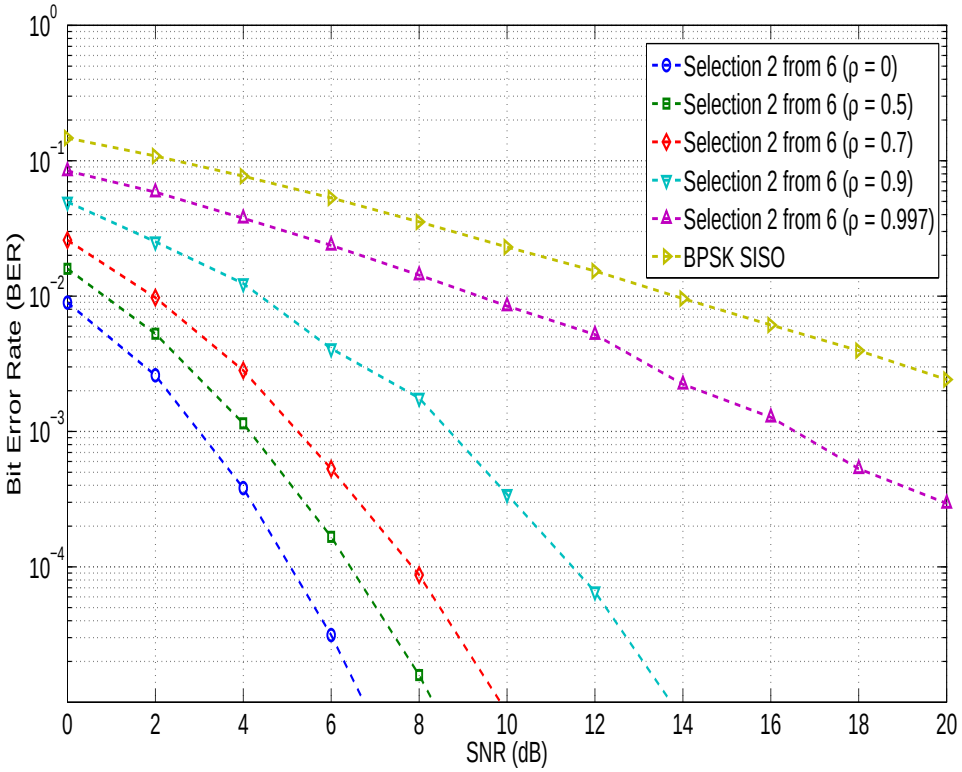

Figure 4.6 Receive Antenna Selection With mixed Correlation ($L_r = 2; N_r = 6$)

BER curves for a fixed value of correlation coefficient and for different values of N_r as well as the results of the 2×2 Alamouti scheme without selection but with the same correlation coefficient. The curve for 2×2 Alamouti without selection and zero correlation is also shown in Figure 4.8. It can be seen from this Figure that for highly correlated channel increasing the number of available antennas for receive antenna selection is also beneficial in terms of SNR gain with respect to the BER performance. As can be seen increasing N_r reduces the average BER and the performances becomes closer to the case of un-correlated 2×2 Alamouti scheme since the best performance is obtained with 8 receive antennas available for selection. The slopes of the curves tend to be different in the high SNR region, indicating that the diversity order is increased by the number of available receive antennas N_r.

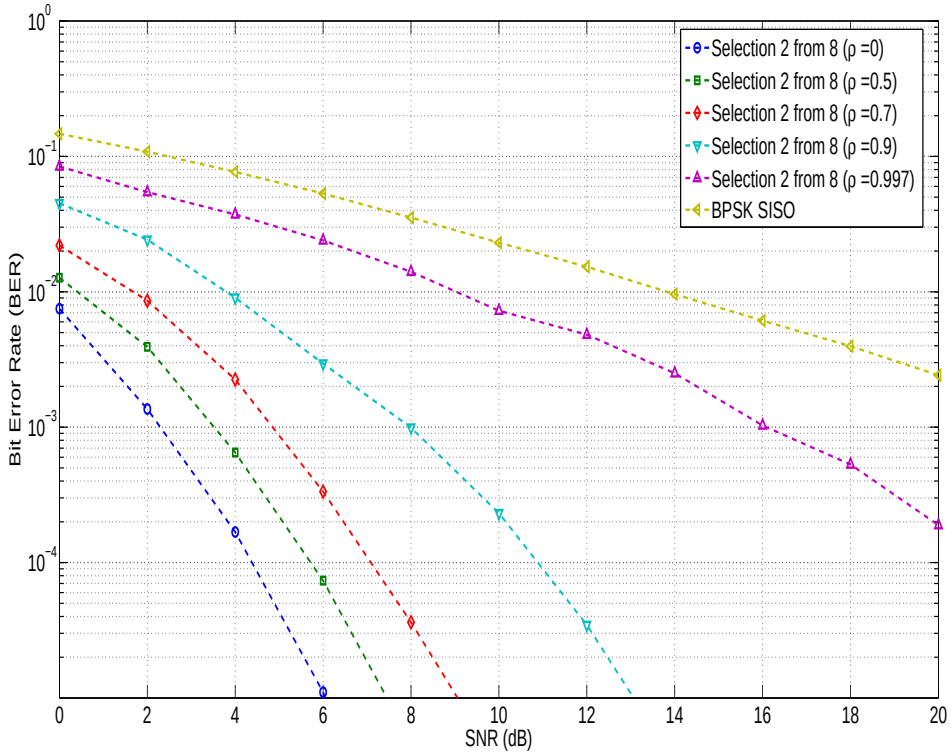

Figure 4.7 Receive Antenna Selection With mixed Correlation ($L_r = 2; N_r = 8$)

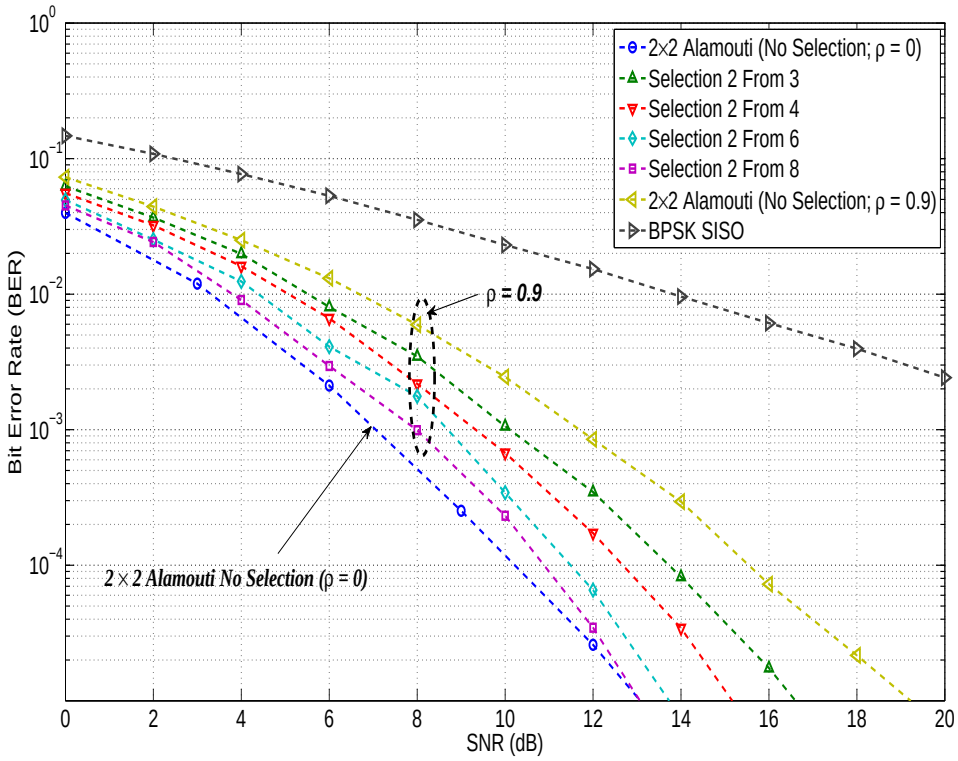

Figure 4.8 BER of Receive Antenna Selection with mixed Correlation ($\rho = 0.9$)

CHAPTER 5

SUMMARY AND CONCLUSIONS

This dissertation consists of two main parts. The first part (Chapter 3) presents an analysis and evaluation of the performance of MIMO-OFDM schemes in 4G LTE systems. More specifically, we derive an average BER performance for two OSTBC diversity MIMO schemes; namely the 2×1 SFBC-OFDM and the 4×2 FSTD-OFDM in the 3GPP 5 MHz Long Term Evolution (LTE) system over a Rayleigh flat fading channel. To show the BER performance improvement of the MIMO-OFDM schemes, the performance is compared to the SISO configuration. To ascertain the accuracy of the analysis, we also performed Monte-Carlo simulation using a LTE Link Level Simulator. The results show a good agreement between numerical results and Monte-Carlo simulation results. To complete the analysis, a study of the channel capacity for 2×1 SFBC-OFDM and 4×2 FSTD-OFDM MIMO schemes in Rayleigh flat fading channel has been performed. We use the probability density function of the instantaneous signal to noise ratio to derive analytical expressions for the capacity in terms of exponential integral and Poisson distribution. Effective data throughput as measured through simulation compare well with the system channel capacity limit.

In the second part of this thesis (Chapter 4) we evaluated the performances of antenna selection in MIMO systems. First, we reviewed antenna selection techniques and algorithms in MIMO systems as well as OSTBC systems. We then presented a performance evaluation for receive antenna selection in Rayleigh flat fading channels, assuming no antenna correlation. We derived analytical expression for the BER performances using order statistics theory to determine the probability density function of the signal to noise ratio of the selected subset of antennas. The analytical results of the BER performance of OSTBC were expressed in terms of an auxiliary integral. This integral can be evaluated using two known analytical defined functions, namely, the incomplete gamma function and the Gauss hypergeometric function. In our analysis, we considered a receive antenna selection where two receive antennas were selected out of N_r available antennas. To verify the accuracy of our analysis, we performed Monte-Carlo simulations and then compared the results to the theoretical analysis. For Monte-Carlo simulations, we implemented the UCBS receive antenna selection algorithm. The results show a good agreement between numerical values and Monte-Carlo simulations results. The order statistics theory is restricted to non correlated channels and hence it cannot be applied for correlated channels. Consequently we were constrained to evaluate the

performance of receive antenna selection in a correlated channels by Monte-Carlo simulations. We used the Kronecker MIMO channel model to generate correlated MIMO channels. Using the kronecker model, the antenna correlation at both sides are applied separately. Our results showed that even in correlated channel, the receive antenna selection is beneficial compared to no selection schemes.

5.1 Future Work

The performance analysis and evaluation presented in this thesis were made based on some assumptions, like flat fading channel and uncorrelated channels. Future work, could consider the following different assumptions.

5.1.1 MU-MIMO Aspects

In our performance evaluation of MIMO schemes in LTE (Chapter 3), we assumed a single user MIMO system (SU-MIMO), where the same time frequency resources are allocated to only one user. In addition to SU-MIMO as prescribed in the initial release of LTE standard, different multi user MIMO schemes (MU-MIMO) have also been defined and hence can be supported [44] by the standard. In MU-MIMO schemes, K UEs out of U active UEs in the cell, where K is much smaller than U, are selected for simultaneous communication over the same time frequency resource. For example, in a system with N_t transmit antennas and UEs with single receive antenna each, N_t different users can be multiplexed, where each stream is allocated to each UE. Thus, a substantial multiplexing gain can be achieved in case of MU-MIMO with single antennas at the UEs. Another advantage of the MU-MIMO is the natural de-correlation between the channels of the different UEs due to the fact that the separation between the UEs is typically large relative to the wavelength. It then becomes worthwhile to consider the performance of such systems.

5.1.2 CSI Aspects

One of the assumption which is consistently used throughout this work is perfect knowledge of the channel state information at the receiver side. However in real implementation, channel information is usually derived through channel estimation techniques which are not always accurate. In LTE, the channel estimation is performed using the Reference Signals (RS). As the signal in LTE evolves both in time and frequency domains, the channel estimation can be performed in both domains, and the impact of each type of estimation on the performance of LTE systems can be considered in the analysis. In the case of transmit

selection, which has not been considered in our work, the impact of the feedback delay should also be considered in the analysis.

5.1.3 Frequency Selective Channel Aspects

In our performance evaluation in Chapter 4 of receive antenna selection , we used a flat fading Rayleigh channel. In many situations the channel may be frequency selective. One of the most important limitation of antenna selection occurs when the channel is frequency selective. Indeed the different channel responses as a function of frequency imply that, in each band, antenna selection should be different. Thus, whenever the channel is highly frequency selective, antenna selection may not be useful or feasible. However, MIMO-OFDM systems are known to view the frequency selective channel as N flat fading channels, where N is the number of subcarriers in the OFDM symbol. In [35], the diversity order analysis of antenna selection scheme over frequency selective channel has been considered while the BER performance was evaluated by simulations only. Further studies of antenna selection in such channels might be worthwhile of interest in the future.

5.1.4 Antenna Correlated Channel Aspects

In addition to the flat fading Rayleigh channel assumption in our performance analysis of the receive antenna selection, we assumed uncorrelated channels in order to be able to apply the theory of order statistics. In [57], an analysis of MIMO systems with receive antenna selection in spatially correlated fading channels is provided using multivariate analysis together with the Wishart distribution [23] but for the case of the selection of only one receive antenna. Extensions to include more selections should be of great interest to investigate whether or not the use of selection diversity is still of practical use in improving the performance.

5.1.5 Contributions and Publications

The results and analysis of the main work obtained in this thesis were published and submitted in the following international conferences and journals:

1. *BER Analysis of Alamouti Scheme with Receive Antenna Selection*, published on 2010 6th International Conference of Wireless and Mobile Communications (ICWMC),
2. Investigation of the correlation effect on the Performance of V-BLAST and OSTBC MIMO Schemes, published on the 2011 Seventh International Conference of Wireless and Mobile Communicationss

3. Performance Evaluation of MIMO Schemes in 5 MHZ Bandwidth LTE Systems, published on the 2012 8th International Conference of Wireless and Mobile Communications
4. Bit Error Analysis of MIMO Schemes in LTE Systems, published on the 2013 9th International Conference of Wireless and Mobile Communications and received a best paper award.
5. Analysis of the Performance for SFBC-OFDM and FSTD-OFDM Schemes in LTE Systems over MIMO Fading Channels, submitted to the International Journal On Advances in Networks and Services as an Invited paper by IARIA Journals
6. Performance Analysis of MIMO Schemes in 3GPP Long Term Evolution System submitted to Springer's Wireless Personal Communications

REFERENCES

[1] 3GPP (2009). Technical specification ts36.211 version 8.7.0 "evolved universal terresterial radio access (e-utra); physical channel and modulation, (release 8)". http://www.3gpp.org.

[2] 3GPP (2009). Technical specification ts36.212 "evolved universal terresterial radio access (e-utra); multiplexing and channel coding". http://www.3gpp.org.

[3] 3GPP (2009). Technical specification ts36.213 "evolved universal terresterial radio access (e-utra); physical layer procedures". http://www.3gpp.org.

[4] 3GPP (2013). Technical specification group radio access network. http://www.3gpp.org.

[5] ALAMOUTI, S. (1998). A simple transmit diversity technique for wireless communications. *Selected Areas in Communications, IEEE Journal on*, 16, 1451 –1458.

[6] ALOUINI, M. S. and SIMON, M. K. (2000). *Digital Communications over Fading Channels: A Unified Approach to Performance Analysis*, Wiley.

[7] ANDREWS, J. G. and GHOSH, A. (2007). *Fundamentals of WiMAX: Understanding Broadband Wireless Networking*, PRENTICE HALL.

[8] ARNOLD, B. C., BALAKRISHNAN, N. and NAGARAJA, H. N. (1992). *A first course in order statistics*. Wiley series in probability and mathematical statistics. J. Wiley, New York. A Wiley-Interscience publication.

[9] BAHCECI, I., DUMAN, T. and ALTUNBASAK, Y. (2003). Antenna selection for multiple-antenna transmission systems: performance analysis and code construction. *Information Theory, IEEE Transactions on*, 49, 2669–2681.

[10] CHOI, Y.-S., MOLISCH, A., WIN, M. and WINTERS, J. (2003). Fast algorithms for antenna selection in mimo systems. *Vehicular Technology Conference, 2003. VTC 2003-Fall. 2003 IEEE 58th.* vol. 3, 1733–1737 Vol.3.

[11] DAVID, H. (1981). *Order statistics*. Wiley series in probability and mathematical statistics. Applied probability and statistics. Wiley.

[12] ESPINOSA, H. C., FONOLLOSA, J. R. and PENIN, J. A. D. (2001). Channel capacity of space-time block coding. *in Proc. IST Mobile Communications*. 9–14.

[13] GHRAYEB, A. (2006). A survey on antenna selection for mimo communication systems. *Information and Communication Technologies, 2006. ICTTA '06. 2nd.* vol. 2, 2104–2109.

[14] GIFFORD, W. M., WIN, M. Z. and CHIANI, M. (2008). Antenna subset diversity with non-ideal channel estimation. *IEEE Transactions on Wireless Communications*, 7, 1527–1539.

[15] GOLDEN, G., FOSCHINI, C. J., VALENZUELA, R. and WOLNIANSKY, P. (1999). Detection algorithm and initial laboratory results using v-blast space-time communication architecture. *Electronics Letters*, 35, 14–16.

[16] GOLDSMITH, A. (2005). *Wireless Communications*. Cambridge University Press, New York, NY, USA.

[17] GORE, D., NABAR, R. and PAULRAJ, A. (2000). Selecting an optimal set of transmit antennas for a low rank matrix channel. *Acoustics, Speech, and Signal Processing, 2000. ICASSP '00. Proceedings. 2000 IEEE International Conference on*. vol. 5, 2785–2788 vol.5.

[18] GORE, D. and PAULRAJ, A. (2002). Mimo antenna subset selection with space-time coding. *Signal Processing, IEEE Transactions on*, 50, 2580–2588.

[19] GOROKHOV, A. (2002). Antenna selection algorithms for mea transmission systems. *Acoustics, Speech, and Signal Processing (ICASSP), 2002 IEEE International Conference on*. vol. 3, III–2857–III–2860.

[20] GRADSHTEYN, I. S. and RYZHIK, I. M. (1994). *Table of Integrals, Series and Products*. Academic Press, San Diego, cinquième édition. Erratum available from `www.mathtable.com`.

[21] GRADSHTEYN, I. S. and RYZHIK, I. M. (2000). *Table of Integrals, Series and Products*. Academic Press, San Diego, sixth édition. Erratum available from `www.mathtable.com`.

[22] GUNTHER, C. (1996). Comment on "estimate of channel capacity in rayleigh fading environment. *Vehicular Technology, IEEE Transactions on*, 45, 401–403.

[23] HAGEDORN, M., SMITH, P., BONES, P., MILLANE, R. and PAIRMAN, D. (2006). A trivariate chi-squared distribution derived from the complex wishart distribution. *Journal of Multivariate Analysis*, 97, 655 – 674.

[24] HEATH, R. and PAULRAJ, A. (2001). Antenna selection for spatial multiplexing systems based on minimum error rate. *Communications, 2001. ICC 2001. IEEE International Conference on*. vol. 7, 2276–2280 vol.7.

[25] IKUNO, J., WRULICH, M. and RUPP, M. (2010). System level simulation of lte networks. *Vehicular Technology Conference (VTC 2010-Spring), 2010 IEEE 71st*. 1 –5.

[26] JOHNSON, C. (2012). *Long Term Evolution IN BULLETS*, PRENTICE HALL. Seconde édition.

[27] KATZ, M., TIIROLA, E. and YLITALO, J. (2001). Combining space-time block coding with diversity antenna selection for improved downlink performance. *Vehicular Technology Conference, 2001. VTC 2001 Fall. IEEE VTS 54th.* vol. 1, 178–182 vol.1.

[28] KERMOAL, J., SCHUMACHER, L., PEDERSEN, K., MOGENSEN, P. and FREDERIKSEN, F. (2002). A stochastic mimo radio channel model with experimental validation. *Selected Areas in Communications, IEEE Journal on*, 20, 1211–1226.

[29] LEGNAIN, R., HAFEZ, R. H. M. and MARSLAND, I. (2012). Ber analysis of three-phase xor-and-forward relaying using alamouti stbc. *Communications Letters, IEEE*, 16, 1458–1461.

[30] LOPEZ-MARTINEZ, F., MARTOS-NAYA, E., WONG, K.-K. and ENTRAMBASAGUAS, J. (2011). Closed-form ber analysis of alamouti-mrc systems with icsi in ricean fading channels. *Communications Letters, IEEE*, 15, 46–48.

[31] MAAREF, A. and AISSA, S. (2005). Capacity of space-time block codes in mimo rayleigh fading channels with adaptive transmission and estimation errors. *Wireless Communications, IEEE Transactions on*, 4, 2568–2578.

[32] MEHLFÜHRER, C., WRULICH, M., IKUNO, J. C., BOSANSKA, D. and RUPP, M. (2009). Simulating the long term evolution physical layer. *Proc. of the 17th European Signal Processing Conference (EUSIPCO 2009)*. Glasgow, Scotland.

[33] MOLISCH, A. (2004). Mimo systems with antenna selection - an overview. *Mitsubishi Electric Research Labs*. 1–22.

[34] MOLISCH, A., WIN, M. and WINTERS, J. (2001). Capacity of mimo systems with antenna selection. *Communications, 2001. ICC 2001. IEEE International Conference on*. vol. 2, 570–574 vol.2.

[35] OHNO, S. and TEO, K. (2009). Diversity analysis of antenna selection over frequency-selective mimo channels. *Acoustics, Speech and Signal Processing, 2009. ICASSP 2009. IEEE International Conference on*. 2813–2816.

[36] ONLINE (2009). Lte link level simulator. Available `http://www.nt.tuwien.ac.at/ltesimulator`.

[37] PARK, J.-S. and PARK, D.-J. (2005). A new antenna selection algorithm with low complexity for mimo wireless systems. *Communications, 2005. ICC 2005. 2005 IEEE International Conference on*. vol. 4, 2308–2312 Vol. 4.

[38] PRASSARD, R. (2001). *OFDM for Wireless Communications Systems*. Artech House.

[39] PROAKIS, J. G. (2001). *Digital Communications*, Mc Graw Hill.

[40] SANDHU, S. and PAULRAJ, A. (2000). Space-time block codes: a capacity perspective. *Communications Letters, IEEE*, 4, 384–386.

[41] SCHWARZ, S., MEHLFUHRER, C. and RUPP, M. (2010). Calculation of the spatial preprocessing and link adaption feedback for 3gpp umts/lte. *Wireless Advanced (WiAD), 2010 6th Conference on*. 1 –6.

[42] SCHWARZ, S., WRULICH, M. and RUPP, M. (2010). Mutual information based calculation of the precoding matrix indicator for 3gpp umts/lte. *Smart Antennas (WSA), 2010 International ITG Workshop on*. 52 –58.

[43] SESIA, S., ISSAM, T. and BACKER, M. (2011). *LTE The UMTS Long Term Evolution From Theory To Practice*, John Wiley.

[44] SESSIA, S., TAOUFIK, I. and BAKER, M. (2011). *LTE The UMTS Long Term Evolution: From THEORY TO PRACTICE*, WILEY. Seconde édition.

[45] SHANNON, C. E. (1948). A mathematical theory of communication. *The Bell System Technical Journal*, 27, 379–423, 623–656.

[46] SHEN, H. and GHRAYEB, A. (2006). Analysis of the outage probability for mimo systems with receive antenna selection. *Vehicular Technology, IEEE Transactions on*, 55, 1435–1440.

[47] SIMKO, M., MEHLFUHRER, C., WRULICH, M. and RUPP, M. (2010). Doubly dispersive channel estimation with scalable complexity. *Smart Antennas (WSA), 2010 International ITG Workshop on*. 251 –256.

[48] SIMON, M. K. and ALOUINI, M.-S. (1998). A unified approach to the performance analysis of digital communication over generalized fading channels. *Proceedings of the IEEE*, 86, 1860–1877.

[49] TAROKH, V., JAFARKHANI, H. and CALDERBANK, A. (1999). Space-time block codes from orthogonal designs. *Information Theory, IEEE Transactions on*, 45, 1456–1467.

[50] TAROKH, V., JAFARKHANI, H. and CALDERBANK, A. (1999). Space-time block codes from orthogonal designs. *Information Theory, IEEE Transactions on*, 45, 1456–1467.

[51] TELATAR, I. E. (1999). Capacity of multi-antenna gaussian channels. *EUROPEAN TRANSACTIONS ON TELECOMMUNICATIONS*, 10, 585–595.

[52] TORABI, M. and HACCOUN, D. (2011). Performance analysis of joint user scheduling and antenna selection over mimo fading channels. *Signal Processing Letters, IEEE*, 18, 235–238.

[53] TSE, D. and VISWANATH, P. (2008). *Fundamnetals of Wireless Communications*, Cambridge University Press.

[54] WONG, W. H. and LARSSON, E. (2003). Orthogonal space-time block coding with antenna selection and power allocation. *Electronics Letters*, 39, 379–381.

[55] WRULICH, M. (2006). *Capacity Analysis of MIMO Systems*. Mémoire de maîtrise, Institut für Nachrichtentechnik und Hochfrequenztechnik, Vienna University of Technology.

[56] XIE, W., XIE, L., ZHAN, J. and LIU, S. (2006). A novel antenna selection algorithm for mimo systems under correlated channels. *ITS Telecommunications Proceedings, 2006 6th International Conference on*. 461–464.

[57] XU, Z., SFAR, S. and BLUM, R. (2009). Analysis of mimo systems with receive antenna selection in spatially correlated rayleigh fading channels. *Vehicular Technology, IEEE Transactions on*, 58, 251–262.

[58] ZENG, X. N. and GHRAYEB, A. (2004). Performance bounds for space-time block codes with receive antenna selection. *Information Theory, IEEE Transactions on*, 50, 2130–2137.

[59] ZHANG, H. and GULLIVER, T. (2005). Capacity and error probability analysis for orthogonal space-time block codes over fading channels. *Wireless Communications, IEEE Transactions on*, 4, 808–819.

APPENDICE A

IMPACT OF RECEIVE ANTENNA CORRELATION

To evaluate the impact of only receive antenna correlation, we performed different simulation when the antenna correlation at the transmitter is equal to 0 (i.e., the transmit correlation matrix is the identity matrix, $R_{tx} = \mathbf{I}$) and only receive antenna correlation is considered. The results for the 2×2 scheme without receive antenna selection and for different values of correlation coefficient ($\rho_{rx} = \{0.5, 0.7, 0.9, 0.99999\}$) are shown in Figure A.1. In this Figure, the BPSK BER performances of the 2×2 Alamouti scheme are shown. It

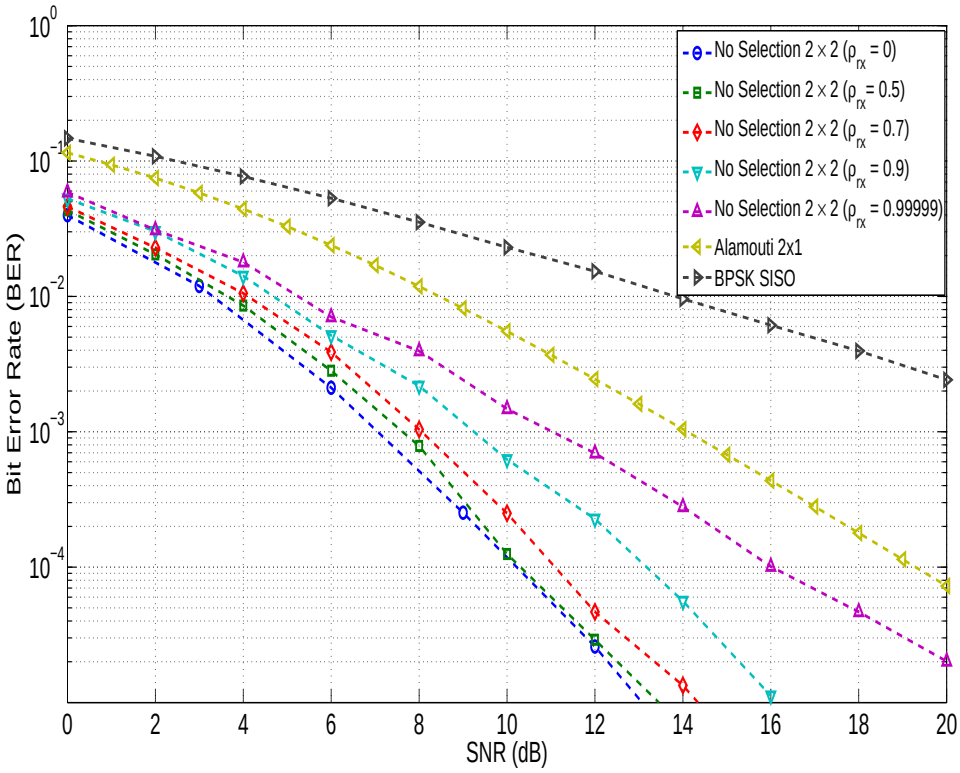

Figure A.1 BER of Receive Antenna Selection with receive antenna Correlation ($\rho_{tx} = 0$)

can be noticed from the Figure that the recieve antenna correlation deteriorate the BER performances. When the correlation coefficient tends to 1 ($\rho_{rx} = 0.99999$), the slope of the BER curve becomes equal to 2. In fact, it is clearly shown in the Figure that the curve of 2×2 scheme with highly receive antenna correlation ($\rho_{rx} = 0.99999$) is almost parallel

to the curve of the 2×1 scheme without any correlation. Also, it can be noticed that the curve of the 2×2 scheme is just shifted by almost 3 dB with respect to the 2×1 scheme, which represents a 3 dB SNR gain with respect to the 2×1 case. This 3 dB improvement with respect to the 2×1 case is explained by the fact that the two receive antennas act as one receive antenna with a double SNR when the correlation coefficient is almost equal to 1. The results for $N_r = 3, 4, 6$, and 8 are shown in Figures A.2, A.3, A.4 and A.5, respectively. In those Figures, we plotted the BPSK BER performance of 2×2 Alamouti scheme with receive antenna selection in correlated channel and where the correlation coefficients values are the same as before. The results when two receive antennas are selected out of three receive available antennas are shown in Figure A.2. We can notice from the Figure that the

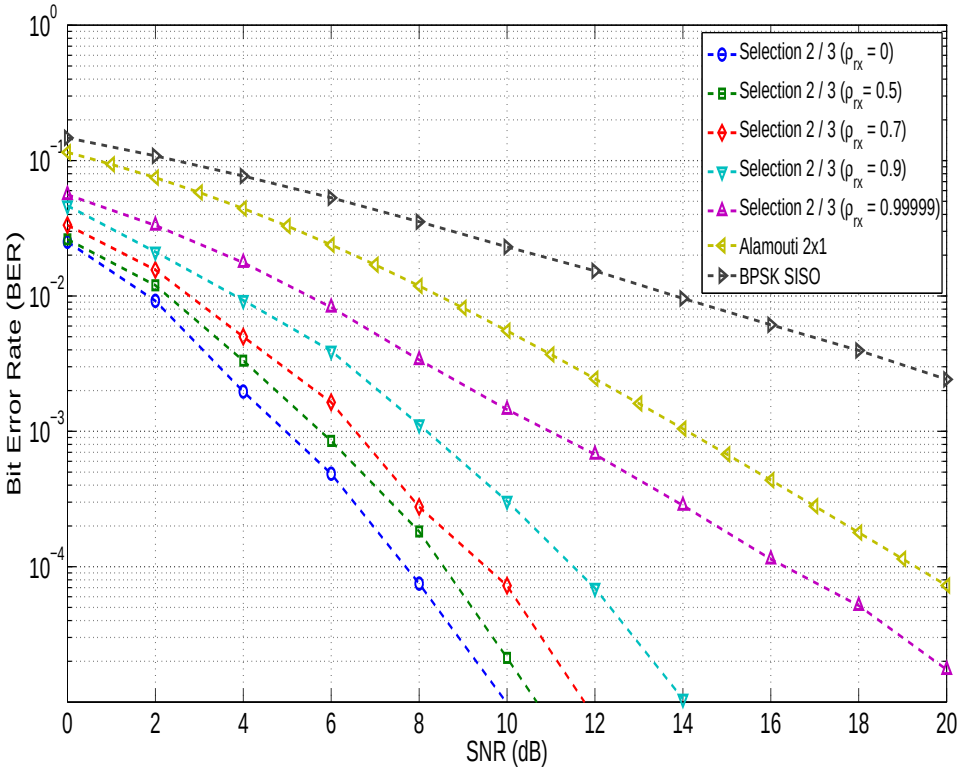

Figure A.2 BER of Receive Antenna Selection with receive antenna Correlation ($\rho_{tx} = 0$ and $N_r = 3$)

receive antenna correlation deteriorates the BER performance. In fact, in case of uncorrelated receive antennas ($\rho_{rx} = 0$), the BER level of 10^{-3} is achieved with SNR value equal to 5 dB, whereas the same BER level is achieved with 11 dB when the correlation coefficient is almost equal to 1 ($\rho_{rx} = 0.99999$), which represents a degradation of 6 dB. It can also be observed from the Figure how the slope of the curve tends to be the same as the 2×1 case as

the correlation coefficient becomes 1. This indicates that the diversity order of 2×2 MIMO system under fully correlated receive antennas ($\rho_{rx} = 1$) is equivalent to the diversity order of 2 MIMO system. The same observations can be made when $N_r = 4, 6$ and 8.

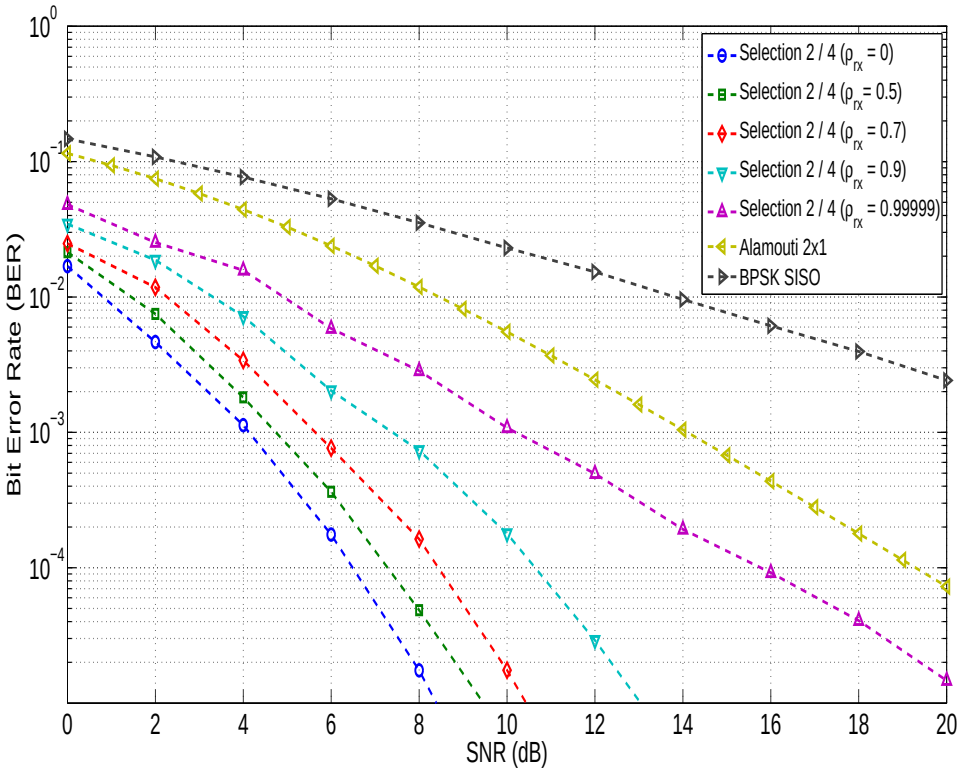

Figure A.3 BER of Receive Antenna Selection with receive antenna Correlation ($\rho_{tx} = 0$)

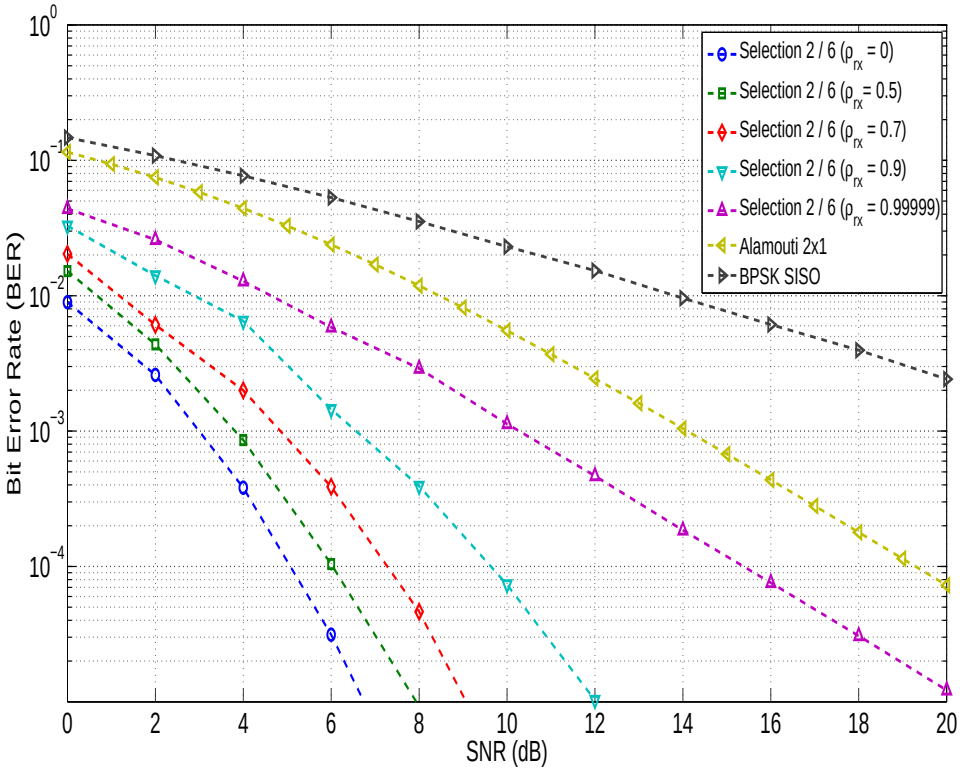

Figure A.4 BER of Receive Antenna Selection with receive antenna Correlation ($\rho_{tx} = 0$)

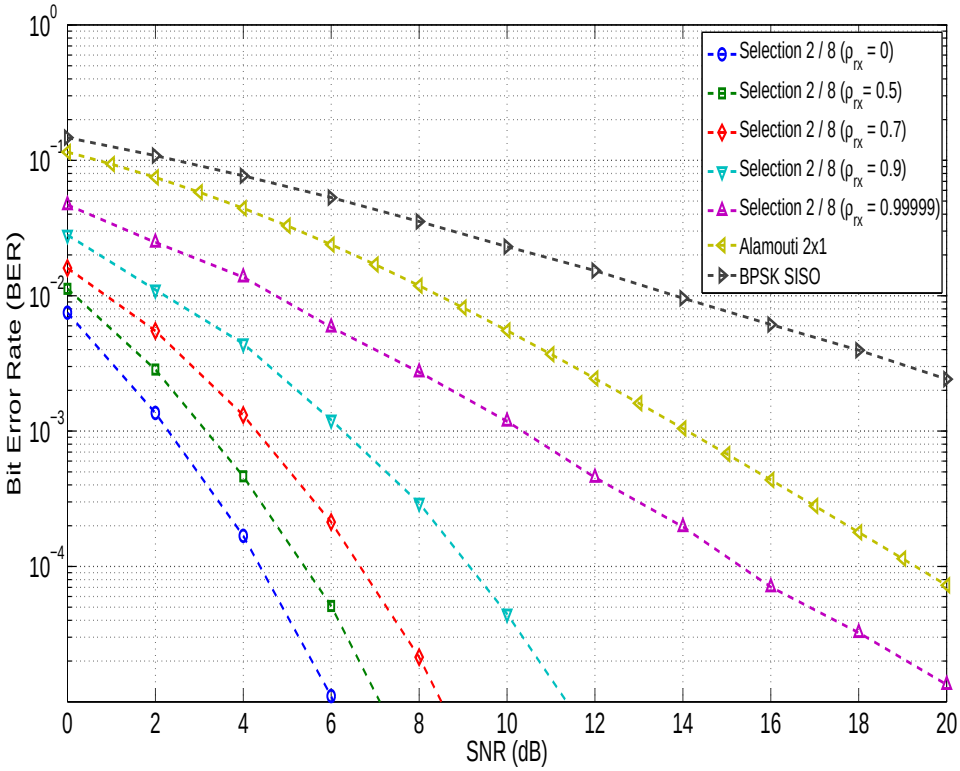

Figure A.5 BER of Receive Antenna Selection with receive antenna Correlation ($\rho_{tx} = 0$)

APPENDICE B

DERIVATION OF THE ALTERNATIVE FORM OF Q-FUNCTION

The classical expression of the Q-function is defined by:

$$Q(x) = \int_x^\infty \frac{1}{\sqrt{2\pi}} \exp\left(-\frac{y^2}{2}\right) dy \tag{B.1}$$

.

The following derivation is aimed to obtain an alternative form of Equation (B.1), where the lower limit of the integral is independent of the variable x and the upper limit is finite. To this end, the starting point of the derivation is to consider the integral due to [20] [p. 362, Eq. (3.363.2)]

$$\int_u^\infty \frac{e^{-\mu x}}{x\sqrt{x-u}} dx = \frac{\pi}{\sqrt{u}} \text{erfc}\left(\sqrt{u\mu}\right) \tag{B.2}$$

.

Putting $u = y^2$ and multiplying both sides of Equation (B.2) by $\frac{1}{2}e^{\mu u}$ gives

$$\frac{1}{2}\int_{y^2}^\infty \frac{e^{-\mu x}}{x\sqrt{x-u}} dx = \frac{\pi}{2y} e^{\mu y^2} \text{erfc}\left(y\sqrt{\mu}\right) \tag{B.3}$$

.

In order to extend the Equation (B.3) to two dimension (x, y), we define $u = x - y^2$. The Equation (B.3) then becomes:

$$\frac{1}{2}\int_0^\infty \frac{e^{-\mu u}}{(u+y^2)\sqrt{u}} du = \frac{\pi}{2y} e^{\mu y^2} \text{erfc}\left(y\sqrt{\mu}\right) \tag{B.4}$$

.

Now, we define $u = t^2$, which leads to $du = 2tdt = 2\sqrt{u}dt$. Hence, Equation (B.4) becomes:

$$\int_0^\infty \frac{e^{-\mu t^2}}{(t^2+y^2)}dt = \frac{\pi}{2y}e^{\mu y^2}\text{erfc}\,(y\sqrt{\mu}) \tag{B.5}$$

.

Putting $y = 1$ and$\mu = z^2$ in the above equation, we obtain:

$$\int_0^\infty \frac{e^{-z^2t^2}}{(t^2+1)}dt = \frac{\pi}{2}e^{z^2}\text{erfc}\,(z) \tag{B.6}$$

.

Equivalently, Equation (B.6) can be written as:

$$\frac{2}{\pi}\int_0^\infty \frac{e^{-z^2(t^2+1)}}{(t^2+1)}dt = \text{erfc}\,(z) \tag{B.7}$$

.

The final step in the derivation of the alternative form of the Q- function is to let $\sin^2\theta = (t^2+1)^{-1}$ and $\cos^2\theta = t^2(t^2+1)$, which leads to a derivation of t with respect to θ as:

$$dt = -(t^2+1)d\theta \tag{B.8}$$

and the Equation (B.7) becomes:

$$\frac{2}{\pi}\int_0^{\frac{\pi}{2}} \exp\left(\frac{-z^2}{\sin^2\theta}\right)d\theta = \text{erfc}\,(z) \tag{B.9}$$

by letting $z = \frac{x}{\sqrt{2}}$, we finally obtain the desired alternative form of the Q-function as:

$$\frac{1}{\pi}\int_0^{\frac{\pi}{2}} \exp\left(-\frac{x^2}{2\sin^2\theta}\right)d\theta = Q(x) \tag{B.10}$$

which conclude the derivation of the alternative form of the Q-function.
It is worth noting that there is another different method to arrive to the form of Equation (B.10), which can be found in [6].

APPENDICE C

BER EVALUATION USING THE ALTERNATIVE Q-FUNCTION

To compute the average error probability, an integral whose integrand consists of the product of the Gaussian Q-function and the probability density function (PDF) of the fading channel have to be evaluated. If one has to use the classical form of the Q-function, the integral for the evaluation will have the following form:

$$I = \int_0^\infty Q(a\sqrt{\gamma}) p_\gamma(\gamma) d\gamma = \int_0^\infty \left[\int_{a\sqrt{\gamma}}^\infty \frac{1}{\sqrt{2\pi}} \exp\left(-\frac{y^2}{2}\right) dy \right] p_\gamma(\gamma) d\gamma \tag{C.1}$$

where γ represents the average signal to noise ratio and a is constant that depends on the specific modulation scheme. As discussed, in general, the evaluation of the integral in Equation (C.1) is difficult because of the presence of $\sqrt{\gamma}$ in the lower limit of the integral. However, if, instead, the alternative form of the Q-function (Appendix A; Equation (B.10)) has to be used, the evaluated integral becomes:

$$I = \int_0^\infty \left[\frac{1}{\pi} \int_0^{\pi/2} \exp\left(-\frac{a^2\gamma}{2\sin^2\theta}\right) d\theta \right] p_\gamma(\gamma) d\gamma \tag{C.2}$$

or equivalently

$$I = \frac{1}{\pi} \int_0^{\pi/2} \left[\int_0^\infty \exp\left(-\frac{a^2\gamma}{2\sin^2\theta}\right) p_\gamma(\gamma) d\gamma \right] d\theta \tag{C.3}$$

where the integral in brackets (inner integral) is i the form of a Laplace transform with respect to the variable γ. In fact, the Laplace transform of $p_\gamma(\gamma)$ represents the Moment Generating Function of γ, which is defined by:

$$M_\gamma(s) = \int_0^\infty e^{s\gamma} p_\gamma(\gamma) d\gamma \tag{C.4}$$

and hence Equation (C.3) can be written as:

$$I = \frac{1}{\pi} \int_0^{\pi/2} M_\gamma\left(-\frac{a^2}{2\sin^2\theta}\right) d\theta \tag{C.5}$$

.

Using the above integral, the evaluation of the error probability is simplified to the eval-

uation a single integral on θ. The first step in the evaluation is then the calculation of the Laplace transform of the probability density function (PDF) of the instantaneous SNR, which represents the Moment Generating Function (MGF) of γ. The second step consists of the evaluation of a single integral on θ.

APPENDICE D

VIENNA LTE LINK LEVEL SIMULATOR

In order to verify the analysis of LTE performances with Monte-Carlo simulation, a full LTE transmission chain have to be implemented to perform those simulations. However, LTE is a complex system and implementing all the functionalities and features of this system would require a huge time. Fortunately, an LTE link level simulator has been made publicly under an academic use license including source code by Vienna Technical University. This enabled academic researches access to an open source LTE simulator, which facilitates the comparison and sharing different algorithm and results. In this thesis, we used the Vienna LTE link level simulation to verify our analysis and perform some evaluations of LTE system performances. The simulator is a software implementation of the physical (PHY) layer procedures. The Link Level Simulator is aimed to simulate one or multiple links between the Evolved base station (eNodeB) and the User Equipment (UE), including channel model. In this appendix, we provide a brief description of the overall structure of the simulator used in this thesis.

The Vienna link level simulator consists of three main blocks, namely Transmitter (TX), Channel Model and Receiver (RX) as shown in Figure D.1.

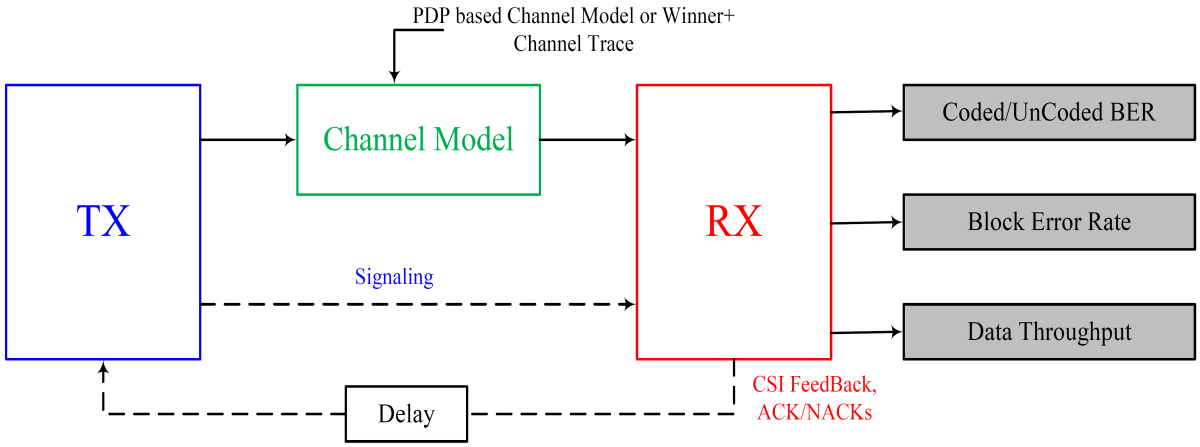

Figure D.1 Functional Block Diagram of Vienna LTE Link Level Simulator

The signaling, from transmitter to the receiver, and the User Equipment feedback, from the receiver to the transmitter and expressed in terms of Channel State Information (CSI)

and acknowledjement/non acknowledgement (ACK/NACK), are assumed to be error free and that is why they are not connected to the channel model.

The functional block diagram of the transmitter is shown in Figure D.1 and represents the implementation of the transmission procedures as described in the corresponding technical specification series (TS). Specifically, the physical layer of LTE are described in TS 36.x series [2], [1], [3].

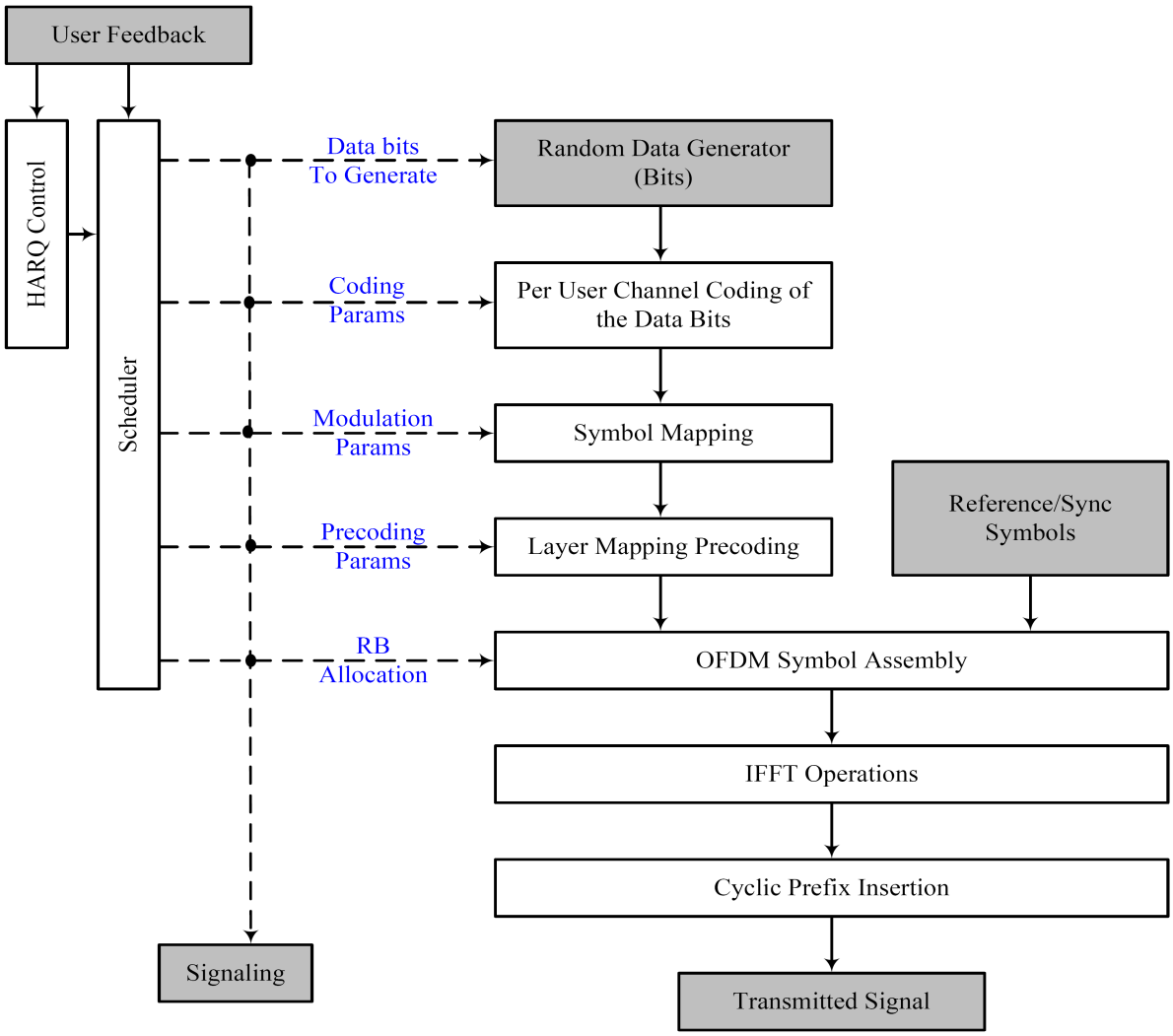

Figure D.2 Functional Block Diagram of the Transmitter of the LTE Simulator

Based on the feedback values received from the UE, the scheduling algorithm in the transmitter assigns each UE specific Resource Blocks (RBs), a modulation and coding scheme (MCS), an MIMO transmission mode and an appropriate pre-coding matrix for spatial mul-

tiplexing. The transmitted signal can be modulated using 4-QAM, 16-QAM or 64-QAM modulations alphabets with discrete set of coding rates as specified in. Three main MIMO modes can be supported by the simulator, namely Transmit Diversity (TxD); Open loop spatial multiplexing (OLSM) and Closed Loop Spatial Multiplexing (CLSM). For each MIMO mode, different antennas configuration can be supported. For example, in TxD mode tho possibilities of antennas configuration can be supported, namely 2×1 and 4×2, where 2×1 means two transmit antennas and one receive antennas.

Two types of fading channels can be supported by the Vienna LTE simulator, namely block fading channels and fast fading channels. In the case of block fading channel, the channel coefficient is constant during the duration of one sub-frame (1 ms). In fast fading channels, time correlated channel impulse response are generated for each sample of the transmitted signal. The channel models that can be supported by the LTE simulator are as follow:

1. Additive White Gaussian Noise (AWGN)
2. Rayleigh Flat Fading Channel
3. Channel models based on the Power Delay Profile (PDP) such as ITU Pedestrian B and ITU Vehicular A channel models.
4. Winner Phase II channel model

The receiver in the LTE simulator is implemented with many options in terms of receiver algorithm, channel estimation and feed back calculations. The overall structure of the implemented receiver in LTE is shown in Figure D.3. As detection algorithms, the receiver can support Zeros Forcing (ZF), Linear Minimum Mean Square Error (LMMSE) and Soft Sphere Decoding (SSD) algorithms. In terms of channel estimation, four different types of channel estimator are implemented, namely Least Square (LS), Minimum Mean Square Error (MMSE), approximate Linear Minimum Mean Square Error (LMMSE) and perfect channel knowledge based on all transmitted symbols. The feedback information to be sent to the transmitter are calculated based on the results of channel estimation. The feedback information include the Channel Quality Indicator (CQI) for all modes of operation, the Rank Indicator (RI) for spatial multiplexing modes and finally the Pre-coding Matrix Indicator (PMI) for Closed Loop Spatial Multiplexing Mode (CLSM). The structure of the receiver allows the investigation of various aspects, such as channel estimation, frequency and time synchronisation algorithms, modeling of the channel encoding and decoding and physical layer modeling for system level simulation.

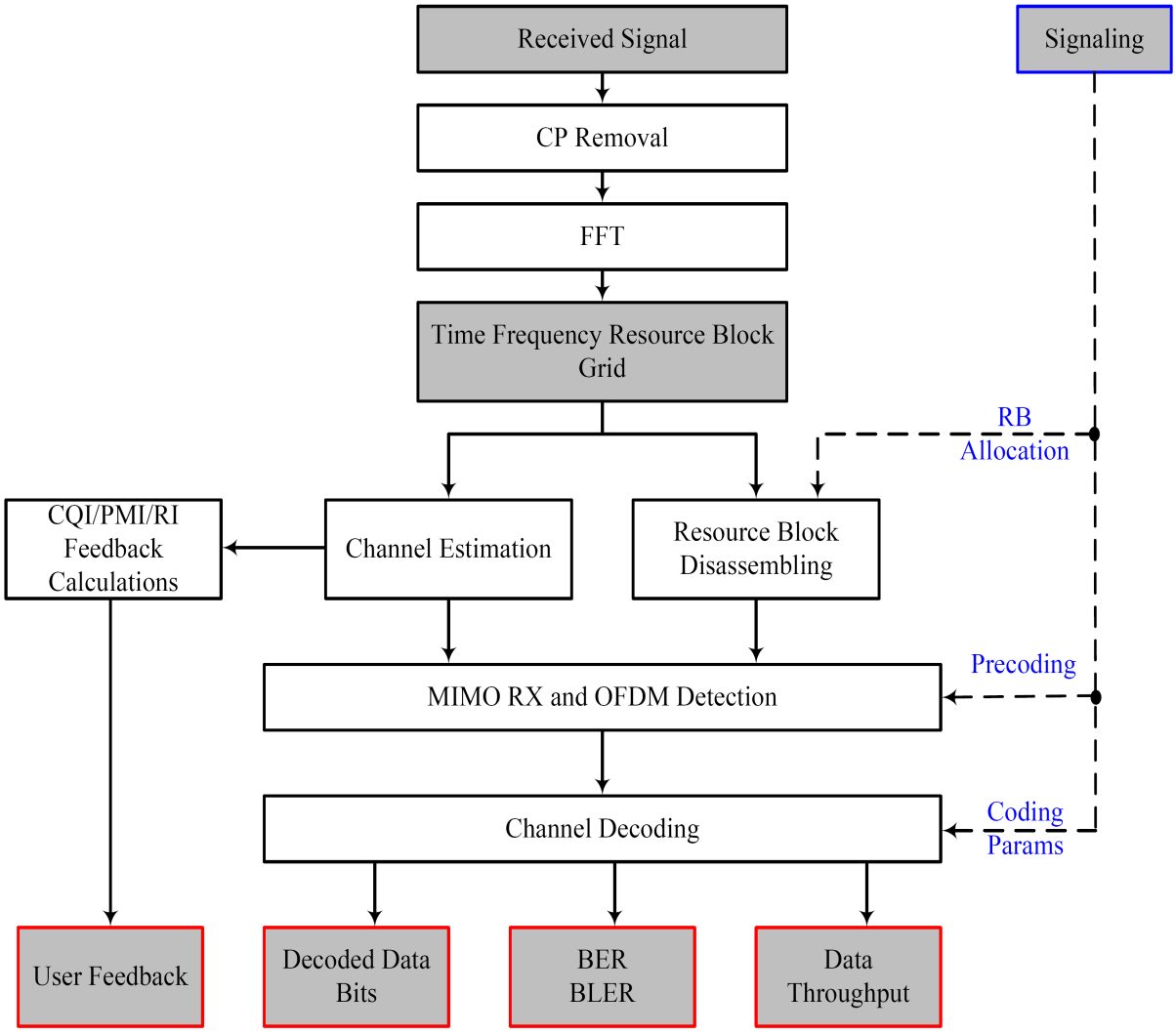

Figure D.3 Functional Block Diagram of the Receiver of the LTE Simulator